2013

An investigation of the bioavailability of heavy metals in tailing run-off sediment at Devon Great Consols

Yin Chi, C.

Yin Chi, C. (2013) 'An investigation of the bioavailability of heavy metals in tailing run-off sediment at Devon Great Consols', The Plymouth Student Scientist, 6(2), p. 211-309.
http://hdl.handle.net/10026.1/14041

The Plymouth Student Scientist
University of Plymouth

*The Plymouth Student Scientist, 2013, **6**, (1), 211-309*

An investigation of the bioavailability of heavy metals in tailing run-off sediment at Devon Great Consols

Chan Yin Chi

Project Advisor: Hywel Evans, School of Geography, Earth and Environmental Sciences, Plymouth University, Drake Circus, Plymouth, PL4 8AA

Abstract

This project focuses on the environmental geochemistry of the Devon Great Consols by determination of the concentrations of chromium, copper, nickel, lead, zinc, cadmium, arsenic, manganese and iron. BCR®701 is a certified reference material (CRM) which was treated by Community Bureau of Reference (BCR) sequential extraction to determine the accuracy and precision of the experiment. Moreover, the CRM was also employed to compare performance of instruments, namely ICP-AES and ICP-MS. The T-test was used to determine any significance of difference between experimental values and certified values. The F- test was used to determine any significance of difference between ICP-AES and ICP-MS presentations. Following comparison, ICP-AES was found to be effective at analysing steps 1 to 3 while ICP-MS was good for the analysis of step 2. The tailing run-off stream sediments collected on 1st November 2011 were extracted by the BCR extraction method. After sieving, samples 2, 4 and 8 had more < 250μm sediment which was used to determine the level of heavy metals. The Folk's classification showed that some of the samples 1, 3, 6 and 7 were classified as muddy sandy gravel sediment. In addition, most sediment samples were yellowish brown while the wet densities in all sediments were higher than 1gcm^{-3} and there were no significant differences between sediment samples. The sampling site 2 had revealed high level of Mn, Zn and Fe in the BCR extraction steps 1 to 3. The high level of metals was due to the mineral dissolution and it was the most contaminated location. The bioavailability of metals is related to the toxicity, mobility and speciation of metal species. Different species have different toxicities. The metals' distribution in the 3 step BCR extraction was used to determinate the electrostatic interaction, adsorption, precipitation and co- precipitation between the metal species and the sediment surfaces. The result showed Mn (0.821-

0.123%) has the most mobility in the environment. The most bioavailable metal was Fe (7837 - 15313 $mgkg^{-1}$) followed by As (68.1 - 3867 $mgkg^{-1}$) and Cu (344.3 - 684.0 $mgkg^{-1}$). These metals were hazardous to the environment (e.g. accumulation in organisms and plants). The bioavailable metals had an effect on Gunnislake, which is a town located downstream of the Tamar River.

Introduction

Heavy metal pollution is a serious environmental problem because of the persistent and non-biodegradable properties of the metals (Cuong *et al*. 2006). Their toxic effect on life in aquatic systems is made worse by their high enrichment factor and slow removal rate (Naji *et al*. 2010). Heavy metal has become a global problem with industrial development and intensive mining activity (Popovic *et al*., 2011).

Sediments are the main source of heavy metals in the marine environment and play an important role in the transport and storage of potentially hazardous metals (Cuong *et al*., 2006). When environmental conditions are changed (e.g. pH and redox potential) metals can remobilize from the sediment to aquatic systems (Gleyzes *et al*., 2010). Metal contamination will transform into more bioavailable or toxic forms (Hoi *et al*., 2006).

BCR sequential extraction is now a well-established method for the fractionation of heavy metal content in sediments (Nemati *et al*., 2009). The method has three steps which are: exchangeable fraction, reducible fraction and oxidizable fraction (Kartal *et al*., 2006). BCR sequential extraction can obtain information about potential toxicity, bioavailability and mobility of elements in the environment depending on the chemical association of the different components and speciation (Alonso Castillo *et al*., 2011). This process can offer a more realistic estimate of actual environmental impact (Morrison *et al*., 2006).

The Devon Great Consols has the highest concentration of heavy metal in sediment in southwestern England, with the intensive exploitation of metal ore deposits in Roman times (Palumbo-Roe *et al*., 2007). The BCR sequential extraction method was chosen to investigate the bioavailability of heavy metals in tailing run-off sediments in the Consols.

Literature Review

The importance of sediment analysis

The sediments in rivers and lakes play an important role in determining water quality and environmental conditions (Yi *et al*., 2008). Sediment is transported through gravity, flowing water, wind and moving ice (Uwumarongie- llori *et al*., 2011). Therefore, the historical record of chemical composition of suspended particles can be obtained through sediment analysis. Moreover, heavy metals are distributed throughout sediment components and associated with them in processes of ion exchange, adsorption, precipitation and complexation (Yuan *et al*., 2004). Furthermore, heavy metals may be accumulated in the sediment due to the interaction (e.g. adsorption and co- precipitation) between the trace metals and sediment matrix (Uwumarongie-llori *et al*., 2011). The accumulation of heavy metals in sediments causes a potential risk to human health because these elements transfer to aquatic media, are absorbed by plants, and enter the food chain (Alonso Castillo *et al*., 2011). The pollutants may be directly or indirectly toxic to the aquatic flora and fauna and may affect the bioaccumulation and bioconcentration in the food web (Yi *et al*., 2008). For example, some organisms may consume the toxic substances, then be eaten by mussels and fish and finally represent a potential hazard for people who consume them as food (Radojevic, 2006). Sediment analysis is widely used in environmental analysis and monitoring because lots of information can be obtained.

The reason for heavy metal investigation

There is a wide range of study areas in sediment analysis including nitrogen, phosphorous, sulfur, organic matter and heavy metals. In this project, heavy metals will be the focus of the sediment analysis. Some toxic metals are harmful to the ecosystem, the environment and human health. Heavy metal pollution is a serious environmental problem due to a number of reasons. First, metal may be dissolved and accumulated in the soils and sediments, causing potential risk to human health due to these elements in aquatic media (Alonso Castillo *et al*., 2011). When the metals are dissolved, metal will be absorbed by the roots together with water. Then, the plant may be damaged. Subsequently, the metals will be introduced into the food chain (Alonso Castillo *et al*., 2011). Second, metals are not the same as organic pollutants which can be broken down according to the reactivity. Heavy metals have persistent and non-biodegradable properties, they cannot be degraded (Yuen *et al*., 2004). Some

anthropogenic activities (e.g. mines, smelters and industrial activities) are the main sources of heavy metals (Radojevic, 2006). When heavy metals are discharged into the environment by soils and sediments, the environment will be polluted. Some heavy metals are toxic and harmful to humans and plants. It is necessary to determine the level of heavy metals in sediments. There are some analytical methods to determine the concentration of heavy metals (e.g. total digestion and Community Bureau of Reference (BCR) sequential extraction).

Tamar Great Consols

The Devon Great Consols Mine is on the east bank of the River Tamar in the Tavistock District in Devon, UK (Palumbo- Roe *et al*., 2007). It is a historical mine site which was one of the biggest producers of copper and arsenic during southwestern England's global dominance of the copper and arsenic mining industry in the 1800s (Palumbo- Roe *et al*., 2007). It produced over 70000t of arsenic between 1848 and 1909 (Palumbo- Roe *et al*., 2007).

The site was derived from the consolidation of five adjacent mines including Wheal Maria, Wheal Fanny, Wheal Anna- Maria, Wheal Josiah and Wheal Emma. The area of the mine site is nearly 3km long, up to 13m wide and at least 600m deep (Plymouth University, 2011) It worked on lodes mainly consisting of chalcopyrite, pyrite, arsenopyrite, cassiterite with quartz, fluorite and brecciated country rock cemented by chlorite or siderite (Palumbo- Roe *et al*., 2007). Mining activity ended in 1930. Devon Great Consols has the highest concentration of As and Cu in the Tamar catchment.

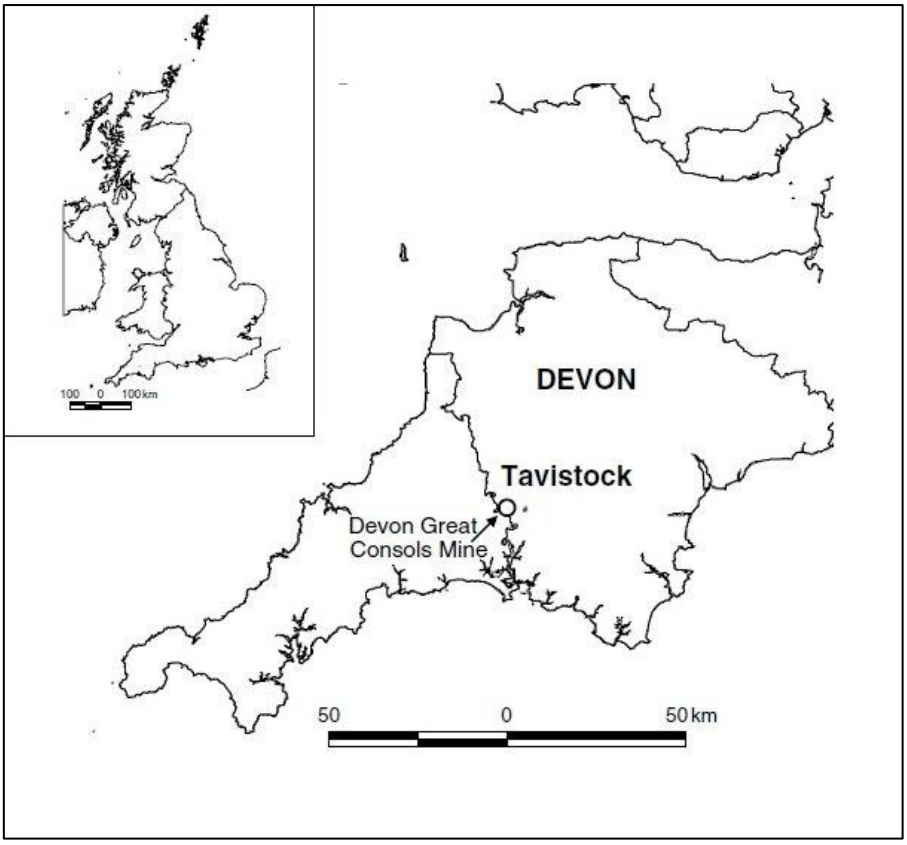

Figure 1: Location of Devon Great Consols Mine (Palumbo-Roe et al., 2007)

Water- sediment interaction

Sediment is a complex assemblage of mineral, biogenic and anthropogenic materials. It is derived from continental and coastal erosion, chemical and biological processes, the atmosphere and industrial activities (Turner *et al*., 2002). Its densities are significantly greater than water. Furthermore, it has a potential to generate successive cycles of deposition-resuspension which provide a crucial link for heavy metals between the aqueous phase, suspension and the bed (Turner *et al*., 2002).

The general structure of the sediment has an inert core where the primary and secondary silicates are surrounded by a more reactive coating which includes iron and manganese oxides, carbonates, sulphides and organic matter (Turner *et al*., 2002). The sediment is enveloped in a film of organic matter which can produce a net negative charge to the surface (Turner *et al*., 2002).

Heavy metals are distributed throughout sediment components and associated with them in different ways (e.g. ion exchange, adsorption, precipitation,

complexation, bound to carbonate phases, bound to Fe- Mn oxides, bound to organic matter and bound to sulfides) (Uwumarongie- llori *et al*., 2011). In sediment, Fe- Mn oxides strongly influence levels of metals due to their tendency to adsorb or co-precipitate them from water (Yuan *et al*., 2004). The association of metal ions with precipitated Fe- Mn oxides from exchangeable forms (loosely adsorbed), through moderately fixed (e.g. with amorphous oxides) to relatively strongly (e.g. occluded) bound in crystalline oxides. Organic matter is an efficient sorbent for hydrophobic organic compounds and divalent metal (Uwumarongie- llori *et al*., 2011).

Heavy metals accumulate in the sediment but are not permanently fixed. When the environmental conditions (e.g. pH, Eh or organic ligand concentration) change, the metals may cause mobilization from the sediment to the liquid phase and cause contamination of surrounding waters (Yuan *et al*., 2004)

Experiment method for heavy metal in sediments

Community Bureau of Reference (BCR) sequential extraction

Although the total concentrations of metals in sediments give valuable information on the overall pollution levels, many studies have also highlighted that measurement of total metal concentration is insufficient to estimate the environmental impact of contaminated sediments (Marin *et al*., 1997; Bacon *et al.*, 2008; Arain *et al*., 2009). Over the last decade, more studies have been undertaken to determine metal species from the speciation of potential toxic elements, bioavailability and mobility dependence on the chemical association of the different components of the sediment sample (Alonso Castillo *et al.*, 2011).

The Community Bureau of Reference (BCR) develops a standardized and harmonized three step sequential extraction for metals in sediment samples. The BCR fractionates the metals into target phases which include exchangeable and bound to carbonate (step 1), reducible which binds to Fe-Mn oxides (step 2) and oxidizable which binds to organic matter and sulphides (step 3) (Kartal *et al*., 2006).

The importance and advantage of BCR extraction method

BCR extraction methods can provide information such as the identification of the main binding sites and strength of metals binding to the particulates and

phases associated with heavy metals in sediment (Yuan *et al.*, 2004). This method can help us to understand the geochemical processes related to heavy metal mobilization and environmental contamination risk (Margui *et al*., 2004).

The advantages of the BCR method are that it can determine the amount of total metal content available for plants or accessible to the environment (Alonso Castillo *et al*., 2011). This is because only a fraction of the metals present in sediments are mobilized and bioavailable (Vasile *et al*., 2008). Moreover, this method is necessary to distinguish and quantify the different forms of metals in sediments in order to predict the mobility, bioavailability, and potential toxicity of metals (Fan *et al.*, 2002). Furthermore, there are reference materials available for the BCR method (e.g. BCR 701) which enables quality control on the measurements of the method (Vieira *et al*., 2009).

Bioavailability

Bioavailability is a specific route of exposure (e.g. oral, inhalation and dermal in the case of humans, and oral, gill and dermal in the case of fish). Oral bioavailability varies with oxidation state, speciation and mineralogy (Langmuir *et al*., 2004). Inhalation bioavailability is strongly dependent on solubility and particle size (Langmuir *et al*., 2004). The bioavailable fraction of metals includes metal species that are environmentally available and have potential to be adsorbed and desorbed by an organism. The route of exposure to an aquatic organism includes uptake from pore water and water above the sediment- water interface, also across body walls and respiratory surfaces as well as ingestion of sediment particles and other food sources (Lopez *et al.*, 2010). Uptake of metals by organisms or bioaccumulation is important for determining concentration, sorption, oxidation state, speciation, and complexation of heavy metals (Langmuir *et al*., 2004).

Mobility

Mobility determines the ability of a metal to be sorbed onto substrate. It is affected by, for example, metal complexes and pH.

The importance of metal complexes

Complexes incorporated in metals play an important role in controlling the availability and fate of metals in the environment. Metal complexing has a direct influence on metal adsorption to organic matter (Langmuir, 1997). Increased fractions of metal complexes increases the solubility and mobility of

metals. For example, metal carbonate, sulfate and fluoride complexes are usually poorly adsorbed while metal hydroxide complexes are strongly adsorbed (Langmuir, 1997).

The stability of metal complexes and toxicity is related to the strength of metal complexing. When the interaction between metal and ligand are week, the influences of metal toxicity become significant (Langmuir *et al*., 2004).

The important of pH

The solubility of metals is strongly pH dependent. When the pH increases, the solubility will increase for most of the metals. For a few metals e.g. Zn(II) and Fe(III)), metal solubility increases again at alkaline pH values (Langmuir *et al*., 2004).

Tyler *et al*., (2001a, 2001b) indicated that when the pH increased, the concentration of Cr and As increased while Fe and Mn concentration decreased. The pH effect on Cu was difficult to define. Moreover, increase in pH will lead to an increase in desorption of anionic elements (e.g. As, Cr). Furthermore, it will lead to an increase in adsorption and precipitation of Fe-Mn oxides.

Toxicity

Toxicity depends on both the oxidation state, form of metal (e.g. cation or anion) and its tendency to form complexes with ligands.

The speciation of metal

Speciation is the distribution of an element among its possible chemical forms, and metal complexes. It has different tendencies to be adsorbed or desorbed and has different effects on the level of toxicity in life. For example, the toxicity of As(III) is significantly different from the As(V) in aquatic life. Moreover, Cr(VI) can cause inhalation of carcinogen within human while Cr(III) has a lower toxicity (Langmuir *et al.*, 2004).

Pourbaix diagram (Eh-pH diagram)

A Pourbaix diagram (Eh-pH diagram) allows a graphical representation of the simultaneous influences of pH and redox potential on metal speciation (Langmuir *et al*., 2004). The diagram can be read as a standard phase diagram with a different set of axes. But like phase diagrams, they do not

involve reaction rates or kinetic effects (Absolute Astronomy, 2011). The diagrams are labeled with two axes. The vertical axis is labeled Eh (V) with respect to the standard hydrogen electrode as calculated by the Nernst equation (equation 1) (Absolute Astronomy, 2011). Temperature and concentration of solvated ions in solution will shift the equilibrium lines in accordance with the Nernst equation.

$$Eh = E^0 - \frac{0.0592}{n} \log \frac{[C]^c[D]^d}{[A]^a[B]^b}$$ Equation 1

The horizontal axis is labeled pH for the –log function of the H^+ ion concentration (Equation 2).

$$pH = -\log[H^+]$$ Equation 2

The diagrams can be drawn for any chemical system. It is important to note that the addition of a ligand will often modify the diagram. For instance, sulfides have a great effect on the diagram for most elements as metal sulfides are extremely insoluble, which reduces the metal concentrations if precipitated (Langmuir *et al*., 2004).

Instrumental Analysis

Inductively coupled plasma atomic emission spectrometry (ICP-AES)

ICP-AES is widely used for the quantitative analysis of metals. Also it can perform multi- element analysis and recording simultaneously with a limit of detection of mgL^{-1} level (Skoog *et al*., 2007), and analytical measurement of emitted visible or UV radiation. ICP-AES greatly reduces chemical interference due to the high temperature of plasma, which leads to multiplicity of intense emission lines in the spectrum (Fifield *et al*., 2000). As a result, the emission intensity retains a linear relationship with the analyte concentration over a wide range e.g. 10^{-3} to 20^2 mg dm^{-3} (Fifield *et al*., 2000). Furthermore, the determination time of ICP-AES is less than a minute.

Plate 1: Photograph of ICP-AES used in the project

Inductively coupled plasma atomic mass spectrometry (ICP-MS)

ICP-MS can be used for quantitative and semi- quantitative analysis. It is widely used in multi element analysis with a dynamic linear range of six orders of magnitude and low detection limits (Fifield *et al*., 2000). Moreover, the analytical signal is only dependent on the mass/charge ratio and the number of ions with a particular ratio as a comprehensive technique for all elements (Fifield *et al*., 2000). The ability to determine isotopic ratios on multiple or single elements at ultra- low levels of concentration (e.g. 0.1µg dm^{-3}) with 0.2-1% RSD (Fifield *et al*., 2000) means that ICP-MS is one of the most sensitive techniques available for elemental analysis.

Plate 2: Photograph of ICP-MS used in this project

Experimental

Site description

Devon Great Consols is located to the east of the Tamar River. The site is located within the Cornish Mining World Heritage Site and includes two County Geological Sites (Wheal Anna Maria CGS and Rementor Mine CGS) and the Devon Great Consols Site of Special Scientific Interest (SSSI) (Educational Register of Geological Sites, 2008).

The site is the largest mine in Devon and is the highest producer of copper and arsenic in Devon and Cornwall (Educational Register of Geological Sites, 2008). In the 19th century, the mines produced 740,000 tons of copper ore and 72,000 tons of refined arsenic which was the highest production in the world (Spiers, 2011). Despite extensive reprocessing of the dumps of the Devon Great Consols complex, significant areas of geological material remain. Traces of mineralization are locally present in mine dumps amongst tailings from ore processing, including evidence of both copper and arsenic mineralization in the Wheal Anna Maria CGS (Educational Register of Geological Sites, 2008).

Now, potentially dangerous buildings also remain as well as arsenic contamination (Educational Register of Geological Sites, 2008).The mining

activity resulted in the release of arsenic remains and other heavy metals which contaminated the environment and was eventually introduced to the Tamar River. The distance between the Devon Great Consols and Gunnislake is just within 2 km (Google map, 2012). The chemical changes in the environment from the past might be revealed by analysis of the Devon Great Consols sediment.

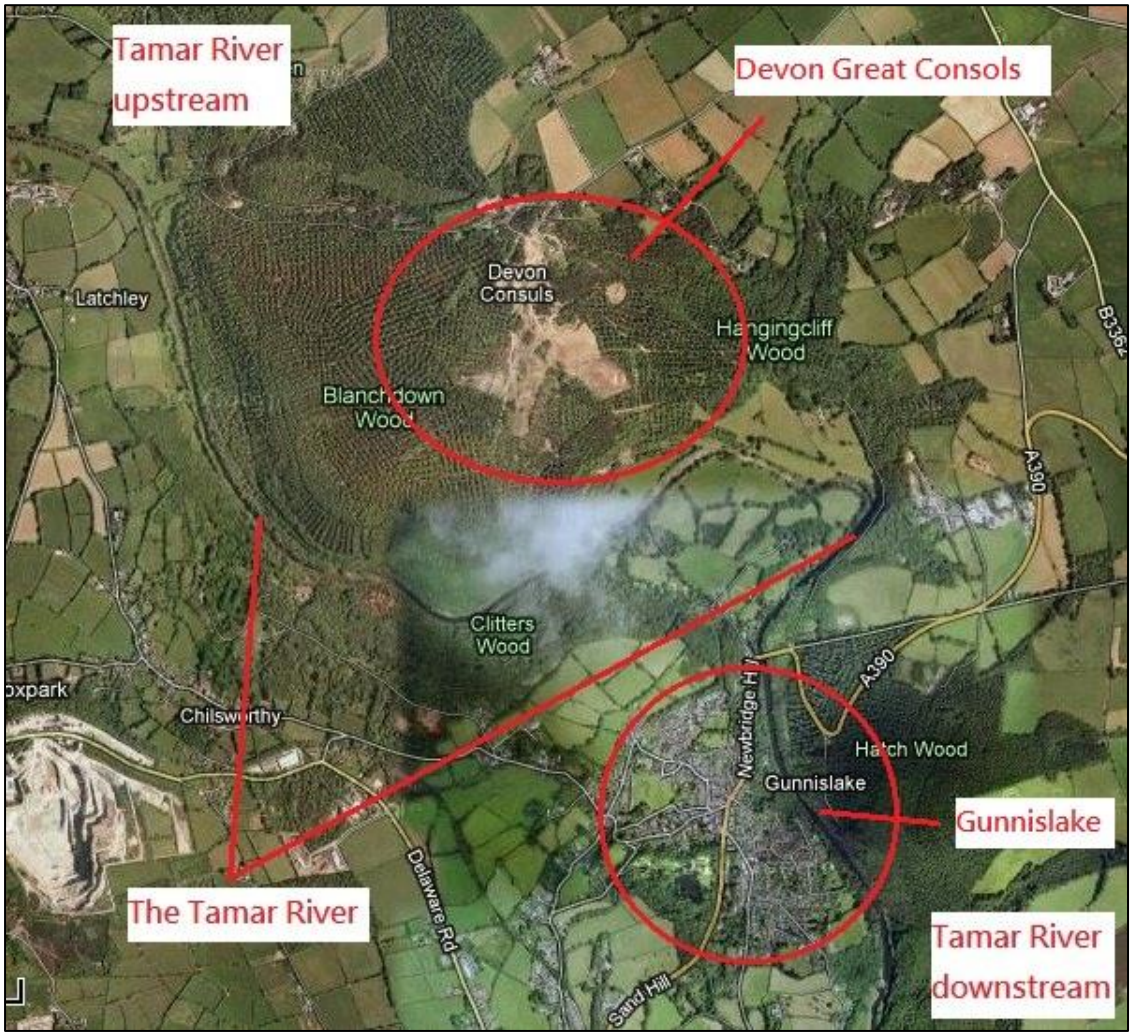

Figure 2: The location of Devon Great Consols and Gunnislake (Google map, 2011)

In this investigation, 8 sites (Figure 5) were chosen as sampling points from the Devon Great Consols. All the sampling sites are from the tailing waste run-off stream. The sampling sites 6, 7 and 8 were in the higher location, while sampling sites 2, 3, 4 and 5 were in the lower location. Sampling site 1 was away from other sites, comparatively. Sampling site 3 was without any water, because there was no water run through the run- off stream on that day.

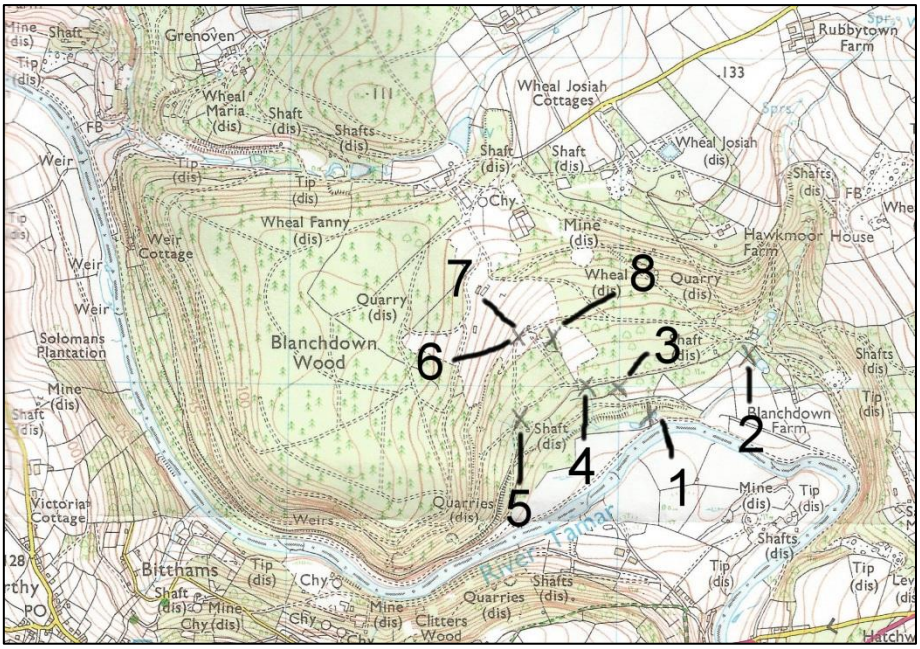

Figure 3: The location of 8 sampling sites in Devon Great Consols (Ordnance Survey)

Table 1: The grid references of eight sampling sites

Sampling site	Grid references
Site 1	431729
Site 2	434731
Site 3	430730
Site 4	429730
Site 5	427729
Site 6	427732 (A)
Site 7	427732 (B)
Site 8	428732

Plate 3: The photograph of Site 1

Plate 4: The photograph of Site 2

Plate 5: The photograph of Site 3

Plate 6: The photograph of Site 4

Plate 7: The photograph of Site 5

Plate 8: The photograph of Site 6

Plate 9: The photograph of Site 7

Plate 10: The photograph of Site 8

Field methodology

Sediment samples were collected at 8 sites from the tailings waste run- off streams of the Devon Great Consols area on 1st November 2011. All the samples were collected using a clean trowel. About 1 kg of sediment in each sampling site was placed in a polyethylene plastic bag and labeled. Then samples were kept in an ice box and frozen prior to analysis. In addition, field data was then measured, including percentage of dissolved oxygen, concentration of dissolved oxygen, water temperature, specific electrical conductivity, salinity, pH and redox potential. This information can be used to reflect the natural condition of the sediments at the time of sampling (Wilde *et al*., 2005).

Sample preparation procedure

Sample sieving

The samples were defrosted and air-dried at 30 ± 2℃ overnight. Then, the sample sediments were sieved with sizes of less than 250μm, between 250μm and 2mm size, and larger than 2mm, using 2mm and 63μm sieves. After sieving, different sizes of samples were centrifuged at 3000 r.p.m. for 5 minutes and the liquid phase was decanted. After that, the samples were dried in an oven at 105 ± 2℃ overnight to obtain a constant weight as this could remove the interstitial water. Too high a temperature might cause the loss of some volatile components and partially destroy the structure of some clay minerals (Loring *et al*., 1992).

Sediment colour

The Munsell Notation was used for the symbols of hue, value and chroma in the format of {hue} {value}/ {chroma}. The symbol for hue is R (red), TR (yellow-red) or Y (yellow) and was preceded by number from 0 to 10. The symbol for value consists of numbers from 0 (absolute) to 10 (absolute white) and the symbol for chroma consists of numbers from 0 (neutral grays) to 20 (equal intervals). Samples of wet sediments were placed on a piece of white paper and the colour chart which corresponds to the correct hue was selected. Then, the samples were held behind the apertures that separated the closest matching colour chips.

Wet density

The clean 5.02 cm^3 phial was taved and was then filled with wet sediments carefully. All air bubbles were removed by tapping the base of the phial on a firm surface and the surfaces of the sediments were smoothed to level of the top edge of the phial. Then, the phial was re-weighed and the weight of the sediments was divided by 5.02cm^3 to determine the wet density.

Weight of the sediment (g) / 5.02 (cm^3) = wet density (g cm^{-3}) Equation 3

Reagents and standards

Reagent for BCR sequential extraction

- Glacial Acetic Acid (Analytical Grade) (Fisher Scientific)
- Hydroxylammonium Chloride (Analytical Grade) (Fisher Scientific)
- 30% Hydrogen Peroxide (Analytical Grade) (Fisher Scientific)
- Ammonium Acetate (Analytical Grade) (Fisher Scientific)

Solution preparation for BCR sequential extraction

Solution A *(acetic acid, 0.11molL^{-1})*

25± 0.2ml of glacial acetic acid was added to about 500ml water in a 1000ml polyethylene volumetric flask and made up to exactly 1000ml with Milli-Q water to prepare a 0.43molL^{-1} acetic acid. 250ml of this solution was diluted to 1000ml with Milli-Q water to obtain an acetic acid solution of 0.11mol L^{-1}.

Solution B *(hydroxylammonium chloride, 0.5molL^{-1})*

34.75g of hydroxylammonium chloride was dissolved in 400ml with Milli-Q water and then the solution was transferred into a 1 L calibrated flask. Then, 25ml of 2molL^{-1} HNO_3 was pipetted using a calibrated pipette to the flask and made up to volume with Milli-Q water. This solution was prepared on the same day the extraction was carried out.

Solution C *(ammonium acetate, 1.0molL^{-1})*

77.08g of ammonium acetic was dissolved in 900ml distilled water. Then the pH was adjusted to 2.0± 0.1 with concentrated HNO_3. Finally it was made up to 1L with Milli-Q water.

Stock standard solution for instrumental analysis

For ICP-AES and ICPMS quantitative analysis:

- Chromium stock solution 10000mgL^{-1} (Prod: 455234Q)
- Copper stock solution 10000mgL^{-1} (Fisher Scientific)
- Nickel stock solution 10000mgL^{-1} (Fisher Scientific)
- Lead stock solution 10000mgL^{-1} (Fisher Scientific)
- Zinc stock solution 10000mgL^{-1} (Fisher Scientific)
- Cadmium stock solution 10000mgL^{-1} (Fisher Scientific)
- Arsenic stock solution 10000mgL^{-1} (Fisher Scientific)

- Manganese stock solution 10000mgL^{-1} (Fisher Scientific)
- Iron stock solution 10000mgL^{-1} (Fisher Scientific)

For ICP-MS semi- quantitative:

- Quality Control Standard 26 100µgmL^{-1} (P/N 4400-013)

Procedure for the BCR sequential extraction

Step 1 ***(Water and acid-soluble fraction, exchangeable and bound to carbonates)***

1.0g of sediment was weighed accurately and 40 ml of solution A was added in a 100ml centrifuge tube. The covers were capped on the tube and extraction was performed by shaking with a mechanical linear shaker (Tecam® Shaking Bath 5B-16) for 16 hours at 22±5℃ overnight. No delay occurred between the addition of the extractant solution and the beginning of the shaking. After 16 hours, the extract was separate from the solid residue by centrifugation at 3000r.p.m. for 20 min and the supernatant liquid was decanted into a polyethylene container and stored in a refrigerator at about 4℃prior to further analysis. Then, the residue was washed by adding 20 ml of milli-Q water and shaken for 15 min on the linear shaker and centrifuged for 20 min at 3000r.p.m. The supernatant liquid was decanted and discarded where there was no solid residue (Rauret *et al*., 1999).

Step 2 ***(Reducible fraction, bound to Fe and Mn oxides)***

40 ml of freshly prepared solution B was added to the residue from step1 in the centrifuge tube. Extraction was performed by shaking with mechanical linear shaker (Tecam® Shaking Bath 5B-16) for 16 hours at 22±5℃ overnight. No delay occurred between the addition of the extractant solution and the beginning of the shaking. The extract was separated from the solid residue by centrifugation and decantation as in step 1. The extract was retained in a stoppered polyethylene container and stored in a refrigerator at about 4℃ prior to further analysis. Then, the residue was washed by adding 20 ml of milli-Q water and shaken for 15 min on the linear shaker and centrifuged for 20 min at 3000r.p.m.. The supernatant was decanted where there was no solid residue (Rauret *et al*., 1999).

Step 3 *(Oxidizable fraction, bound to organic matter and sulfides)*

10 ml of 30% hydrogen peroxide was added to the residue in the centrifuge tube in small aliquots to avoid loss due to possible violent reaction. The vessel was covered loosely with its cap and digested at room temperature for 1 hour at 85±2℃ in a water bath. Then, the volume was reduced to less than 3 ml by further heating of the uncovered tube. A further aliquot of 10 ml of 30% hydrogen peroxide was added to the tube and the uncovered vessel was heated again at 85±2℃ and digested for 1 hour. The cover was removed and the volume of liquid was reduced to about 1 ml. Then, 50 ml of solution D was added to the cool moist residue. Extraction was performed by shaking with a mechanical linear shaker (Tecam® Shaking Bath 5B-16) for 16 hours at 22±5 ℃ overnight. No delay occurred between the addition of the extractant solution and the beginning of the shaking. The extract was separated from the solid residue by centrifugation and decantation as in step 1. The extract was retained in a stoppered polyethylene container and stored in a refrigerator at about 4℃ prior to further analysis (Rauret *et al*., 1999)

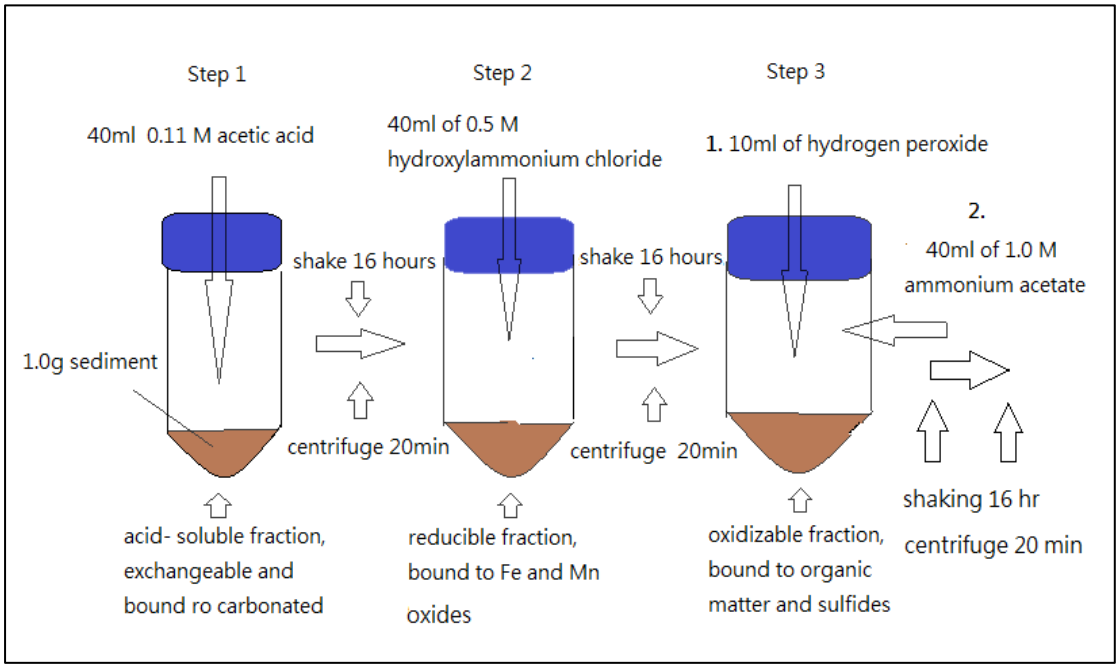

Figure 4: Picture of BCR extraction procedure (step 1 to 3)

Determination of heavy metal in CRMs

Certified Reference Materials (CRM) are reference materials which are accompanied by a certificate. CRMs can be either pure materials or matrix materials. Matrix materials are used for the validation of the whole method from sample preparation to the final analysis and have a certified reference value to compare the accuracy of the measurement (Filield *et al*., 2000). In this investigation, CRM BCR 701 was used to validate the BCR sequential extraction method. The extraction procedure was as per previous, but 0.25g of sample was used rather than 1.0g. The certificate of CRM BCR701 is shown in the Appendixes.

Instrumentation

Inductively coupled plasma atomic emission spectrometry (ICP-AES)

Instrument:

Varian 725-ES ICP Optical Emission Spectrometer

ICP-AES Condition:

Power (kW): 1.40
Plasma Flow (L/min): 15.0
Auxiliary Flow (L/min): 1.50
Nebulizer Flow (L/min): 0.68
Viewing Height (mm): 8
Replicate read time (s): 4.00
Instr stabilization delay (s): 10

Inductively coupled plasma mass spectrometry (ICP-MS)

Instrument:

Thermo Scientific ICP-MS XSERIES 2

ICP-MS Condition:

Forward Power (kW): 1.40
Horizontal: 68
Vertical: 566
Auxiliary Flow (L/min): 0.7
Nebulizer Flow (L/min): 0.78
Acquisition Tine (s): 5

Sweeps: 50
Dwell (ms): 10.0

Calibration standard preparation

CRM analysis

For ICP-AES:

For NI, Cr, Pb, Cd, Zn, Cu multi element standard

An intermediate standard with concentration of 10mgL^{-1} was prepared by pipetting 100.0µL of the stock solutions to a 100.0ml volumetric flask, then 0.5mL, 2.0mL and 5.0ml of the intermediate standard in the 100.0 mL volumetric flask were pipetted to three 100.0 mL volumetric flasks and made up to mark with 2 % nitric acid respectively.

For ICP-MS:

For NI, Cr, Pb, Cd, Zn, Cu multi element standard

An intermediate standard with concentration of 10mgL^{-1} was prepared in the previous ICP-AES analysis, then 5.0µL, 100.0µL, 1.0mL and 5.0mL of the intermediate standard in the 100.0 mL volumetric flask were pipetted to four 100.0 mL volumetric flasks and made up to mark with 2 % nitric acid respectively.

Overall working standard series:

Table 2: Calibration standard of each multi elements standards for ICP-AES for CRM samples in step1 to step 3

CRM sample for step 1 to step 3						
Standard solution	Concentration of each metal (mg/L)					
	Cr	Cu	Ni	Pb	Zn	Cd
1	0	0	0	0	0	0
2	0.1	0.1	0.1	0.1	0.1	0.1
3	0.4	0.4	0.4	0.4	0.4	0.4
4	1	1	1	1	1	1

Table 3: Calibration standard of each multi elements standards for ICP-MS for CRM samples in step1 to step 3

CRM sample for step 1 to step 3						
Standard solution	Concentration of each metal (µg/L)					
	Cr	Cu	Ni	Pb	Zn	Cd
1	0	0	0	0	0	0
2	0.5	0.5	0.5	0.5	0.5	0.5
3	10	10	10	10	10	10
4	100	100	100	100	100	100
5	500	500	500	500	500	500

Semi-quantitative analysis

For ICP-MS:

For all metal multi element standard:

50.0µL of the quality control standard with concentration of 100µgL^{-1} was pipetted to 50.0 mL volumetric flask. Then 50.0µL of internal standard was added and made up to mark with 2 % nitric acid respectively.

Sediment sample standard

For ICP-AES:

For Ni, Cr, Pb, Zn, Cu, Mn multi element standard

An intermediate standard with concentration of 100mgL^{-1} was prepared by pipetting 1.0 mL of the stock solutions to a 100.0ml volumetric flask, then 250.0µL, 500.0µL and 2.0ml of the intermediate standard in the 100.0 mL volumetric flask were pipetted to three 50.0 mL volumetric flasks and was made up to mark with 2 % nitric acid respectively.

For As multi element standard

25.0µL, 50.0µL and 200.0µL of the stock standard with concentration of 10000 mgL^{-1} were pipetted to those 50.0 ml volumetric flasks and made up to mark with 2 % nitric acid respectively.

For Fe multi element standard

250.0µL, 500.0µL and 2.0ml of the stock standard with concentration of 10000 mgL^{-1} were pipetted to those 50.0 ml volumetric flasks and made up to mark with 2 % nitric acid respectively.

For ICP-MS:

For Pb working standard

250.0µL, 500.0µL and 2.0ml of the standards which prepared from ICP-AES were pipetted to three 50.0 ml volumetric flasks, then 50.0µL of internal standard was added to both and made up to mark with 2 % nitric acid respectively.

For Cd working standard

0.50ml and 10.0ml of the working standard which prepared in semi quantitative analysis were pipetted to two 50.0 mL volumetric flasks. Then 50.0µL of internal standard was added to and made up to mark with 2 % nitric acid respectively.

Blank solution

All 50mL blank solutions were prepared by adding 50.0µL of internal standard and make up with 2% nitric acid.

Overall working standard series

Table 4: Calibration standard of each multi elements standards for sediment samples in step1

Sediment sample for step 1									
Standard solution	Concentration of each metal (mg/L)								
	Cr	Cu	Ni	Pb	Zn	Cd	As	Mn	Fe
1	0	0	0	0	0	0	0	0	0
2	0.5	0.5	0.5	0.005	0.5	0.001	5.0	0.5	50
3	1.0	1.0	1.0	0.01	1.0	0.02	10.0	1.0	100
4	4.0	4.0	4.0	0.04	4.0	0.1	40	4.0	400

Table 5: Calibration standard of each multi elements standards for sediment samples in step 2

Sediment sample for step 2									
Standard solution	Concentration of each metal (mg/L)								
	Cr	Cu	Ni	Pb	Zn	Cd	As	Mn	Fe
1	0	0	0	0	0	0	0	0	0
2	0.5	0.5	0.5	0.5	0.5	0.001	5.0	0.5	50
3	1.0	1.0	1.0	1.0	1.0	0.02	10	1.0	100
4	4.0	4.0	4.0	4.0	4.0	0.1	40	4.0	400

Table 6: Calibration standard of each multi elements standards for sediment samples in step 3

Sediment sample for step 3									
Standard solution	Concentration of each metal (mg/L)								
	Cr	Cu	Ni	Pb	Zn	Cd	As	Mn	Fe
1	0	0	0	0	0	0	0	0	0
2	0.5	0.5	0.5	0.005	0.5	0.001	5.0	0.5	50
3	1.0	1.0	1.0	0.01	1.0	0.02	10	1.0	100
4	4.0	4.0	4.0	0.04	4.0	0.1	40	4.0	400

Data analysis

Calibration and standardization

Calibration and standardization processes are very important in all analytical procedures. Calibration determines the relationship between the analyte concentration and the analytical response (Skoog *et al*., 2007). The least squares method was used in the experiment. The linear curve equation shows the relationship between the analyte concentration (X) and the measured response (y) (Skoog *et al.,* 2007).

The equation is represented as

$$y=mx+c \qquad \text{Equation 4}$$

Where y is the analytical response, x is the analytical concentration, m is the slope of the curve; c is the y- intercept.

Limit of detection (LOD)

Limit of detection (LOD) is the lowest concentration of analyte that can be detected at a known confidence level (e.g. 68%, 95% and 99.7 confidence level) (Skoog *et al.,* 2007). Furthermore, LOD is the power of detection of any method of analysis. The LOD is derived from the smallest measured y which can be accepted with confidence and not suspected to be an accidentally high value. The value of LOD at 99.7 % confidence level is given by

$$y_{LOD} = Y_B + 3S_B \qquad \text{Equation 5}$$

Where Y_B is the sample blank mean, $3S_B$ is the sample blank standard deviation.

T-Test

The t- test is a statistical and significance test used to compare mean values and certified values. The two tailed test was used in the experiment. From the experimental data, the t value can be calculated in equation 6 and compared with the table of t distribution. The t distribution table includes different confidence intervals against degrees of freedom (DF). Then, the critical t value (95% confidence level) can be compared with the (n-1) DF and the calculated t value obtained. If the $t_{calculated} > t_{crit}$, the concentration of the metal, there would be significance difference between the true values, therefore it should be rejected (Skoog *et al*., 2007).

$$t = \frac{\overline{x} - \mu_0}{s/\sqrt{n}}, \qquad \text{Equation 6}$$

Where S was the sample standard deviation, n is the number of items,

$\overline{x}$ was the sample mean and μ_0 was true value.

F- Test

The f- test is a significance test used to compare the standard deviation of the sample results for the data of two methods in order to determine whether the data comes from the same parent distribution. The variance is the square of

the standard deviation. The ratio of the variance is the calculated F value which can be used to compare the critical F value. The F- ratio has been rearranged to F>1 with one-side test at 97.5% confidence level. The critical F value can be found from the F- Test table using (n_1-1) and (n_2-1) DF. If the F_{crit} > $F_{calculated}$ we can conclude that the standard deviations in the data of the two methods are not significantly different from each other and it is reasonable to combine the standard deviations of each method (Bialkowski, 2004).

$$F = \frac{s_1^2}{s_2^2}$$

Equation 7

$$s_p^2 = \frac{\sum_{i=1}^{k}((n_i - 1)s_i^2)}{\sum_{i=1}^{k}(n_i - 1)}$$

Equation 8

Where S_1 and S_2 are the sample standard deviation, n is the number of items, S_p is the pooled standard deviation

The pooled standard deviation is used to calculate the t-value which combines the sample means of the two methods. Finally, the two- side value of t_{crit} at 95% confidence level for (n_1 +n_2-2) DF is compared with the calculated t value. If t calculated > t_{crit}, the two methods will have significance difference and can then be rejected (Bialkowski, 2004).

$$t = \frac{\bar{X}_1 - \bar{X}_2}{S_{X_1X_2} \cdot \sqrt{\frac{2}{n}}}$$

Equation 9

Where S_{X1X2} is the pooled standard deviation

Recovery

The recovery is the factor of the mean concentration and the true concentration that is obtained in a method.

Recovery (%) = (mean concentration/ true concentration) x100 Equation 10

Results and Discussion

CRM analysis

Analytical figures of merit

The gradient, intercept and R^2 of ICP-AES for the BCR extraction and determination of CRM are shown in table 7. Also, the calibration data of ICP-MS is shown in table 8. Equation 4 was used to calculate the concentration of selected metal in sample.

Table 7: Calibration Graph information for determination of BCR extraction for CRM by ICP-AES

Date	Wave Length(nm)	Element	Gradient (m, eql)	Intercept (c, eql)	R^2
5th Dec 11	267.7	Cr	3694.4	12.422	1
	231.6	Ni	282.9	0.5247	1
	327.4	Cu	5876	33.336	1
	213.9	Zn	2735.1	20.044	1
	214.4	Cd	1328.9	2.037	1
	220.4	Pb	113.11	4.8099	0.999

Table 8: Calibration Graph information for determination of BCR extraction for CRM by ICP-MS

Date	Atomic mass	Element	Gradient (m, eql)	Intercept (c, eql)	R^2
8th Dec 11	52	Cr	3121.7	3639.9	0.999
	60	Ni	1250.8	2374.5	1
	65	Cu	1898.3	5547.9	0.999
	66	Zn	891.2	5040.5	0.999
	111	Cd	1893.7	858	0.999
	208	Pb	24335.3	15535.2	0.999

In ICP-AES and ICP-MS measurements, the value of R^2 of each element calibration curve for each element was approximately 0.999 to 1. It revealed that the calibration curves worked in linear portion and the least squares method could be applied to calibration (Skoog *et al*., 2007).

Concentration of CRM analysis

CRM analysis for ICP-AES

The certificate, experimental concentration and recovery of the 6 elements using the BCR extraction method (step 1 to 3) by ICP-AES are shown in table 9, 10 and 11 respectively. The experimental concentrations were used to calculate the recovery of the metal. The calculated concentration of metal by equation 4 and calculated recovery by equation 10 was shown previously.

Step 1 in ICP-AES

In step 1, some of the recoveries of metals were below 120% except Cu and Pb. This could suggest that the instrumental analysis of the extraction was accurate. The recovery of Cu and Pb were 125% and 223% respectively. The high recovery might due to contamination of metal presented in the CRM samples, thus leading to an increase in the concentration of metals.

Table 9: The certified value, experiment value, recovery of six elements using BCR extraction method of BCR sample for step 1 by ICP-AES

Step	Metal	Certified Value (mg/kg) ± 2SD	Experiment Value (mg/kg) ± 2SD	Recovery (%)
1	Cr	2.26 ± 0.16	2.36 ± 0.82	105
	Ni	15.4 ± 0.9	16.58 ± 2.74	108
	Cu	49.3 ± 1.7	61.44 ± 11.76	125
	Zn	205 ± 6	224.48 ± 19.82	110
	Cd	7.34 ± 0.35	8.50 ± 0.68	116
	Pb	3.18 ± 0.21	7.09 ± 4.42	223

Step 2 in ICP-AES

In step 2, most of the recoveries of the metals were higher than 80% except Zn. It suggests that the metals in step 2 were accurate. On the other hand, Zn had 76% recovery; this was caused by the use of a different concentration or volume of solution B. Moreover, the low recovery could also be due to the analyte loss during analysis.

Table 10: The certified value, experiment value, recovery of six elements using BCR extraction method of BCR sample for step 2 by ICP-AES

Step	Metal	Certified Value (mg/kg) ± 2SD	Experiment Value (mg/kg) ± 2SD	Recovery (%)
2	Cr	45.7 ± 2.0	37.38 ± 1.13	82
	Ni	26.6 ± 1.3	22.08 ± 1.71	83
	Cu	124 ± 3	99.81 ± 9.08	80
	Zn	114 ± 5	87.1 ± 12.74	76
	Cd	3.77 ± 0.28	3.03 ± 0.49	80
	Pb	126 ± 3	110 ± 9.87	83

Step 3 in ICP-AES

In step 3, the recoveries of all metals were below 70%. The result was inaccurate. The low recovery could be explained by too small a CRM sample used in the experiment. The BCR certificate stated that the minimum mass of CRM sample used should be 1.0 g. However, only 0.25 g was used in the experiment. Moreover, matrix effects and spectroscopic interference might present during analysis. This led to dramatic decreases in recovery of each metal. In addition, the ICP-AES could not determine the level of Cd. It was estimated that the concentration of Cd was close to the detection limit. Moreover, the poor recovery could be explained by the washing of sediments with water between two extraction steps. It was likely that the sample washed with water between the two extractions, which was discarded after extraction, caused the low recovery of all metals in the experiment as the water could contain a significant amount of metals (Cappuyns *et al*., 2007).

Table 11: The certified value, experiment value, recovery of six elements using BCR extraction method of BCR sample for step 3 by ICP-AES

Step	Metal	Certified Value (mg/kg) ± 2SD	Experiment Value (mg/kg) ± 2SD	Recovery (%)
3	Cr	143 ± 7	78.7 ± 18.3	55
	Ni	15.3 ± 0.9	10.32 ± 1.95	67
	Cu	55.2 ± 4.0	23.9 ± 1.79	43
	Zn	45.7 ± 4.0	22.9 ± 2.27	50
	Cd	0.27 ± 0.06	0	0
	Pb	9.3 ± 2.0	0.190 ± 0.368	2

CRM analysis for ICP-MS

The certificate, experimental concentration and recovery of the 6 elements by the BCR extraction method (step 1 to 3) by ICP-MS are shown in table 12, 13 and 14 respectively.

Step 1 in ICP-MS

In step 1, only the recovery of Ni was below 120%. The recovery of other metals was quite high. It could explain that contamination of metals presented in the CRM sample. It thus led to high concentration of metals in step 1.

Table 12: The certified value, experiment value and recovery of six elements using BCR extraction method of BCR sample for step 1 by ICP-MS

Step	Metal	Certified Value (mg/kg) ± 2SD	Experiment Value (mg/kg) ± 2SD	Recovery (%)
1	Cr	2.26 ± 0.16	2.93 ± 0.7	129
	Ni	15.4 ± 0.9	17.4 ± 2.47	113
	Cu	49.3 ± 1.7	75.02 ± 14.23	152
	Zn	205 ± 6	261 ± 36.21	127
	Cd	7.34 ± 0.35	9.72 ± 1.33	132
	Pb	3.18 ± 0.21	6.94 ± 1.17	218

Step 2 in ICP-MS

In step 2, the recoveries of some metals were higher than 80%. This shows that the result was inaccurate. On the contrary, the recoveries of Zn and Cd were only 77% and 73%. This might be caused by using a different concentration or volume of solution B. Moreover, there might be analyte loss during the analysis. For these reasons, the recoveries of Zn and Cd could decrease slightly compared to other metals.

Table 13: The certified value, experiment value and recovery of six elements using BCR extraction method of BCR sample for step 2 by ICP-MS

Step	Metal	Certified Value (mg/kg) ± 2SD	Experiment Value (mg/kg) ± 2SD	Recovery (%)
2	Cr	45.7 ± 2.0	38.05 ± 1.54	83
	Ni	26.6 ± 1.3	22 ± 1.97	83
	Cu	124 ± 3	112 ± 13.2	91
	Zn	114 ± 5	88.03 ± 14.03	77
	Cd	3.77 ± 0.28	2.74 ± 0.6	73
	Pb	126 ± 3	112 ± 2.83	89

Step 3 in ICP-MS

In step 3, all the recovery results were lower than 60% except Zn. This means that the result was inaccurate in step 3. This might be caused by the low amount of sediment (e.g. 0.25g) used in the experiment, or incorrect concentration or volume of reagent added. Such an incorrect method could cause a dramatic decrease in the recovery. In addition, the matrix effects and spectroscopic interference of the ICP-MS might significantly decrease the recoveries of the metals. Although ICP-MS could determine the level of Cd, the recovery of Cd was lower than 50%. It was estimated that the concentration of Cd was close to the detection limit. In addition, the poor recovery could be explained by the washing with water between the two extraction steps. It was likely that the sample washing with water between two extractions, which was discarded after extraction, led to extremely low recovery for all metals as the water could contain a significant amount of metals (Cappuyns *et al*., 2007).

Table 14: The certified value, experiment value and recovery of six elements using BCR extraction method of BCR sample for step 3 by ICP-MS

Step	Metal	Certified Value (mg/kg) ± 2SD	Experiment Value (mg/kg) ± 2SD	Recovery (%)
3	Cr	143 ± 7	79.7 ± 22	56
	Ni	15.3 ± 0.9	8.78 ± 1.2	57
	Cu	55.2 ± 4.0	26.7 ±2.96	48
	Zn	45.7 ± 4.0	32.64 ± 4.38	71
	Cd	0.27 ± 0.06	0.13 ± 0.04	48
	Pb	9.3 ± 2.0	5.49 ± 0.52	59

Comparison of ICP-AES and ICP-MS result

In this section, results of CRM are measured and the certified values analyzed to determine the optimum BCR extraction in the 3 steps with six metal elements from the sediment. The optimum extraction method was then used to extract the heavy metals in the Devon Great Consols sediment in order to discuss its geochemistry.

Tables 15, 16 and 17 show the relative standard deviation % (RSD), recovery, T-Test and F-Test of the BCR extractions (step 1 to 3) by the ICP-AES and ICP-MS.

RSD% was a very useful parameter to show the precision of instrumental analysis. Moreover, this precision provided a means to measure the random or indeterminate errors in analysis (Skoog *et al*., 2007). If the RSD value was lower than 10%, then the analysis method was generally acceptable (Cappuyns *et al*., 2007). If the T-Test value was positive, then there was no significance difference between the certified and experiment values. Equation 6 is shown in table 15. The experimental value might be accepted in the instrumental analysis. If the F-Test value was positive, then there was no significance difference between the two instruments. Equations 7, 8 and 9 were shown earlier. The red highlights in the table show where the recovery was not accepted.

Step 1 comparison

From the F-Test, only Cd was rejected, there being a significance difference between the two instruments, therefore should not be considered for comparison between the two instrumental sets of data. The RSD of Cr was higher than 10% in both data sets, indicating that the Cr data should not be accepted. In contrast, the RSD of the other metals was similar in the two sets of data. In terms of recovery, the recovery of metal in ICP-AES was better than that of ICP-MS, because the overall metal recovery in ICP-AES was close to 100% and only a few metals were over 120%. The Pb recovery might not be considered suitable as a factor for comparison between the two instrumental data of results, because the Pb recovery was higher than 150% on both counts. More metals were accepted with no significance difference between the certified values in ICP-AES. This could demonstrate that ICP-AES is more preferable using step 1.

Table 15: The summary of RSD%, recovery, T-Test and F-Test of BCR extraction in CRM sample for step 1 by ICP-AES and ICP-MS

Step 1	Metal	Relative standard deviation (RSD)(%)		Recovery (%)		T-Test		F-Test
		ICP-AES	ICP-MS	ICP-AES	ICP-MS	ICP-AES	ICP-MS	combine
	Cr	17.5	12.0	105	129	Accept	Accept	Accept
	Ni	8.25	7.10	108	113	Accept	Accept	Accept
	Cu	9.57	9.49	125	152	Accept	Reject	Accept
	Zn	4.41	6.95	110	127	Accept	Reject	Accept
	Cd	3.98	6.86	116	132	Reject	Reject	Reject
	Pb	31.2	8.46	223	218	Accept	Reject	Accept

Step 2 comparison

The RSD of six metals in ICP-AES were all below 10%, the ICP-AES represented the high precision in step 2. In terms of recovery, the two sets of data were similar. The recovery of nine out of 12 metals was higher than 80%. The recovery of ICP-AES was as good as ICP-MS. From the T-Test, 11 out of 12 metal results showed that there were significance differences between the certified and the experimental values in the two sets of data. Hence, the T-Test should not be considered as a factor for optimum instrument analysis in step 2.

From the F-Test, all the results showed that there was no significance difference between the two instruments. On the whole, ICP-AES and ICP-MS were preferable in step 2.

Table 16: The summary of RSD%, recovery, T-Test and F-Test of BCR extraction in CRM sample for step 2 by ICP-AES and ICP-MS

Step 2	Metal	Relative standard deviation (RSD)(%)		Recovery (%)		T-Test		F-Test
		ICP-AES	ICP-MS	ICP-AES	ICP-MS	ICP-AES	ICP-MS	combine
	Cr	1.51	2.03	82	83	Reject	Reject	Accept
	Ni	3.87	4.48	83	83	Reject	Reject	Accept
	Cu	4.55	5.86	80	91	Reject	Accept	Accept
	Zn	7.32	7.97	76	77	Reject	Reject	Accept
	Cd	8.04	10.7	80	73	Reject	Reject	Accept
	Pb	4.48	1.26	83	89	Reject	Reject	Accept

Step 3 comparison

From the F-test, only Cr and Ni had no significance difference between the two instruments; the matrix effects and spectroscopic interference might not be factors affecting the comparison. Also, it indicated that only Cr and Ni could be considered for the comparison of the results of the two instruments and for optimizing the instrument for analysis in step 3. The RSD of Cr and Ni in ICP-AES and ICP-MS was similar. The RSD of Cr was higher than 10% for both instruments, while Ni values were both lower than 10%. In terms of recovery, the recovery obtained by the 2 metals using the two instruments was quite similar, but the recovery of Ni in ICP-AES was higher than ICP-MS by 10%. Although these 2 metals were rejected in the T-test, the test was able to identify that the ICP-AES was more preferable in step 3. Table 17 shows the RSD of Cd and Pb was very high for ICP-AES, possibly due mainly to the low concentration of these elements in the extracts and to the fact that the third step accumulated the errors of the previous steps (Pueyo *et al*., 2001)

Table 17: The summary of RSD%, recovery, T-Test and F-Test of BCR extraction in CRM sample for step 3 by ICP-AES and ICP-MS

Step 3	Metal	Relative standard deviation (RSD)(%)		Recovery (%)		T-Test		F-Test
		ICP-AES	ICP-MS	ICP-AES	ICP-MS	ICP-AES	ICP-MS	combine
	Cr	11.6	13.8	55	56	Reject	Reject	Accept
	Ni	9.47	6.82	67	57	Reject	Reject	Accept
	Cu	3.74	5.55	43	48	Reject	Reject	Reject
	Zn	4.96	6.71	50	71	Reject	Reject	Reject
	Cd	173	15.5	0	48	/	Reject	Reject
	Pb	96.9	4.78	2	59	Reject	Reject	Reject

Semi- quantitative analysis

The concentration of 9 selected metals for the BCR extraction method (step 1 to 3) by ICP-MS is shown in tables 18, 19, and 20 respectively. The semi-quantitative analysis of ICP-MS was used to roughly determine all the metal presented in the sediment samples. This method was convenient for the preparation of the range of calibration curves for the samples. In this investigation, the 9 selected metals (e.g. Cr, Mn, Fe, Ni, Cu, Zn, As, Cd and Pb) were fully determined in terms of the concentration and bioavailability by the BCR extraction method.

Table 18: The concentration of 9 selected metals for semi-quantitative analysis for step 1 by ICP-MS

BCR step 1									
concentration (mg/kg)									
	Cr	Mn	Fe	Ni	Cu	Zn	As	Cd	Pb
sample 1	0.230	21.96	166.4	0.608	142.9	11.39	1.277	0.128	0.057
sample 2	0.329	558.6	384.7	8.042	96.36	347.3	20.63	0.703	0.105
sample 3	0.491	148.1	63.84	2.214	212.6	10.88	11.80	0.028	0.090
sample 4	0.173	14.83	68.46	0.274	191.2	13.26	113.3	0.037	0.019
sample 5	0.132	16.92	141.4	0.651	171.3	6.296	76.36	0.019	0.068
sample 6	0.118	13.45	124.5	0.258	178.1	6.411	42.75	0.047	0.004
sample 7	0.172	11.06	198.7	0.164	159.4	3.670	18.90	0.022	0.068
sample 8	0.066	7.504	75.80	0.218	145.4	8.993	68.92	0.089	0.009

Table 19: The concentration of 9 selected metals for semi-quantitative analysis for step 2 by ICP-MS

BCR step 2									
concentration (mg/kg)									
	Cr	Mn	Fe	Ni	Cu	Zn	As	Cd	Pb
sample 1	2.733	34.95	8251	0.267	156.2	5.757	60.54	0.063	9.716
sample 2	2.796	130.4	11073	7.992	191.9	181.6	506.2	0.569	14.85
sample 3	8.803	122.2	6477	2.733	185.8	7.519	804.5	0.041	12.44
sample 4	4.285	34.79	5947	0.654	214.7	16.29	1358	0.151	8.608
sample 5	4.087	44.68	6668	0.919	172.4	6.782	1423	0.038	12.97
sample 6	4.897	43.34	10783	0.618	216.0	9.229	2519	0.108	11.46
sample 7	3.499	27.22	10243	0.385	211.5	5.155	1447	0.061	13.60
sample 8	3.289	34.03	6316	0.539	208.9	17.49	1752	0.194	14.60

Table 20: The concentration of 9 selected metals for semi-quantitative analysis for step 3 by ICP-MS

BCR step 3									
concentration (mg/kg)									
	Cr	Mn	Fe	Ni	Cu	Zn	As	Cd	Pb
sample 1	5.921	14.58	779.7	0.788	133.1	10.58	5.697	0.016	1.585
sample 2	13.64	64.76	2277	6.364	208.3	100.4	290.4	0.090	3.142
sample 3	5.596	26.40	251.4	3.020	128.9	9.804	301.0	0.032	0.052
sample 4	4.789	18.03	358.1	0.756	115.9	13.07	352.9	0.070	0.050
sample 5	5.839	24.03	676.6	2.236	708.4	22.49	330.0	0.069	0.852
sample 6	2.596	38.55	734.9	0.771	124.0	21.28	359.5	0.063	0.395
sample 7	2.452	77.78	1629	0.640	425.3	18.80	501.5	0.060	1.009
sample 8	0.305	8.332	76.26	0.249	85.56	8.829	267.1	0.032	0.179

Devon Great Consols sediment analysis

Devon Great Consols field data

The field data collected are shown in table 21. As site 3 was without water on the sampling date, its water quality was not determined. The percentage and concentration of dissolved oxygen and water temperature was similar on all the sampling sites. The conductivity shows the amount of electrolyte in water and sediment. They were important parameters for environmental analysis. Site 5 had the lowest conductivity (4.6μs) and no salinity was determined. In this investigation, pH and Eh were the main foci for discussion regarding the dominant metal species in the environment. The pH and Eh were essential values for predicting the abundance of metal species in the sediment and water. The results will be discussed later.

Table 21: Field data from Great Consols tailing run-off stream on 1st November 2011

Diameter\samples	Site1	Site2	Site3	Site4	Site5	Site6	Site7	Site8
DO (%)	94.0	98.0	/	92.2	93.3	91.4	95.5	89.3
DO(mg/L)	10.1	9.90	/	9.64	10.10	9.74	10.14	9.62
Temp(℃)	12.2	12.6	/	13.3	11.4	12.4	12.5	12.7
Conductivity(μs)	277	179	/	595	4.6	476	580	500
Salinity	0.2	0.1	/	0.4	0.0	0.3	0.4	0.3
pH	4.34	6.54	/	3.94	5.10	3.72	3.41	3.65
Eh (mV)	425	98	/	370	306	499	507	481

The physical treatment for sediment

Different types of sediment after sieving

The classification for sizing the particles from the eight samples is shown in table 22. In this investigation, sediments <250μm were preferable for BCR extraction. Usually the trace metal concentration increases with decreases in grain size of the sediment (Loring *et al.*, 1992). Table 22 shows that sediment <250μm could be classified into find sand, very find sand and mud. In this section, only the fine grained size sediment was considered for the eight samples.

Table 22: Wentworth particle size classification (Wiki, 2012)

φ scale	Size range (metric)	Size range (approx. inches)	Aggregate name (Wentworth Class)	Other names
−8 <	256 mm <	10.1 in <	Boulder	
−6 to −8	64–256 mm	2.5–10.1 in	Cobble	
−5 to −6	32–64 mm	1.26–2.5 in	Very coarse gravel	Pebble
−4 to −5	16–32 mm	0.63–1.26 in	Coarse gravel	Pebble
−3 to −4	8–16 mm	0.31–0.63 in	Medium gravel	Pebble
−2 to −3	4–8 mm	0.157–0.31 in	Fine gravel	Pebble
−1 to −2	2–4 mm	0.079–0.157 in	Very fine gravel	Granule
0 to −1	1–2 mm	0.039–0.079 in	Very coarse sand	
1 to 0	½–1 mm	0.020–0.039 in	Coarse sand	
2 to 1	¼–½ mm	0.010–0.020 in	Medium sand	
3 to 2	125–250 µm	0.0049–0.010 in	Fine sand	
4 to 3	62.5–125 µm	0.0025–0.0049 in	Very fine sand	
8 to 4	3.90625–62.5 µm	0.00015–0.0025 in	Silt	Mud
< 8	< 3.90625 µm	< 0.00015 in	Clay	Mud
< 10	< 1 µm	< 0.000039 in	Colloid	Mud

The Wentworth Scale

$\Phi = - \log_2 D$ D in mm

Surface area effect

Spherical grains

$SA = 4\pi R^2$

$SA = \pi D^2$

$SA/V = 6/D$ Equation 11

Where SA is the surface area, R is the radius, D is the diameter and V is the volume.

Equation 11 shows that the proportion of particle volume (e.g. reactive coating) generally increases with decreasing particle diameter (Turner *et al*., 2002).

Figure 5 shows that the largest proportion of sediment <250µm presented in

sample 2, followed by samples 4 and 8 respectively. In contrast, sample 5 had the smallest amount of <250μm sediment.

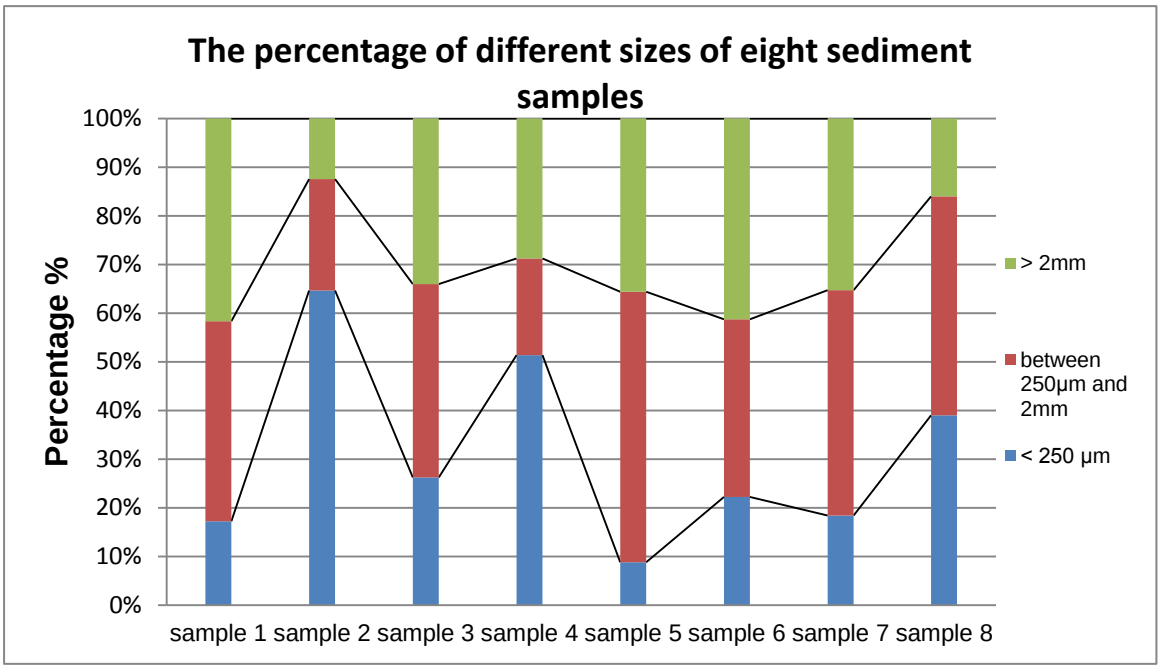

Figure 5: The percentage of different sizes of sediment samples

Table 23 shows the name of eight sediments using the Folk's classification. Some of the samples (sample 1, 3, 6 and 7) were classified as muddy sandy gravel sediment. Samples 2 and 4 were gravelly mud, while sample 8 was gravelly muddy sand. Figure 6 shows that these types of sediment contain less than 30% gravel (>2mm) and more mud (<250μm) in the sampling site. The result was the same as figure 5.

Table 23: The Folk's classification in eight samples

samples	types of sediments
sample 1	muddy sandy gravel
sample 2	gravelly mud
sample 3	muddy sandy gravel
sample 4	gravelly mud
sample 5	sandy gravel
sample 6	muddy sandy gravel
sample 7	muddy sandy gravel
sample 8	gravelly muddy sand

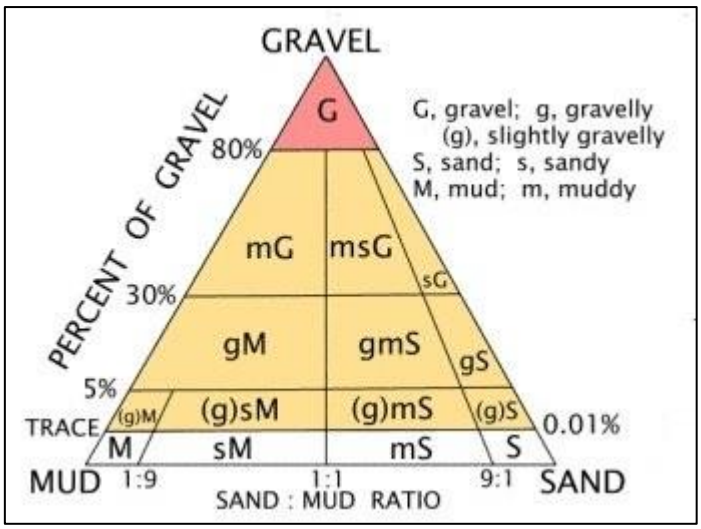

Figure 6: The Folk's classification chart (USGS, 2012)

Sediment colour

All the samples presented in symbol 10YR in the Munsell notation. In addition, most sediment samples were yellowish brown. The fine grained sediments usually have a thin, dark yellowish brown surface layer resulting from the oxidation of iron compounds in the sediment and water surface (Loring *et al*., 1992).

Table 24: The Munsell notation of eight sediments using Munsell soil colour chart

samples	Munsell notation symbol	colour
sample 1	10YR 6/4	Light yellowish brown
sample 2	10YR 4/3	Brown
sample 3	10YR 7/3	Very pale brown
sample 4	10YR 3/4	Dark yellowish brown
sample 5	10YR 7/4	Very pale brown
sample 6	10YR 4/3	Brown
sample 7	10YR 4/4	Dark yellowish brown
sample 8	10YR 3/3	Dark brown

Wet density

The density of the sediment was determined by its composition. Variation In sediment core in density down the core indicated fluctuations in sediment composition, suggesting more than one sediment source presented.

Table 25 shows the wet density of the eight samples. The wet density of sample 2 had the lowest density of all the samples, thus this sample may have more than one source.

Table 25: The wet density of eight samples

samples	wet density(g/cm3)
sample 1	1.84
sample 2	1.15
sample 3	1.70
sample 4	1.99
sample 5	1.88
sample 6	1.90
sample 7	2.08
sample 8	1.97

Analytical figures of merit

The gradient, intercept, R^2 and the limit of detection (LOD) for optimum ICP-AES and ICP-MS by BCR extraction (step 1 to 3) for determination of samples are shown in table 26 to 32. Equation 5 was used to calculate the LOD and equation 4 given in the same section was used to calculate the concentration of selected metal in sample sediment.

Step 1

LOD is the power of detection for any method of analysis. According to the LOD equation, LOD is affected by the means of the blank concentration and the standard deviation of the sample. The steeper the slope, the better the precision and the lower the LOD. In step 1, Mn had the highest gradient (1940.6), but the LOD was not the smallest in all metals. This could explain the high standard deviation seen in the analysis of Mn replicates. The precision of Mn was poor. The LODs of the metals were of the following order: As< Cr< Mn< Zn< Ni< Fe< Cu for ICP-AES. For ICP-MS, the LODs of Cd and Pb were zero. The values of R^2 for each calibration curve were higher than 0.99. This revealed that the calibration curves were in linear portion, and the least squares method could be applied to the calibration (Skoog *et al*., 2007).

Table 26: Calibration Graph information for determination of BCR extraction for sample by ICP-AES for step 1

Date	Wave Length (nm)	Element	Gradient (m, eql)	Intercept (c, eql)	R^2	Limit of detection (mg/L)
17th Jan 12	267.7	Cr	412.55	18.894	0.999	0.001
	327.4	Cu	527.14	17.155	1	0.151
	213.9	Zn	339.78	21.121	1	0.006
	189	As	62.222	77.648	0.998	0
	257.6	Mn	1940.6	40.528	1	0.004
	234.4	Fe	718.97	1464.8	0.999	0.137
1st Feb 12	231.6	Ni	309.14	14.039	0.999	0.010

Table 27: Calibration Graph information for determination of BCR extraction for sample by ICP-MS for step 1

Date	Wave Length (nm)	Element	Gradient (m, eql)	Intercept (c, eql)	R^2	Limit of detection (mg/L)
16th Jan 12	111	Cd	3694.4	55.984	1	0
3rd Feb 12	208	Pb	63345.4	33616.8	0.999	0

Step 2

In step 2, the gradient of Cu was the highest (5910), but the LOD was not the lowest of all the metals. This case was similar to step 1. The order of LODs were Mn< Cu< Ni< Cr< Zn< Pb< As< Fe for ICP-AES. The LOD of Cd was also zero. The values of R^2 for each calibration curve were higher than 0.999. This indicated that calibration curves were in linear portion and the least squares method could be used (Skoog *et al*., 2007).

Table 28: Calibration Graph information for determination of BCR extraction for sample by ICP-AES for step 2

Date	Wave Length (nm)	Element	Gradient (m, eql)	Intercept (c, eql)	R^2	Limit of detection (mg/L)
17th Jan 12	189	As	62.222	77.648	0.998	0.243
	257.6	Mn	1940.6	40.528	1	0.006
	234.4	Fe	718.97	1464.8	0.999	0.790
1st Feb 12	267.7	Cr	4067.3	136.8	0.999	0.024
	327.4	Cu	5910	271.14	0.999	0.007
	231.6	Ni	309.14	14.039	0.999	0.013
	220.4	Pb	141.38	10.128	0.999	0.027
	213.9	Zn	3387.7	125.2	0.999	0.020

Table 29: Calibration Graph information for determination of BCR extraction for sample by ICP-MS for step 2

Date	Wave Length (nm)	Element	Gradient (m, eql)	Intercept (c, eql)	R^2	Limit of detection (mg/L)
16th Jan 12	111	Cd	3694.4	55.984	1	0

Step 3

In step 3, the gradient of Cr was the highest (4067.3) for ICP-AES, but the LOD was not the lowest of all the metals. On the other hand, the gradient of Pb was the highest (63345.4) in ICP-MS. The results could be explained by the low precision. The order of LOD was Mn< Cr< Zn< Ni< Cu< As< Fe for ICP-AES. The LODs of Cd and Pb were zero and 0.002 mgL^{-1}. The value of R^2 of each calibration curve was approximately 0.99. This showed that the calibration curves were in linear portion and the least squares method could be used (Skoog *et al*., 2007).

Table 30: Calibration Graph information for determination of BCR extraction foe sample by ICP-AES for step 3

Date	Wave Length (nm)	Element	Gradient (m, eql)	Intercept (c, eql)	R^2	Limit of detection (mg/L)
17th Jan 12	327.4	Cu	527.14	17.155	1	0.026
	231.6	Ni	31.33	3.6458	0.999	0.014
	213.9	Zn	339.78	21.121	1	0.013
	257.6	Mn	1940.6	40.528	1	0.004
	234.4	Fe	718.97	1464.8	0.999	0.203
1st Feb 12	267.7	Cr	4067.3	136.8	0.999	0.008
	189	As	66.903	102.82	0.997	0.116

Table 31: Calibration Graph information for determination of BCR extraction for sample by ICP-MS for step 3

Date	Wave Length (nm)	Element	Gradient (m, eql)	Intercept (c, eql)	R^2	Limit of detection (mg/L)
16th Jan 12	111	Cd	3694.4	55.984	1	0
3rd Feb 12	208	Pb	63345.4	33616.8	0.999	0.002

Toxicity of heavy metals

Toxicity depends on the form of occurrence of the individual species. In the aquatic environment, heavy metals could occur in a free ion form which is most toxic to living organisms (Namiesnik *et al*., 2010).

Figures 7 to 15 show the Eh-pH diagrams of the nine selected metals speciation. According to the water quality of the sampling sites, the pH and Eh were measured at eight sampling sites. The pH and Eh data were used to estimate the metal's speciation in water and sediment.

Chromium (Cr)

Figure 7 shows that sample 1 and 4 were $Cr(OH)^{2+}$, sample 2 and 5 were Cr_2O_3, sample 6 to sample 8 were Cr^{3+} species. Cr (III) was strongly bound to sediment particles (Namiesnik *et al.*, 2010). Also, Cr was the most dissolved

ionic species, which complexed with inorganic ligands like hydroxide, and organic compounds (Morel *et al*., 1994). In nature, chromium occurs almost exclusively in the form of compounds with oxygen (Morel *et al*., 1994). Cr easily formed complexes and oxides, hence the amount of Cr free ions were not high. The toxicity of Cr is not serious and has no negative impacts on the organism.

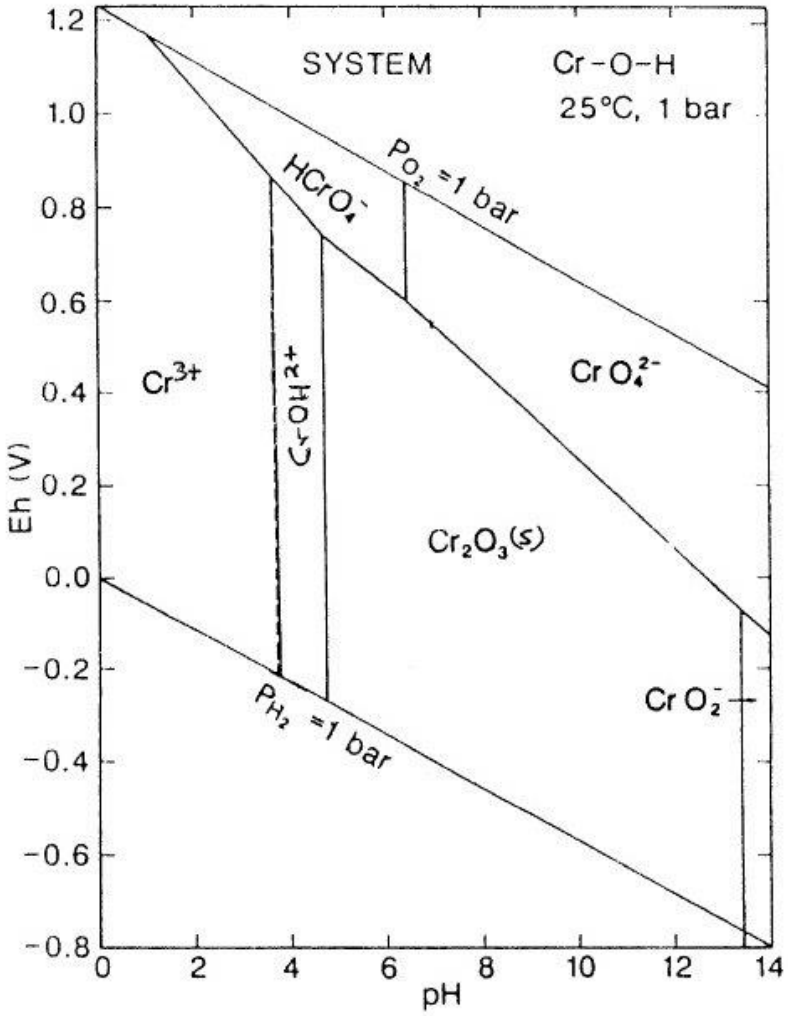

Figure 7: Simplified Eh-pH diagram for the system Cr-O_2-H_2O at 25 and 1 atm. (Langmuir *et al*., 2004)

Copper (Cu)

Figure 8 shows that sample 2 was Cu_2O while other samples were all Cu^{2+} species. The toxicity of copper (Cu) in organisms is highly dependent on its chemical forms. Indeed, free Cu^{2+} ions are believed to be the most important factor controlling the bioavailability and toxicity of Cu because they can pass through biological membranes easily (Campbell, 1995; Brown et al., 2000).

Also, Cu has a stronger tendency to bind to the barley roots rather than to the malate ligands. Cu is the most toxic metal, after mercury and silver, to the wild marine life (Clark, 2001). Nonetheless, copper does not generally accumulate in the food chain (Clark, 2001). In humans, the toxicity of copper can functionally disturb the nervous system, kidneys and liver (Ayres, 1998).

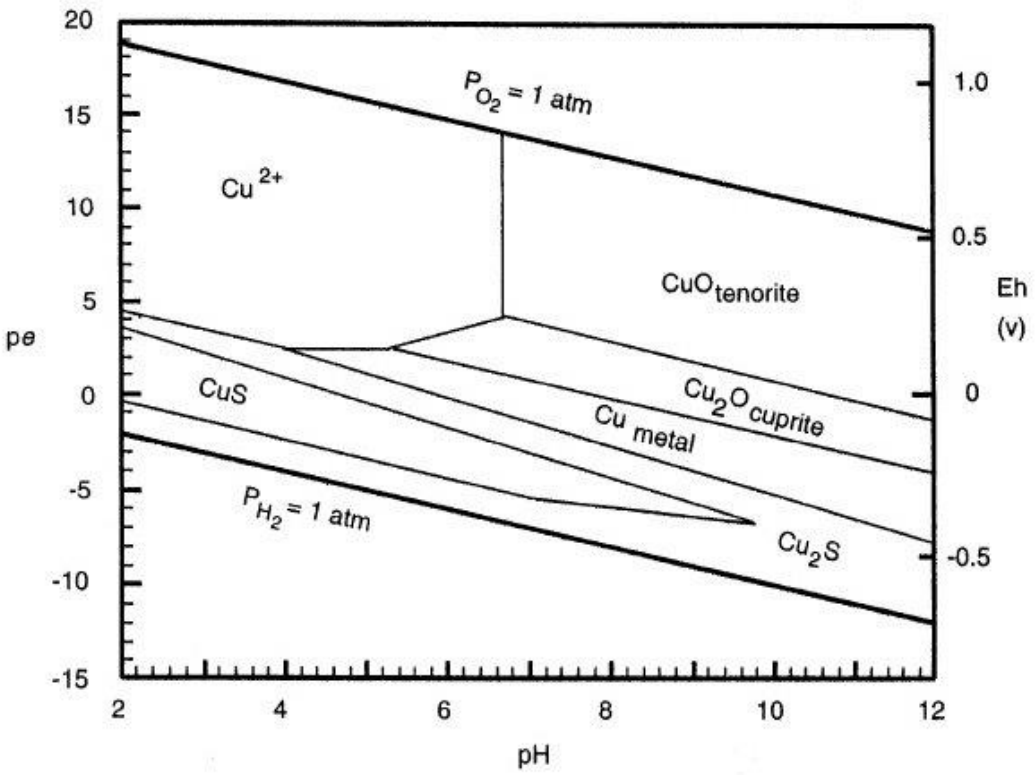

Figure 8: Simplified Eh-pH diagram for the system Cu-O_2-S-H_2O at 25 and 1 atm. (Langmuir *et al*., 2004) (Remark: pe x 0.0592= Eh(V))

Nickel (Ni)

Figure 9 shows that all the samples were NI^{2+} species. The toxicity of nickel varied widely and was influenced by salinity and the presence of other ions. Therefore, Ni was regarded as only moderately toxic. No organisms have been found to contain very high concentrations of nickel. There was no evidence that nickel was bioaccumulated in the marine food webs (Clark, 2001).

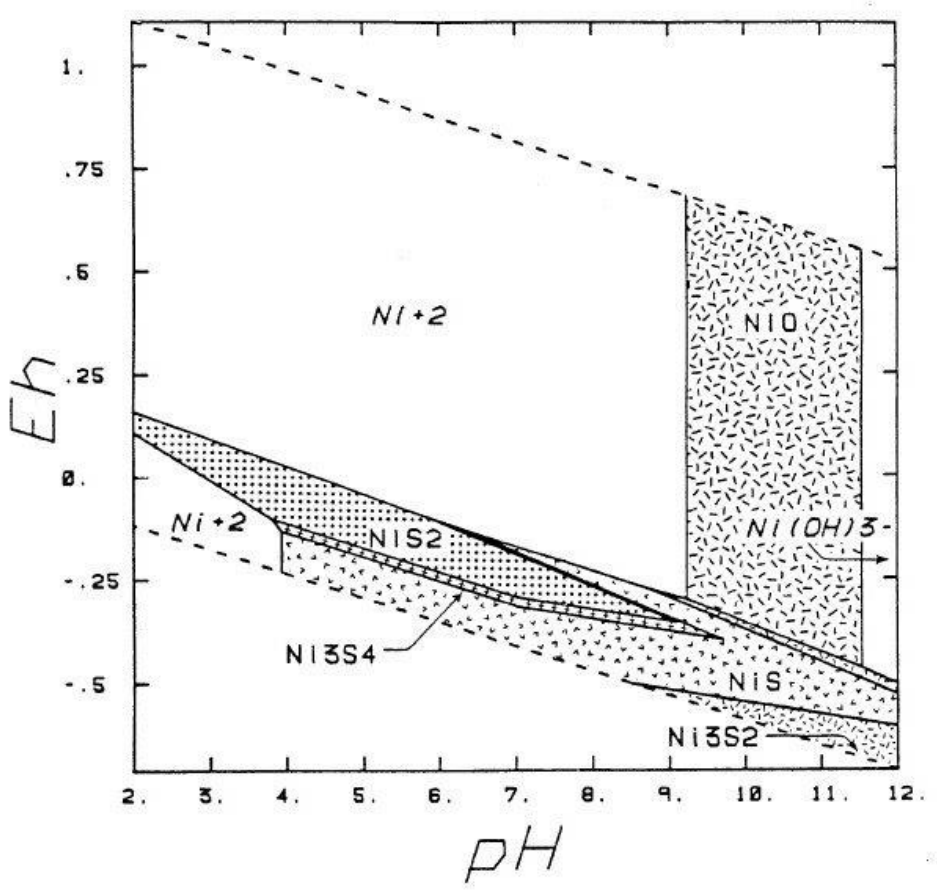

Figure 9: Simplified Eh-pH diagram for the system Ni-O_2-CO_2-S-H_2O at 25 and 1 atm. (Langmuir *et al*., 2004)

Lead (Pb)

Figure 10 shows that all the samples were Pb^{2+} species. In soluble form, the metal occurred mainly as Pb^{2+}. Compared with other metals, lead in the sea is not particularly toxic (Clark, 2001). Lead is readily accumulated by both living organisms and in bottom sediments (Rickard et al., 1978; Kabata-Pendias *et al*., 2000). Under extremely polluted conditions or when contaminants are acidic, lead could enter the food chain (Namiesnik *et al*., 2010). The toxicity of Pb is from human ingestion which can lead to cumulative poisoning (Standard methods, 2004).

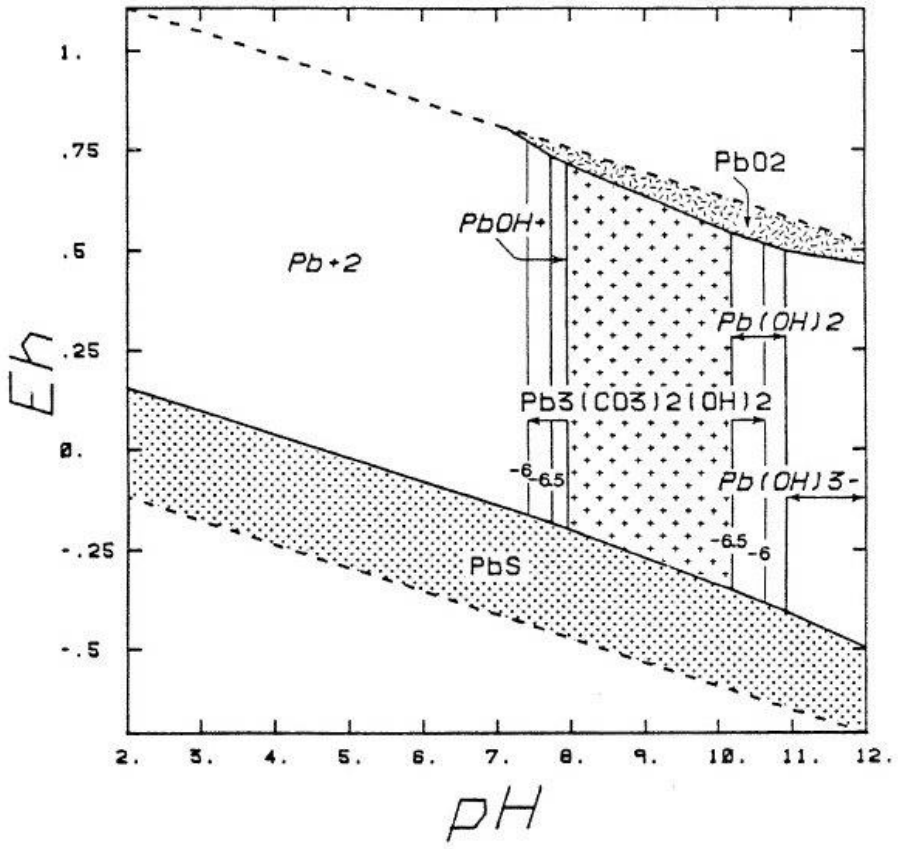

Figure 10: Simplified Eh-pH diagram for the system Pb-O_2-CO_2-S-H_2O at 25 and 1 atm. (Langmuir et al., 2004)

Zinc (Zn)

Figure 11 shows that all samples were Zn^{2+} species. The wide variety of Zn applications might pose a significant threat to the environment. At pH<7, Zn is generally present as a divalent ion which could readily form complexes with organic and inorganic compounds. It is rapidly adsorbed on the surface of organic matter and bottom sediments (Bertling et al., 2006; Directive 76/464/EEC). There is an associated risk that Zn could enter the food chain. Zn compounds have excellent solubility. The migration of zinc in the environment and its uptake by plants and other soil organisms are favored by acidic pH (Simon-Hettich *et al*., 2001). The toxicity of zinc species is dependent. It is easily bioaccumulated in zooplankton (Directive 76/464/EEC). When Zn concentration is higher than 300 to 400 mg/kg in sediments, it could cause growth retardation in plants, while a level range of 1 to 10 ppm could cause lethal effects in some fish species. Zinc is very toxic and can cause acute toxicity in humans and animals (Ayres, 1998).

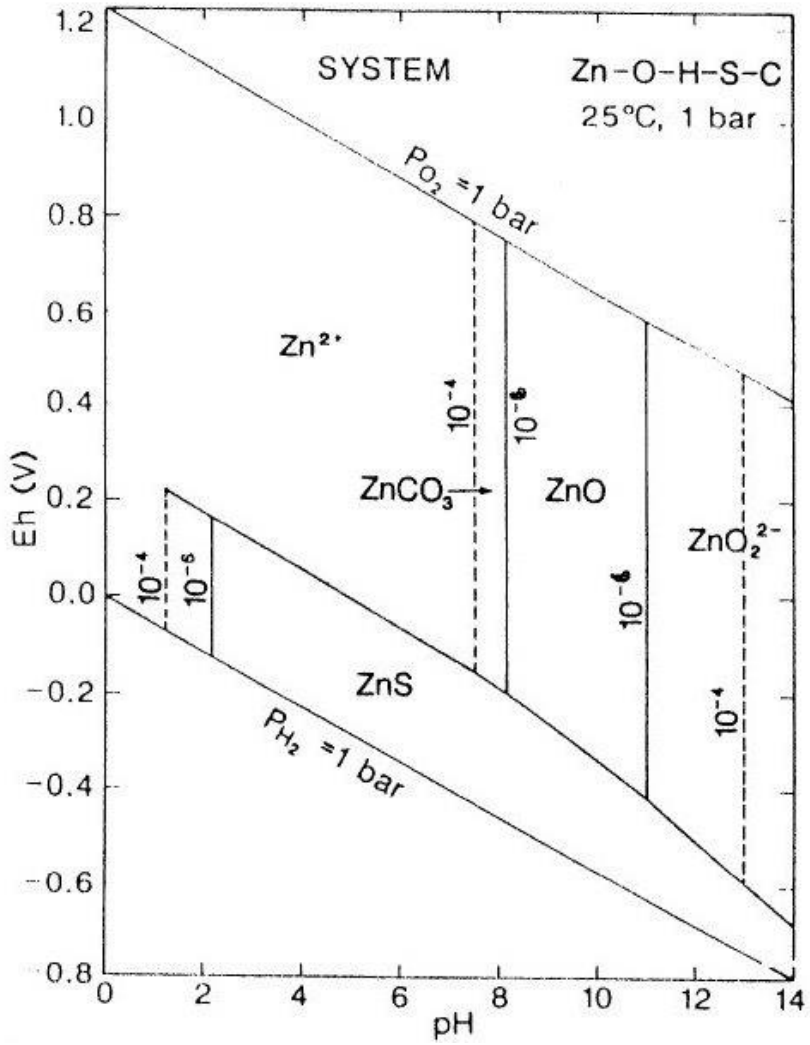

Figure 11: Simplified Eh-pH diagram for the system Zn-O_2-CO_2-S-H_2O at 25 and 1 atm. (Langmuir *et al*., 2004)

Cadmium (Cd)

Figure 12 shows that all samples were Cd^{2+} species. Cadmium is readily mobilized by weathering, and can be bound by minerals containing iron hydroxide and organic substances (Kabata-Pendias *et al*., 2000; Lai et al., 2002). The free Cd^{2+} ions show that it might be easily transferred into the food chain through uptake by plants growing in the sediment. These characteristics show that the hazards of Cd are harmful to human health (e.g. Minamata disaster) (Yusuf, 2007). Cadmium is extremely toxic and could accumulate in human kidneys and the liver (Standard methods, 2004). Furthermore, when intakes of cadmium are at a low concentration, it would lead to the dysfunction of the kidneys. In marine systems, Cd is assumed to be taken up by phytoplankton. Nonetheless, it does not appear to be accumulated in the food

chain (Clark, 2002).

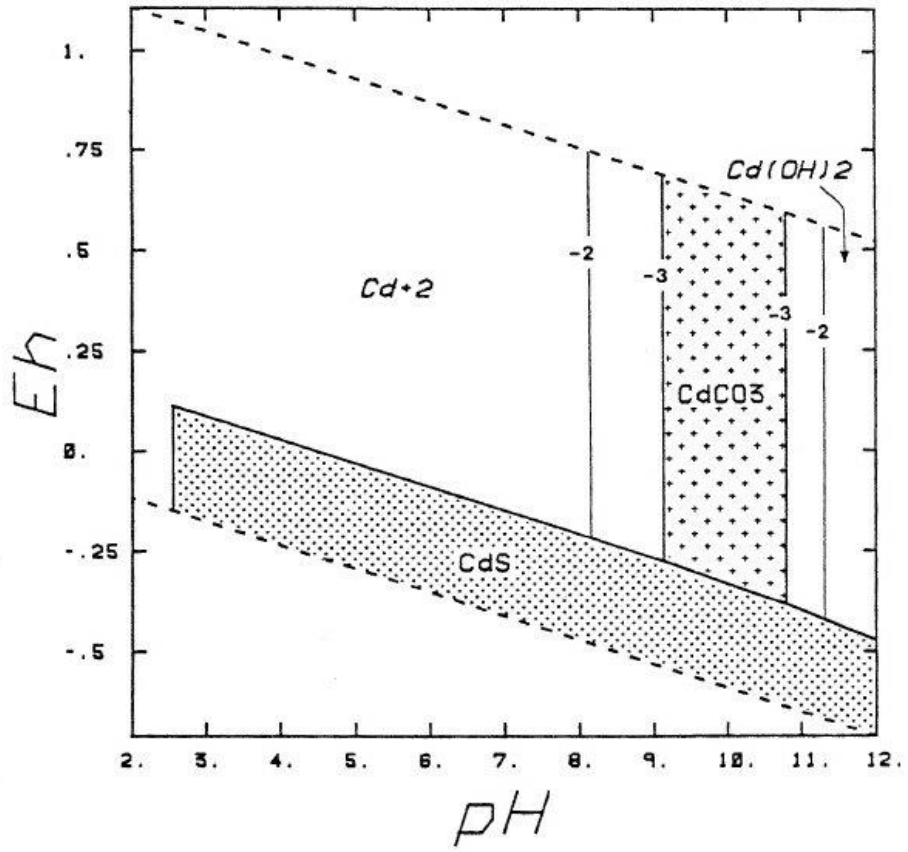

Figure 12: Simplified Eh-pH diagram for the system Cd-O_2-CO_2-S-H_2O at 25 and 1 atm. (Langmuir *et al.*, 2004)

Arsenic (As)

Figure 13 shows that all samples were $H_2AsO_4^-$ species. Arsenic is an element of great concern in terrestrial as well as aquatic environments because of its high toxicity to living organisms. Depending on environmental conditions, As (V) in sediments could be mobilized into ground and surface water, where living organisms are readily exposed to it, and where it might accumulate in the trophic chain (Mello et al., 2006). Moreover, organisms are able to metabolize As (V) into organic arsenic compounds (Smedley *et al*., 2002). Furthermore, inorganic arsenic compounds (As (V)) are more toxic than organic arsenic compounds and have been classified as human carcinogens mainly related to lung and skin cancer (Baig *et al.*, 2009).

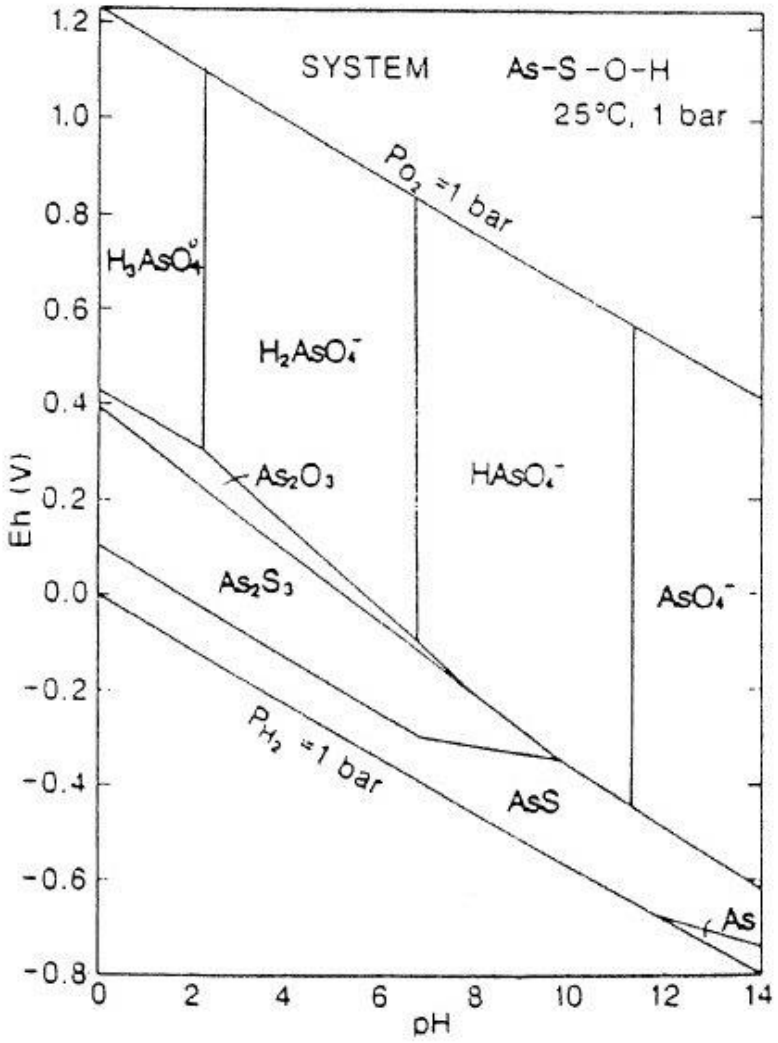

Figure 13: Simplified Eh-pH diagram for the system As-O_2-S-H_2O at 25 and 1 atm. (Langmuir et al., 2004)

Manganese (Mn)

Figure 14 shows that all samples were Mn^{2+} species. Manganese is toxic in high concentrations, also as a cytotoxic and neurotoxic compound which can cause muscle weakness and increased incidence of upper respiratory infections and pneumonia (Ayres, 1998).

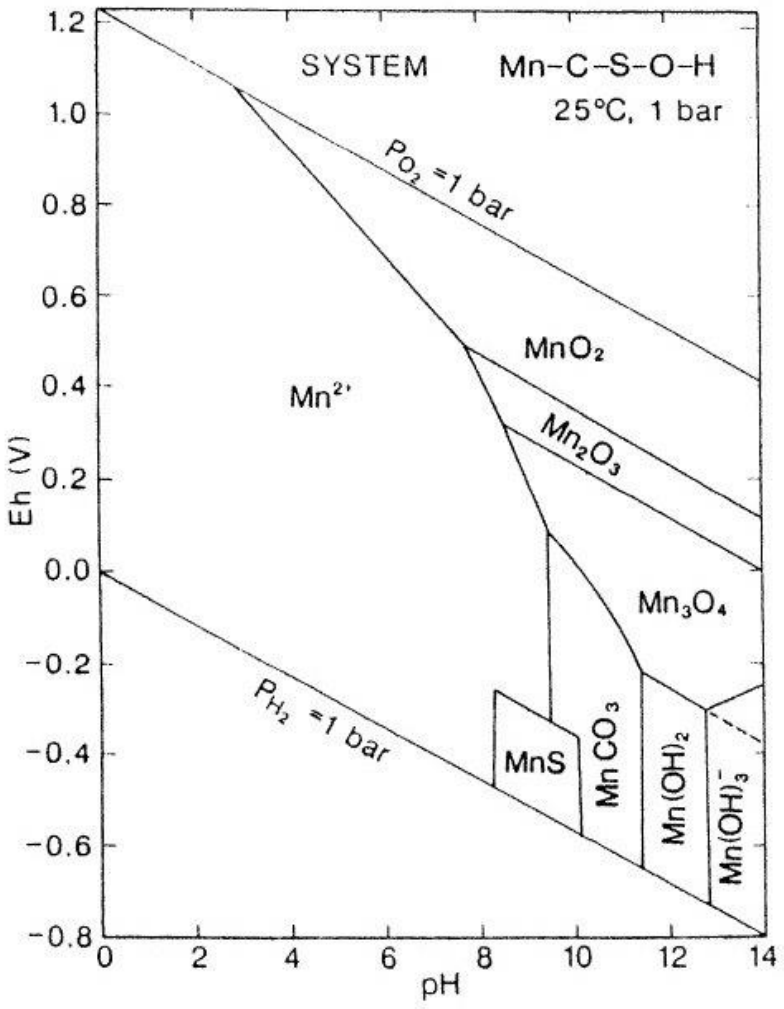

Figure 14: Simplified Eh-pH diagram for the system Mn-O_2-CO_2-S-H_2O at 25 and 1 atm. (Langmuir *et al.*, 2004)

Iron (Fe)

Figure 15 shows that sample 2 was $FeCO_3$, while other samples were Fe^{2+} species. It has been found difficult to identify the environmental impact of Fe. Moreover, Fe^{2+} can easily oxidize to Fe^{3+} and precipitate as hydrated oxides of iron (Clark, 2002), thus decreasing its toxicity. Nonetheless, Fe-Mn oxides exist as nodules, concretions and cement between particles or as a coating on particles, which are excellent trace element scavengers (Ikem *et al.*, 2003). Fe encourages other metals to adsorb onto its surface, potentially leading to increases in other metal free ions in the sediments. Moreover, excess Iron can cause toxicity to plants and animals. In animal bodies, excess iron can store up and cause damage to the liver (Ayres, 1998).

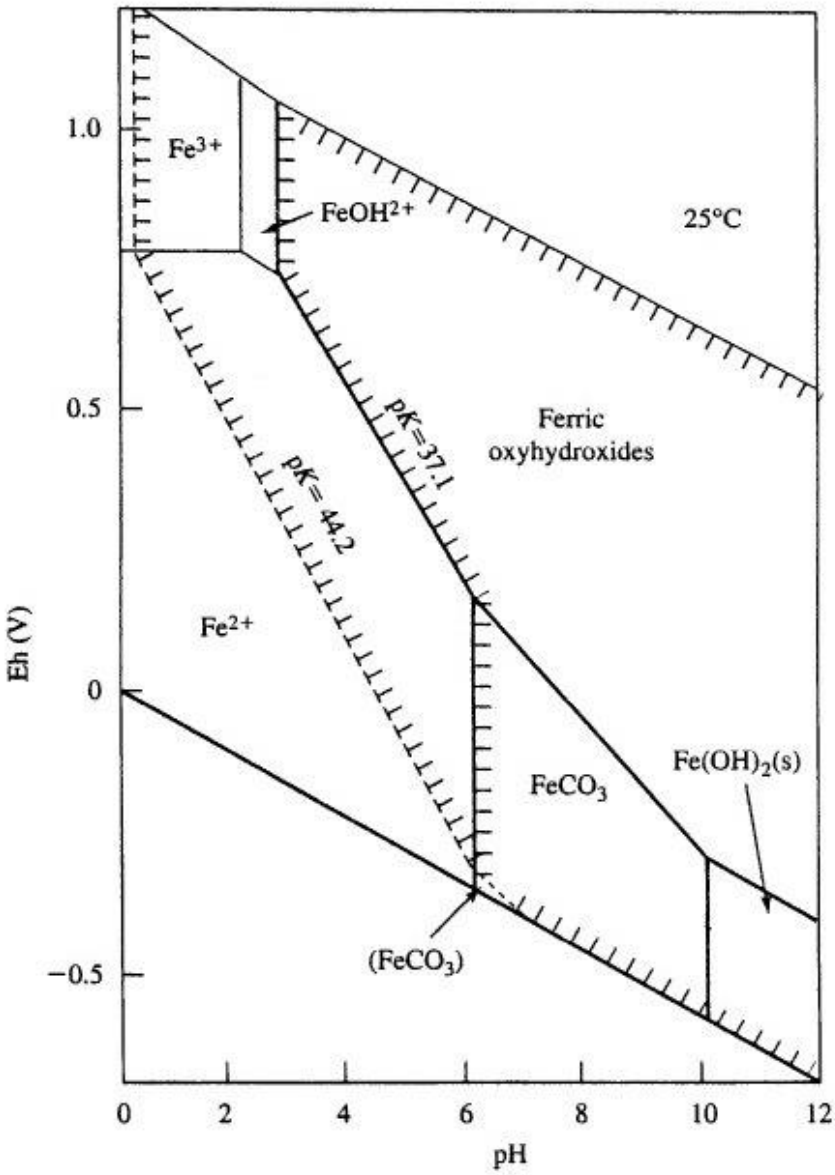

Figure 15: Simplified Eh-pH diagram for the system Cd-O_2-CO_2 –H_2O at 25 and 1 atm. (Langmuir *et al*., 2004)

BCR sequential extraction data

The BCR sequential extraction method was useful in determining the speciation of the selected metals. After extraction, it provided three different fractions (e.g. exchangeable, reducible and oxidisable) for the analysis. The results and graphs of BCR sequential extraction (3 steps) with nine selected heavy metals are shown in table 32 and figures 16 to 18 respectively.

Water and acid soluble, exchangeable and bound to carbon fraction (step 1)
This fraction showed the amount of the selected element that would be released into the environment when conditions become acidic. The fraction produces adverse impacts to the environment (Nemati *et al*., 2009). Moreover, this fraction is very important because of the high mobility of metals to the aqueous phase (Uwumarongie-llori et al., 2011). The extent of mobility provided information on the potential for contamination. Also, the form of metals in the fraction is the most accessible for plant uptake and they could be released by changing the ionic strength of the medium (Geanina *et al*., 2008).

Soluble metals in the Great Consols run off stream were adsorbed as outer-sphere complexes, but not necessarily for metals adsorbed as inner sphere complexes. In an outer- sphere complex, the ion kept being surrounded by a hydration shell and it was not binding to the surface directly. The adsorption was caused by attraction between a positively-charged cation in the water and a negatively- charged surface. Also, negatively- charged anions could have been adsorbed onto positively- charged surfaces (Langmuir *et al*., 2004).

Metal adsorption onto sediments was probably dependent on changes in pH. For a divalent metal cation (e.g. M^{2+}), the general sorption reaction could be written: (Langmuir *et al*., 2004)

$$SOH + M^{2+} = SOM^{+} + H^{+}$$

For adsorption of a divalent metal anion (e.g. L^{2-}):

$$SOH_2^{+} + L^{2-} = SOH_2L^{-}$$

Where SOH and SOM+ were surface sites with an adsorbed proton and a metal ion.

In this investigation, a significant amount of Fe (78.66- 616.2 $mgkg^{-1}$) was released in step 1, followed by Cu (175.9- 387.4 $mgkg^{-1}$), As (5.976- 128.5 $mgkg^{-1}$), Mn (6.534- 154.8$mgkg^{-1}$) (except sample 2), Ni (0.224- 10.93 $mgkg^{-1}$), Zn (3.029- 9.907$mgkg^{-1}$) (except sample 2), Cd (0.028- 0.675 $mgkg^{-1}$), Cr (0.053- 0.195 $mgkg^{-1}$), and Pb (0.0003- 0.086 $mgkg^{-1}$). The high concentration of Fe in step 1 could be explained by the dissolution of minerals that contained Iron (e.g. arsenopyrite FeAsS and Scorodite $FeAsO_4{\cdot}2H_2O$). There is the largest production of As minerals in Devon Great Consols, in the UK. The

minerals might be released from weathering of rocks and subsequently ended up in the run off stream. Also, the Fe speciation was $FeCO_3$ and $Fe^{2+,}$ demonstrated in the previous section. $FeCO_3$ and Fe^{2+} were easily adsorbed onto the sediment surface by electrostatic interaction. In sample 2, $FeCO_3$ could strongly adsorb in higher pH (6.54), accounting for the high concentration of Fe when compared to other samples.

The amount of Cu was significantly high in step 1, possibly caused by the dissolution of $CuFeS_2$ minerals. Furthermore, As also had high concentrations in step 1, for the same reasons as Fe and Cu. The Devon Great Consols contained active As and Cu ores in the 19th century. The heavy metals might have been released by mining activity as the ores and impermeable rocks were broken up and exposed to run off streams (Palumbo-Roe *et al*., 2007). In sample 2, the extra high concentrations of Mn, Zn and Fe were observed, compared to the other samples. The location of sampling site 2 could explain this in that it was far away from the others. The high level of Mn, Zn and Fe might be due to the most contaminated region or ore that was near the site 2, especially Mn and Zn metals.

The order of concentration of selected metals in BCR sequential extraction (step 1) was Fe> Cu> As> Mn> Ni> Zn> Cd> Cr> Pb. The metal distribution of the selected metals was most important in determining the mobility and bioavailability of the metals in the sequential extraction. The distribution, mobility and bioavailability of all selected metals in the step 1 fraction is discussed later.

Reducible manganese and iron oxides fraction (step 2)

This fraction represents the metals associated with Fe-Mn oxides. The metals are released in the reducible fraction when Fe-Mn oxides fractions are dissolved by reduction (Asagba *et al.*, 2007; Singh *et al.*, 1998). This fraction can extract these metals from inner sphere complexes. Metals associated with the Fe-Mn oxide can be remobilized and be available to the biota when the pH and redox conditions of water-sediment system are changed (Iwegbue *et al.*, 2007).

In the experiment, the concentration of Fe (7759- 14697mgkg^{-1}) was the highest, followed by As (62.19- 3827 mgkg^{-1}), Cu (163.9- 387.6 mgkg^{-1}), Mn (23.42- 94.31 mgkg^{-1}) (except sample 2), Pb (10.78- 20.32 mgkg^{-1}), Zn (5.007-

14.19 $mgkg^{-1}$) (except sample 2), Ni (0.065- 7.827 $mgkg^{-1}$), Cr (0.532- 2.129 $mgkg^{-1}$), and Cd (0.035- 0.566 $mgkg^{-1}$).

The high concentration of Fe in the Fe-Mn oxides fraction can be explained by the precipitation effect of Fe-Mn oxyhydroxides in water. The significant high levels of As and Cu were due to the dissolution of minerals (as per step 1). Table 33 and figure 16 show that large amounts of all heavy metals were extracted in step 2. This explains why Fe-Mn oxides occurred in various physical forms in the sediments. The Fe-Mn oxides strongly influence levels of trace metals due to their tendency to adsorb or co-precipitate them from the run off stream (Pickering, 1996). Also, manganese and iron have civilizational effects such as extreme eutrophication that can cause other metal elements to accumulate in sediments (Uwumarongie-Ilori *et al.*, 2011). Furthermore, Fe-Mn oxides could bind with the trace metals since it has high scavenging efficiencies for trace metals (Naji *et al.*, 2010). For example, the excellent scavengers of trace metals tended to control Cu, Mn and Zn solubility in sediments (Pickering, 1996). These are the reasons why the levels of Cu, Mn and Zn were higher than Ni, Cr and Cd. In sample 2, the results evidenced the extra amount of Zn and Mn when compared with the other samples. This could be explained by the location and the level of contamination in this area.

The order of concentration of selected metals in the BCR sequential extraction in step 2 was Fe> As> Cu> Mn> Pb> Zn> Ni> Cr> Cd. The metal distribution of all selected metals in step 2 fraction will be discussed later.

Organic complex and sulphide fraction (step 3)

The oxidisable fraction shows the amount of heavy metal binding to the organic matter and sulfur that would be released into the environment if the conditions became oxidative (Nemati *et al*., 2009). The size of organic matter in fresh water is relatively small. Metals generally attract organic matter, and might form chelate complexes (Drever, 1997). For example, carboxyl, carbonyl, hydroxyl and phenolic functional groups could bind with metals (Jnr *et al*., 2005). Such binding makes the heavy metals temporarily immobilized.

In the experiment, the concentration of Fe (452.1- 2710$mgkg^{-1}$) was the highest, followed by Cu (125.3- 1143 $mgkg^{-1}$), As (4.084- 331.6 $mgkg^{-1}$), Mn (13.70- 49.23 $mgkg^{-1}$), Zn (6.448- 12.06 $mgkg^{-1}$), Ni (0.377- 5.577 $mgkg^{-1}$), Cr (0.565- 4.212 $mgkg^{-1}$), Pb (~0- 3.425 $mgkg^{-1}$), and Cd (0.021- 0.076 $mgkg^{-1}$).

The high concentration of Fe was due to dissolution of the Fe minerals. The speciation of Fe was demonstrated in the previous section. The Eh-pH diagram showed that sample 2 was $FeCO_3$ and the other samples were all the Fe^{2+} species. It was easier for the free Fe ions to form a complex and adsorb to the organic matter surfaces. Also, Cu had a high binding affinity to the ligands presented. In most water systems, the majority of copper residing in complexes would dissolve the organic matter, hence Cu occurs at a relatively high level in the step 3 fraction (Jnr *et al.*, 2005). The significant high level of As can be explained by the mineral dissolution. On the other hand, sample 2 revealed extra high levels of Zn and Fe compared to the other samples, due to the site being nearer the high contaminated region.

The order of concentration of selected metals in BCR sequential extraction in step 3 was Fe> Cu> As> Mn> Zn> Ni> Cr> Pb> Cd. The metal distribution of all selected metals in step 3 fraction will also be discussed later.

Table 32: The table of selected metals for eight samples in BCR sequential extraction ($mgkg^{-1}$)

		Cr	Cu	Ni	Pb	Zn	Cd	As	Mn	Fe
	Step 1	0.195	180.4	1.184	0.042	9.106	0.107	5.976	22.81	373.3
sample 1	Step 2	0.532	163.9	0.065	10.86	4.442	0.054	62.19	29.28	9554
	Step 3	1.986	192.2	0.585	1.922	6.448	0.025	4.084	13.70	1109
	Step 1	0.132	175.9	10.93	0.086	287.2	0.675	25.65	936.5	616.2
sample 2	Step 2	0.795	318.2	7.827	17.52	122.4	0.566	746.7	156.1	14697
	Step 3	4.212	364.6	5.577	3.425	46.49	0.076	177.0	48.71	2710
	Step 1	0.169	387.4	2.521	0.082	8.064	0.031	13.30	154.8	78.66
sample 3	Step 2	2.129	288.9	2.655	10.78	5.079	0.035	1283	94.31	7759
	Step 3	2.330	198.1	3.225	0.564	6.560	0.021	195.1	25.66	470.6
	Step 1	0.053	296.4	0.304	0.0003	9.907	0.057	128.5	13.26	96.90
sample 4	Step 2	1.378	387.6	0.774	10.82	11.92	0.167	2715	31.27	7761
	Step 3	1.658	125.3	0.917	0.488	6.529	0.029	234.6	15.18	459.7
	Step 1	0.104	255.1	0.792	0.063	4.590	0.030	85.34	19.15	235.6
sample 5	Step 2	1.154	217.3	0.968	15.68	5.384	0.049	2791	39.36	8602
	Step 3	1.946	1143	1.918	<LOD	12.06	0.049	186.9	19.81	821.3
	Step 1	0.056	212.6	0.331	0.002	4.519	0.041	40.87	14.42	167.6
sample 6	Step 2	1.100	359.2	0.543	14.87	7.293	0.104	3827	32.07	12697
	Step 3	0.887	217.5	0.556	0.731	9.758	0.031	218.0	32.00	982.0
	Step 1	0.044	185.3	0.275	0.060	3.029	0.028	19.59	10.52	327.3
sample 7	Step 2	1.091	274.4	0.525	19.23	5.007	0.058	2521	23.42	12721
	Step 3	0.898	628.5	0.454	<LOD	11.63	0.038	331.6	49.23	1287
	Step 1	0.061	177.7	0.224	0.017	6.006	0.049	66.96	6.534	86.86
sample 8	Step 2	1.005	411.1	0.929	20.32	14.19	0.194	3283	29.77	7958
	Step 3	0.565	125.9	0.377	0.705	7.190	0.048	158.5	16.73	452.1

Remark: <LOD means that the concentration of Pb is below the limit of detection.

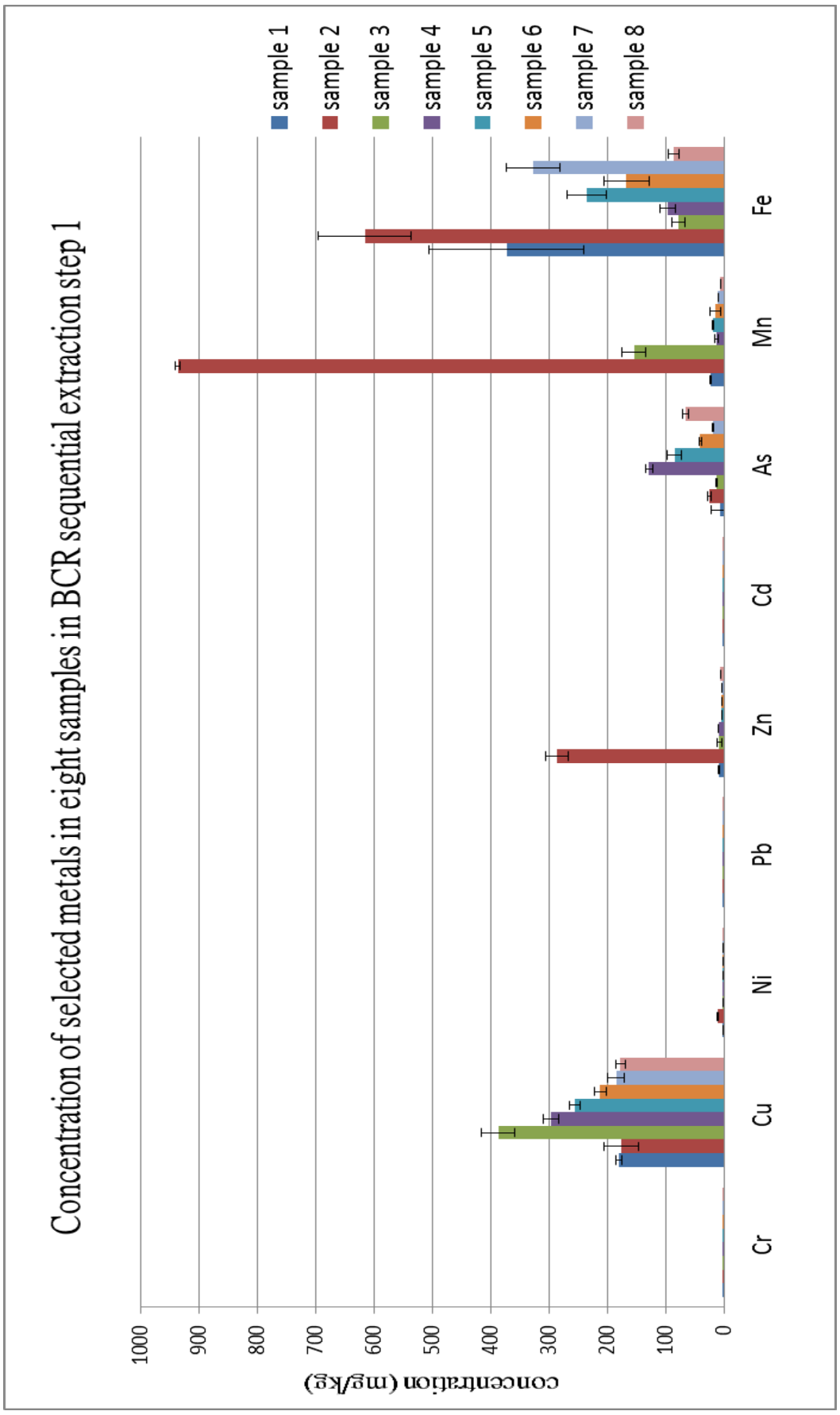

Figure 16: Concentration of selected metals in eight samples in BCR sequential extraction step 1 (±2 SD)

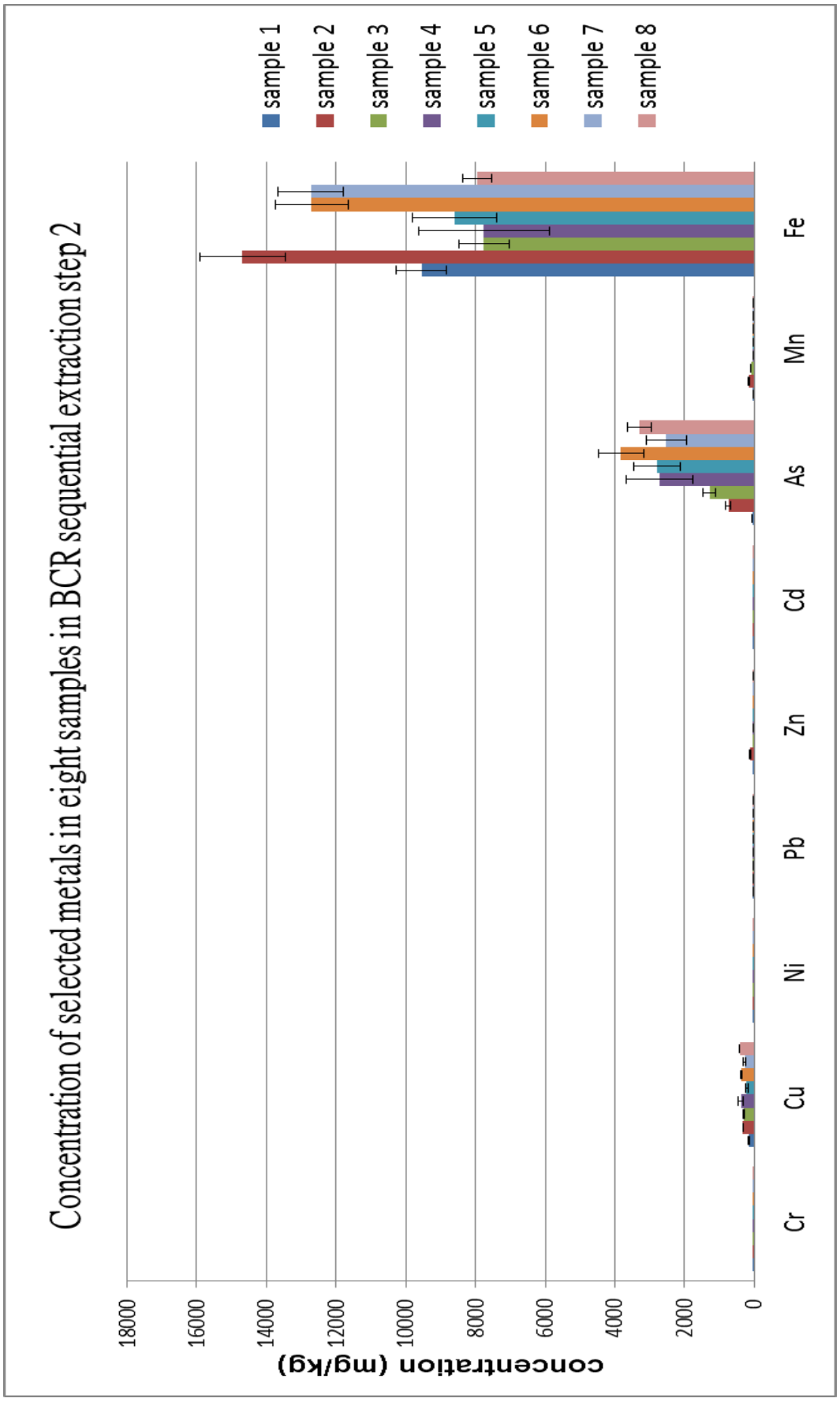

Figure 17: Concentration of selected metals in eight samples in BCR sequential extraction step 2 (±2 SD)

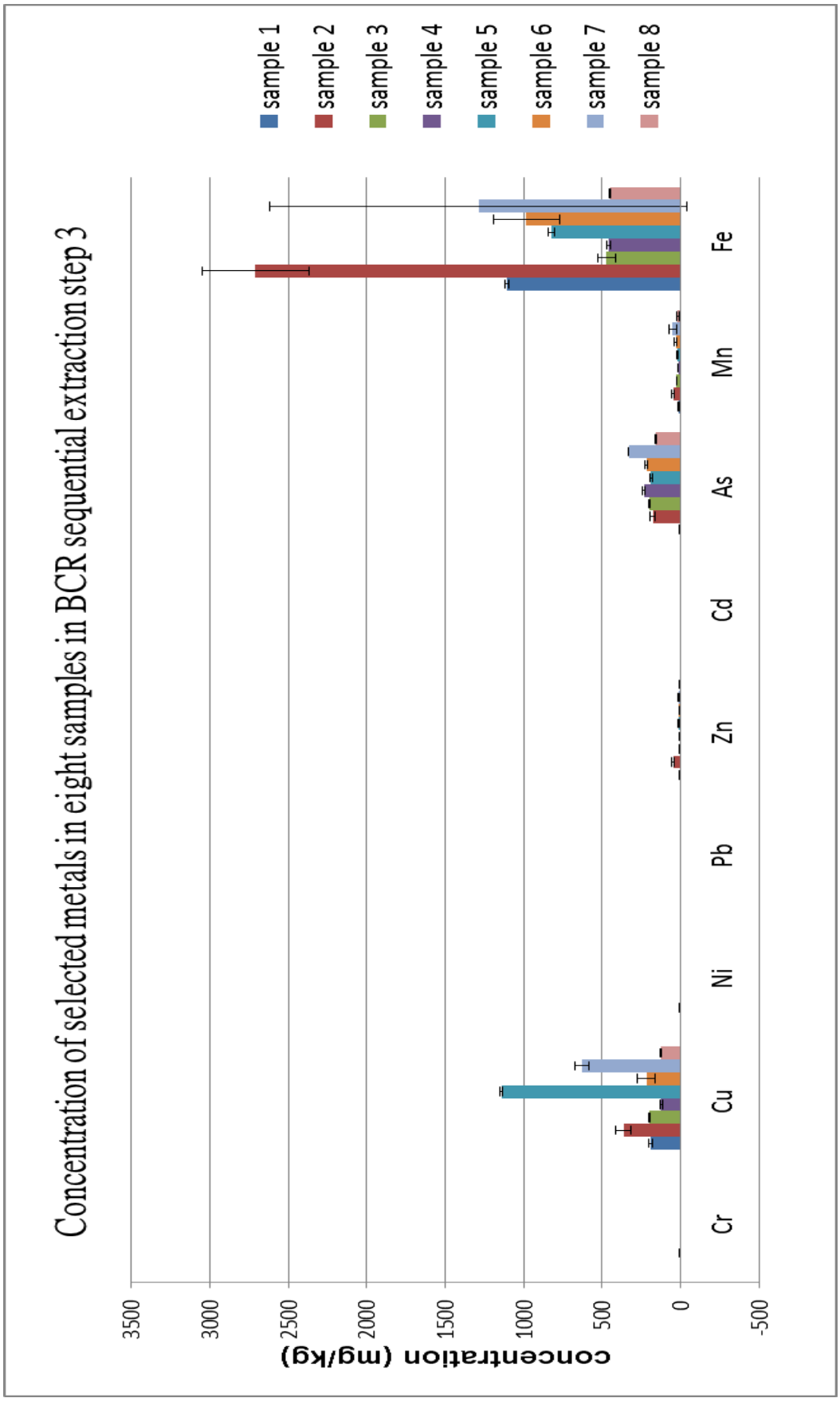

Figure 18: Concentration of selected metals in eight samples in BCR sequential extraction step 3 (±2 SD)

The distribution of each metal fraction for eight samples in BCR extraction

Chromium (Cr)

Figure 19 shows the Cr fraction of the BCR extraction with 3 steps. In samples 1 to 5, Cr has a large percentage range (from ~50% to 72%) in the step 3 fraction. The speciation of Cr in samples 1 to 5 is $Cr(OH)^{2+}$ and Cr_2O_3 species. The high proportion of Cr bounded to organic material and sulphides could be explained by Cr(III). Cr(III) readily forms complexes with hydroxyl, sulfate, organic ligands and other species. These complexes could increase its stability and raise the Cr_2O_3 boundary (Langmuir *et al.*, 2004). Also, some organic matter and Fe^{2+} could reduce Cr(VI) to Cr(III) (Langmuir *et al*., 2004). Hence the large amount of Cr(III) could form complexes and be adsorbed in the organic matter which could lead to high organic fraction in samples 1 to 5.

In samples 6 to 8, Cr has a significant percentage range (from ~35% to 44%) in the step 2 fraction. The speciation of Cr in these samples was Cr^{3+} species. The majority of Cr was associated with Fe-Mn oxide fraction (Figure 19). This is consistent with numerous studies which indicate that chromium is insoluble in these types of sediments (McGrath *et al*., 1990; McLean *et al.*, 1992; Ryan *et al*., 2002). Moreover, Cr(III) can form poorly soluble compounds, and is readily adsorbed by Fe-Mn oxides (Namiesnik *et al.*, 2010). This explains the high level of Cr that was extracted in step 2.

Figure 19 shows a low percentage range of Cr (from ~25 to 7%) associated with the exchangeable and carbonate fraction (step 1).

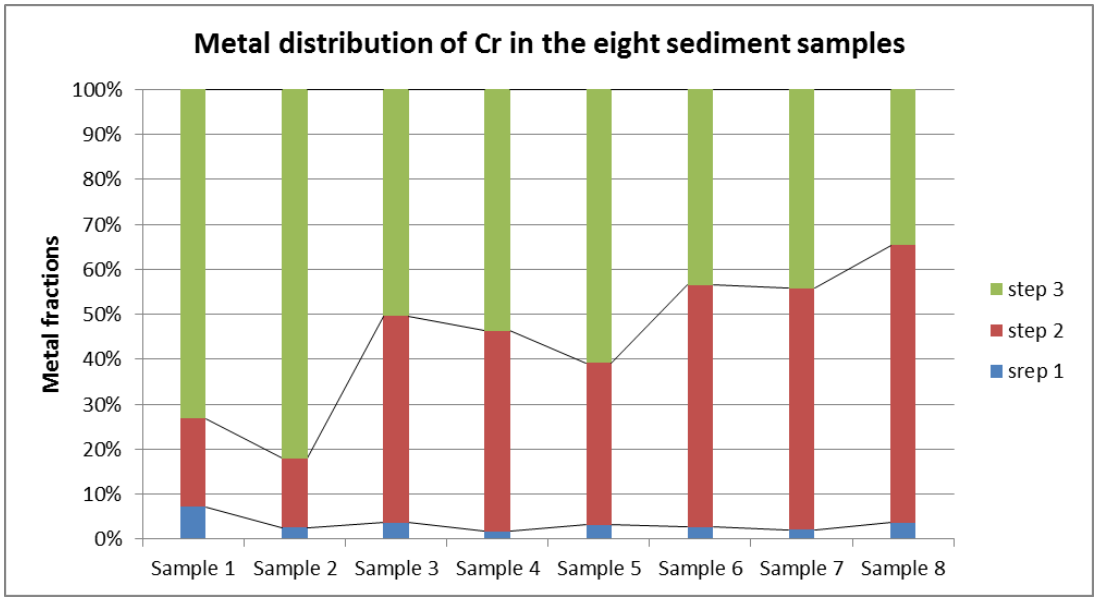

Figure 19: The metal fractions of Cr in the eight sediment samples

Copper (Cu)

Figure 20 shows the Cu fraction of the BCR extraction with 3 steps. In samples 1, 2, 5 and 7, Cu has a large percentage range (from ~36% to 71%) in the step 3 fraction. The high percentage of Cu bound to organic material and sulphides (step 3) could be explained by several factors. When metal is adsorbed by organic matter such as Cu^{2+} in particular, it may be strongly adsorbed, and be virtually independent of concentrations of the major metals (Lu et al., 2002). Also, Rozan *et al*., (2000) suggest that metal-sulfide complexes can dominate the speciation of some soft acid metals such as Cu, which give such inorganic complexes that are stable in sediment. Moreover, the high stability of organic Cu compounds result in stable complex formation between Cu and organic matter (Morillo *et al.*, 2004).

In samples 4, 6 and 8, the high percentage range of Cu (from ~45% to 58%) in the Fe-Mn oxide fraction suggests that adsorption might be an important control of Cu in the sediment. In a high percentage of the Cu sampling sites, the sediment might have a high surface and adsorbing capacity of Fe-Mn oxides which can combine with the ability of Cu^{2+} to replace Fe^{2+} in some Fe-oxides (Taylor, 1965). Hence, a higher amount of Cu in this fraction suggests that it might be remobilized under reducing conditions (Iwegbue *et al.*, 2007).

The low percentage range of Cu (from ~17% to 37%) in each sample except

sample 3 in the exchangeable fraction (step 1) suggests that Cu was low in the soluble form and tends to complex with organic matter or co-precipitate with hydrous Fe-Mn oxides (Iwegbue *et al.*, 2007).

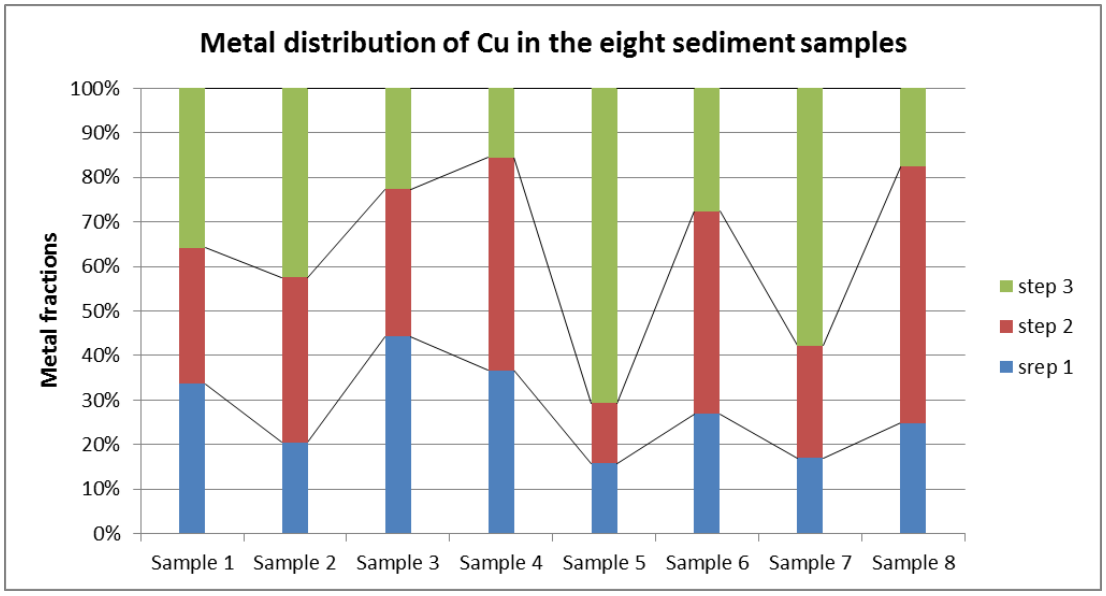

Figure 20: The metal fractions of Cu in the eight sediment samples

Nickel (Ni)

Figure 21 shows the Ni fraction of the BCR extraction with 3 steps. In samples 1 and 2, Ni has a large percentage range (from ~45% to 65%) in the step 1 fraction. The high percentage of Ni associated with the exchangeable fraction (step 1) could be explained by the speciation of Ni. All samples show the presence of Ni^{2+} species. However, Ni^{2+} might have a considerable electrostatic interaction between the positive ion and the negatively charged sediment surface. The step 1 fraction of Ni is more mobile and potentially more bioavailable within sediments (Cuong *et al.*, 2006).

The high percentage of Ni in the step 2 and step 3 fractions ranged from ~70% to 85%, as seen in samples 3 to 8. These sediments may have high surface and adsorbing capacity of Fe-Mn oxides. Also, pH might affect the metal adsorption and dissolution in steps 2 and 3. Generally, the Fe-Mn oxide adsorption capacity of metals increases with decreasing pH. Hence, a high percentage of step 2 and 3 fractions in samples 6 to 8 record a lower comparative pH than other samples.

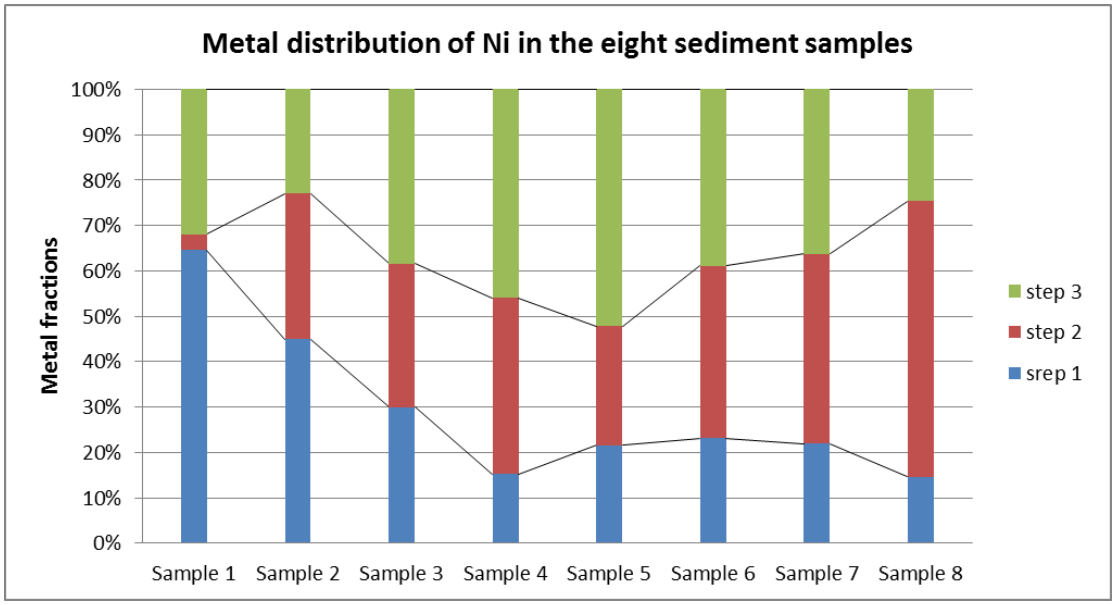

Figure 21: The metal fractions of Ni in the eight sediment samples

Lead (Pb)

Figure 22 shows the Pb fraction of the BCR extraction with 3 steps. All of the samples that were collected in the Great Consols reveal a large percentage range (from ~83% to 100%) in the step 2 fraction. The high percentage of Pb bounded to Fe-Mn oxides identifies with other studies. Pb is known to bind strongly onto hydrous Fe oxide surfaces {e.g. Balistneri et al., 1992}. The reason is that Pb is relatively immobile in sediments and ground waters, and has a strong tendency to be adsorbed by Fe and Mn oxides (Langmuir et al., 2004). Moreover, Pb can form stable complexes with Fe and Mn oxides (Ramos et al., 1994; Li et al., 2001; Gao et al., 2008). When environmental conditions become reducible, the insoluble complexes may be remobilized into the environment. Pb has a negligible percentage in the exchangeable fraction. The level of threat may not seriously affect the environment.

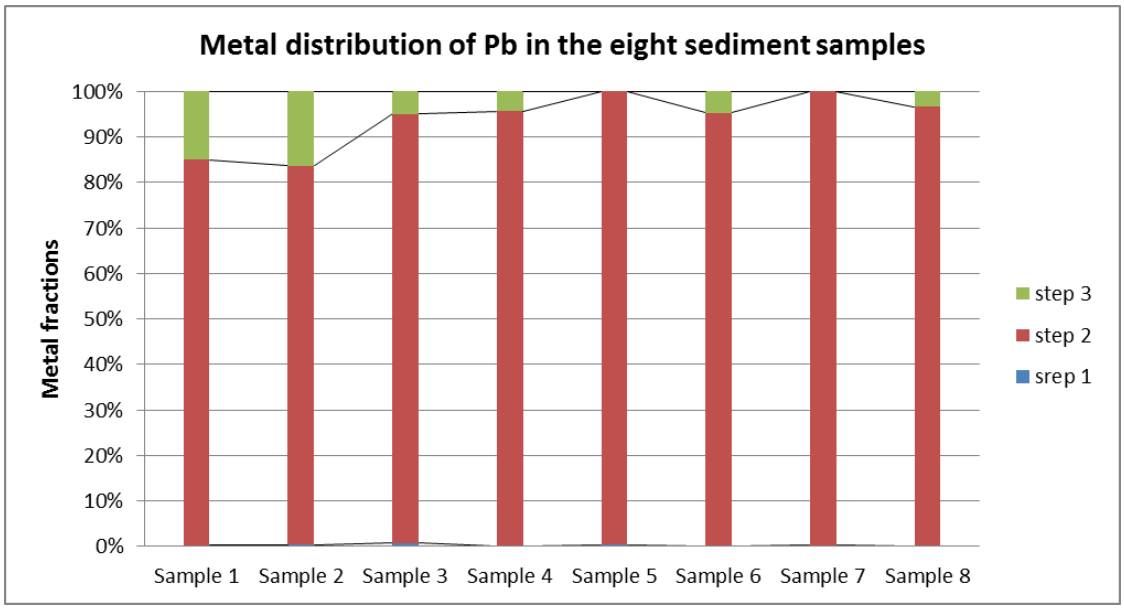

Figure 22: The metal fractions of Pb in the eight sediment samples

Zinc (Zn)

Figure 23 shows the Zn fraction of the BCR extraction with 3 steps. In samples 1 to 3, Zn has a large percentage range (from ~41% to 63%) in the step 1 fraction. The high percentage of Zn bounded to the exchangeable fraction (step 3) could be an indication of high mobility within this fraction. This metal could have potentially hazardous effects on the environment (Margui *et al*., 2004). Also, the result predicts that Zn associated with the exchangeable and acid soluble fraction might be released if acidic conditions were created (Vieira *et al*., 2009).

In samples 4 and 8, the percentage of the reducible fraction (step 2) in Zn was high, ranging from ~40% to 52%). Chlopecka *et al*. (1996) finds Zn to be strongly bound to the Fe-Mn oxide fraction. The reason is that Zinc oxide has stability constants that are high enough to be concentrated in this fraction.

In samples 5 to 7, the highest value for Zn (ranging from ~45% to 60%) is observed in the oxidizable fraction (step 3) in the sediments. Zn is mostly adsorbed by organic matter. Also, the high percentage of Zn in the step 3 fraction might result from the input of different types of organic matter from the anthropogenic discharges like the ores or industries.

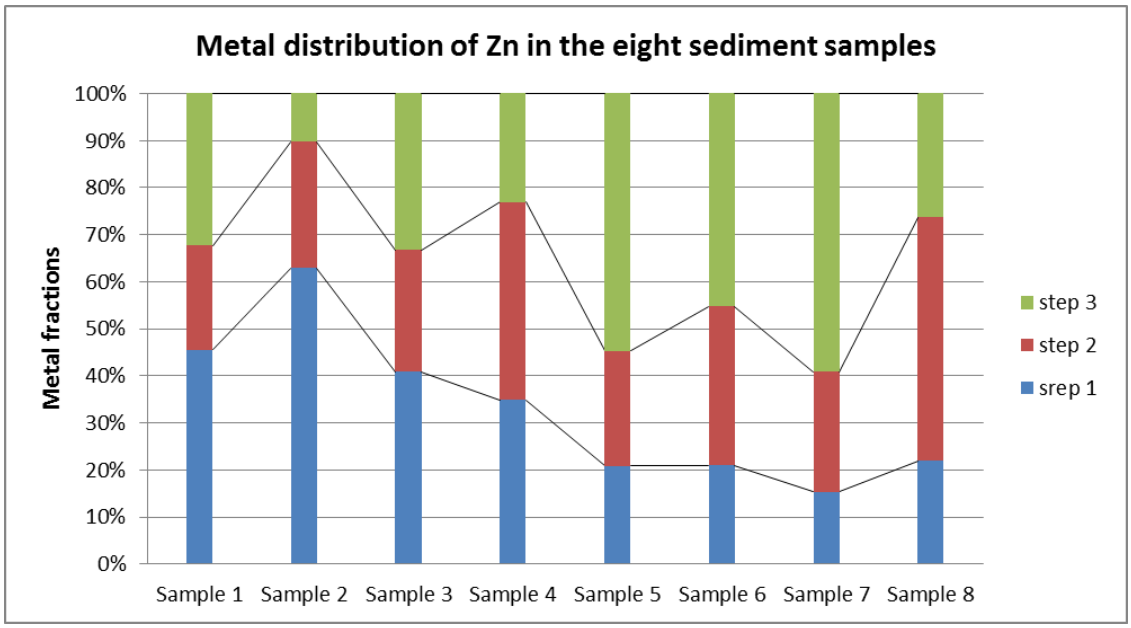

Figure 23: The metal fractions of Zn in the eight sediment samples

Cadmium (Cd)

Figure 24 shows that significant amounts of Cd (51% to 57%) in samples 1 and 2 were found in the exchangeable fraction (step 1). Taking into consideration the fact that high mobility of heavy metals presented in this fraction, it could be concluded that Cd may have a potentially hazardous effect on the environment (Margui *et al*., 2004). Moreover, the dominant proportion of Cd in step 1 indicates that Cd is held by electrostatic adsorption and is specifically adsorbed (Christensen *et al.*, 1999).

The high percentage of the reducible fraction of Cd (40% to 66%) in samples 3, 4, 6 to 8, with other fractions, demonstrates that the affinity for this metal in the reducible fraction of the surface sediments is high (Naji *et al.*, 2010).

The minor role of the organic fraction in the speciation of Cd in all samples except sample 5, noted in the present study, is consistent with findings of the low adsorption of Cd to organic matter (Baron *et al*., 1990; Chlopecka *et al*., 1996), with evidence that Cd does not appear to form strong organic complexes (Sposito *et al*., 1982; Keefer *et al*., 1984).

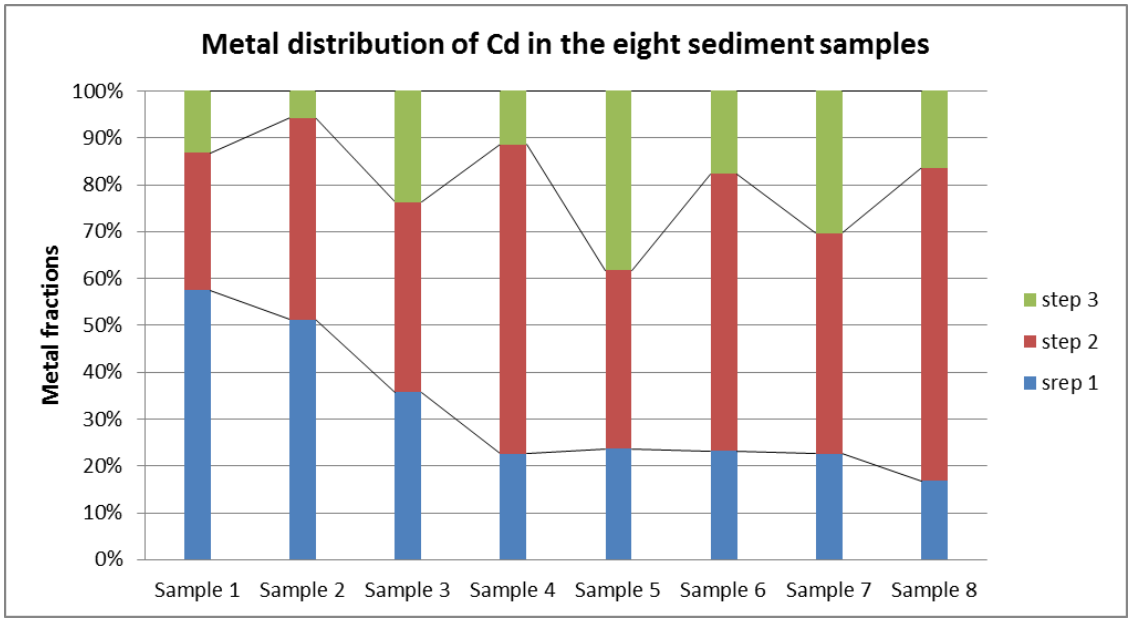

Figure 24: The metal fractions of Cd in the eight sediment samples

Arsenic (As)

Figure 25 shows the As fraction of the BCR extraction with 3 steps. A dominant proportion of As is found in the reducible fraction (78% to 93%) within all samples. The sequential extraction data shows that As is mainly bound to Fe-Mn oxides. Also, Fe-Mn oxides are the most significant As carriers in the mine wastes sediment from the Devon Great Consols Mine. This supports the role of the Fe-Mn oxides as a stable As binding phase in an oxidizing and acidic environment (Palumbo-Poe *et al.*, 2007a). Furthermore, Fe-Mn oxides are excellent scavengers for As and are affected by Eh and pH changes which commonly form on grains in the presence of dissolved O_2 during the transport of sediment (Anawar *et al*., 2010). In addition, all As species are present as $H_2AsO_4^-$. Under weakly acidic conditions, As(V) could be co-precipitated with hydrous iron oxides (Wilson *et al*.,1978). It is presumed that both adsorption of As on the Fe rich oxides exists on the surfaces of the sediments, and that the incorporation of As into the sediments by co-precipitation at the time of formation of hydrous iron oxides controls the As distribution in sediments (Mok *et al*., 1989).

In the Devon great Consols, there are high levels of As adsorbed in the soil and sediment. A large proportion of the As mineral was Arsenopyrite which was the primary ore mineral. This was brought to the arsenic works from various working mines (Palumbo-Roe *et al*., 2007b). In its environmental

condition, As occurs as oxyanions in oxidizing environments. As is relatively mobile, so determination of mobility is necessary. The mobility of metals will be discussed later.

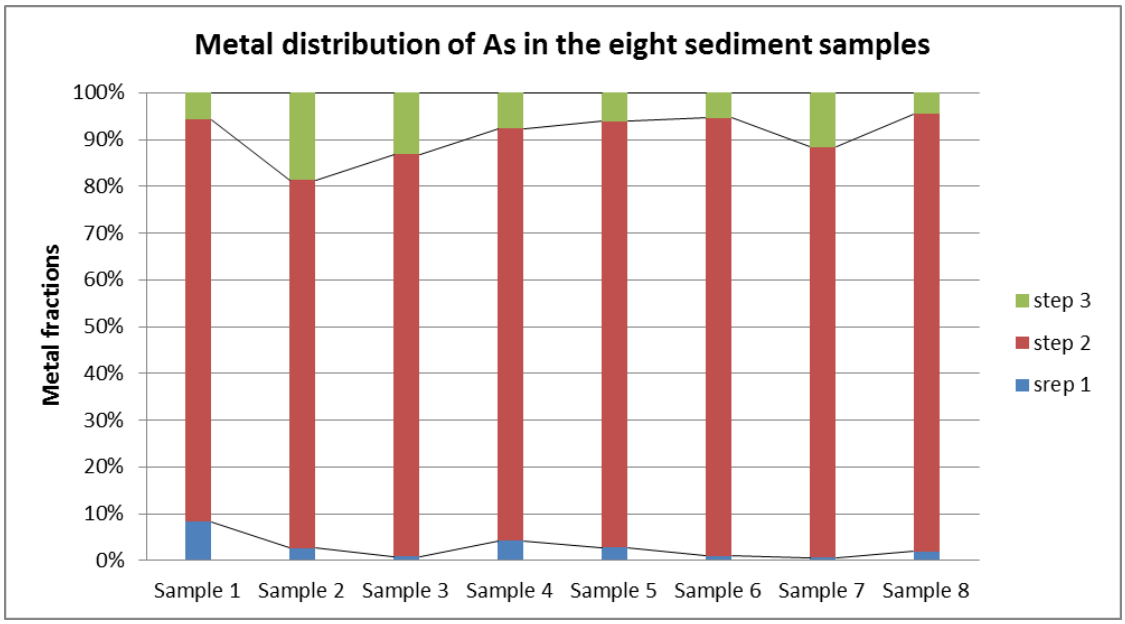

Figure 25: The metal fractions of As in the eight sediment samples

Manganese (Mn)

Figure 26 shows the Mn fraction of the BCR extraction with 3 steps. The highest proportion of Mn is found in the exchangeable fraction (78% to 93%) in samples 2 and 3. In this fraction, weakly adsorbed Mn is retained on the sediment surface by relatively weak electrostatic interactions (Tuan *et al*., 2004). Mn might be released by ion-exchange processes and dissociation of the Mn-carbonate phase (Tessier *et al*., 1979). The results indicate that a considerable amount of Mn might be released into the environment if conditions become more acidic (Thomas *et al*., 1994).

The most dominant fraction was the Mn extracted with hydroxylammonium chloride in samples 1, 4, 5 and 8, with extraction yields ranging from 13 to 54%, thus indicating that Mn is mainly associated with Fe-Mn oxides. The reason could be explained by the precipitating effects of Fe-Mn oxide hydroxide in water (Iwegbue *et al*., 2007). Also, Fe oxide surfaces also have the ability to desorb the Mn ions from water (Lopez *et al*., 2010). In addition, large proportions of Mn existing as oxides might be released if the sediment is subjected to more reducing conditions (Panda *et al*., 1995).

In samples 6 and 7, Mn is speciated into organic or sulfide fractions. This could be mobilized to more available forms as a result of chemical and biological transformations in sediment—water systems (Gambrell *et al*., 1983).

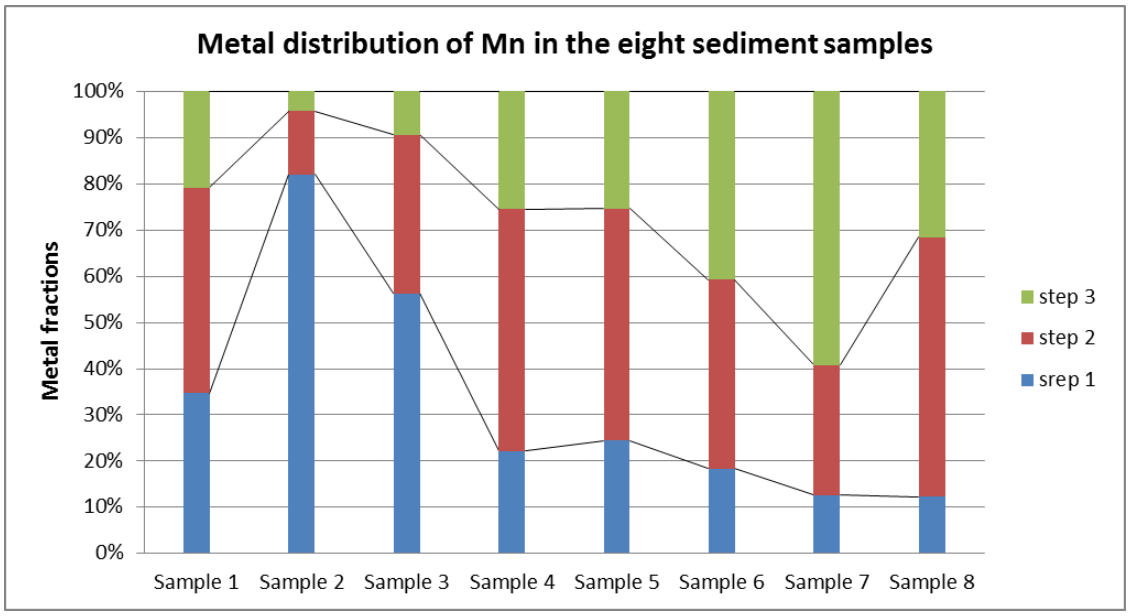

Figure 26: The metal fractions of Mn in the eight sediment samples

Iron (Fe)

Figure 27 shows the Fe fraction of the BCR extraction with 3 steps. The most dominant proportion of Fe was found in the reducible fraction (81% to 93%) in all samples. The high levels of Fe in the Fe-Mn oxide fraction could be explained by the precipitation effects of Fe-Mn oxyhydroxides in water (Iwegbue *et al*., 2007).

The result shows that the highest yield of Fe in the exchangeable fraction in sample 2 was about 3%. The speciation of Fe in sample 2 presents as $FeCO_3$ in the Eh-pH diagram. It is consistent with experimental results. Sequestration of heavy metals by carbonates is an important mechanism in the mobility and availability of heavy metals in the environment. Carbonates have been implicated as immobilizing most of the heavy metals by providing an adsorbing surface and by buffering the soil and sediment pH (Uwumarongie-Ilori *et al*., 2011). In addition, Lambert *et al*., (1997) states that carbonates are only stable in soils and sediments with high pH. Moreover, sample 2 was affected by man-made activities that influence the metal levels in sediments (Uwumarongie-Ilori *et al*., 2011).

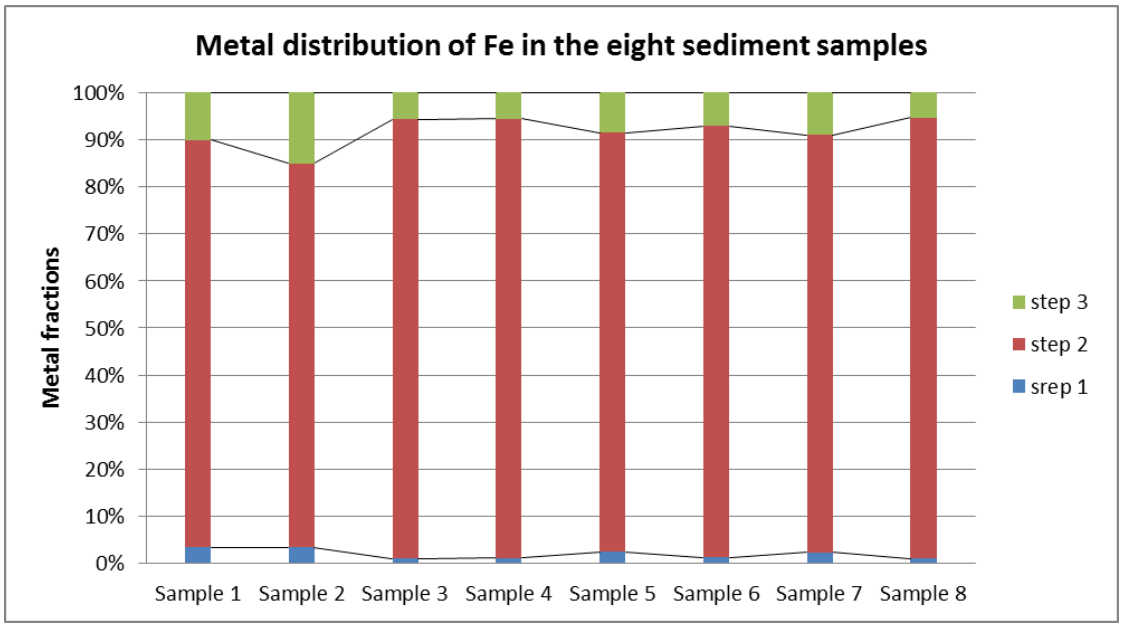

Figure 27: The metal fractions of Fe in the eight sediment samples

Mobility of heavy metals in eight locations

The step 1 fraction was the most mobile that could be easily released into the environment. The higher percentage of metals in the step 1 fraction might produce high mobility within the environment.

The mobility of Cr decreased in the order of sample 1 (0.072%) > sample 8 (0.037%) ~ sample 3 (0.037%) > sample 5 (0.032%) > sample 6 (0.027%) > sample 2 (0.026%) > sample 7 (0.022%) > sample 4 (0.017%).

The mobility of Cu decreased in the order of sample 3 (0.443%) > sample 4 (0.366%) > sample 1 (0.336%) > sample 6 (0.269%) > sample 8 (0.249%) > sample 2 (0.205%) > sample 7 (0.170%) > sample 5 (0.158%).

The mobility of Ni decreased in the order of sample 1(0.646%) > sample 2 (0.449%) > sample 3 (0.300%) > sample 6 (0.231%) > sample 7 (0.219%) > sample 5 (0.215%) > sample 4 (0.152%) > sample 8 (0.147%).

The mobility of Pb decreased in the order of sample 3 (0.007%) > sample 2 (0.004%) ~ sample 5 (0.004%) > sample 1 (0.003%) ~ sample 7(0.003%) > sample 8 (0.001%) > sample 6 (~0%) ~ sample 4 (~0%).

The mobility of Zn decreased in the order of sample 2 (0.630%) > sample 1 (0.455%) > sample 3 (0.409%) > sample 4 (0.349%) > sample 8 (0.219%) >

sample 6 (0.210%) > sample 5 (0.208%) > sample 7 (0.154%).

The mobility of Cd decreased in the order of sample 1 (0.575%) > sample 2 (0.512%) > sample 3 (0.357%) > sample 5 (0.237%) > sample 6 (0.232%) > sample 4 (0.226%) ~ sample 7 (0.226%) > sample 8 (0.169%).

The mobility of As decreased in the order of sample 1 (0.083%) > sample 4 (0.042%) > sample 5 (0.028%) > sample 2 (0.027%) > sample 8 (0.019%) > sample 6 (0.010%) > sample 3 (0.009%) > sample 7 (0.007%).

The mobility of Mn decreased in the order of sample 2 (0.821%) > sample 3 (0.563%) > sample 1 (0.347%) > sample 5 (0.245%) > sample 4 (0.222%) > sample 6 (0.184%) > sample 7 (0.127%) > sample 8 (0.123%).

The mobility of Fe decreased in the order of sample 1 (0.034%) ~ sample 2 (0.034%) > sample 5 (0.024%) > sample 7 (0.023%) > sample 4 (0.012%) ~ sample 6 (0.012%) > sample 8 (0.010%) > sample 3 (0.009%).

The overall mobility of selected metals in the eight samples decreased in the following order: Mn (0.0821% - 0.123%) > Ni (0.646% - 0.147%) > Zn (0.630% - 0.154%) > Cd (0.575% - 0.169%) > Cu (0.443% - 0.158%) > As (0.083% - 0.007%) > Cr (0.072% - 0.017%) > Fe (0.034% - ~0%).

The highest proportion of Mn (0.0821% - 0.123%) was present in all samples due to the presence of Mn coating around silicate grains and discrete grains of oxide mineral. This generally occurs as poor crystallized manganese oxides (Drever, 1997). Therefore, it is relatively easy to extract compared to other metals. Hence, the concentration of Mn was highest in this step and the most mobile in the environment.

Figure 28 indicates a high percentage of Mn, Ni and Zn present in the step 1. It reflects the greater mobility of these metals and could have potential hazardous effects on the environment (Margui *et al*., 2004). The low percentage of Fe in the step 1 may be due to precipitation of Fe oxides and accumulation of Fe-Mn oxides, which were not easy to extract in the step1 (Iwegbue *et al*., 2007).

Figure 29 shows the mobility of selected metals in the eight samples. The mobility of all the metals in all locations decreased in the order of: sampling site 2 > sampling site 1 > sampling site 3 > sampling site 4 > sampling site 6 > sampling site 5 > sampling site 8 > sampling site 7. The results identified that site 2 had the overall largest percentage of heavy metals in the exchangeable fraction (step 1), and that a considerable proportion of metals might be released to the into environment when conditions become more acidic (Nemati *et al*., 2009).

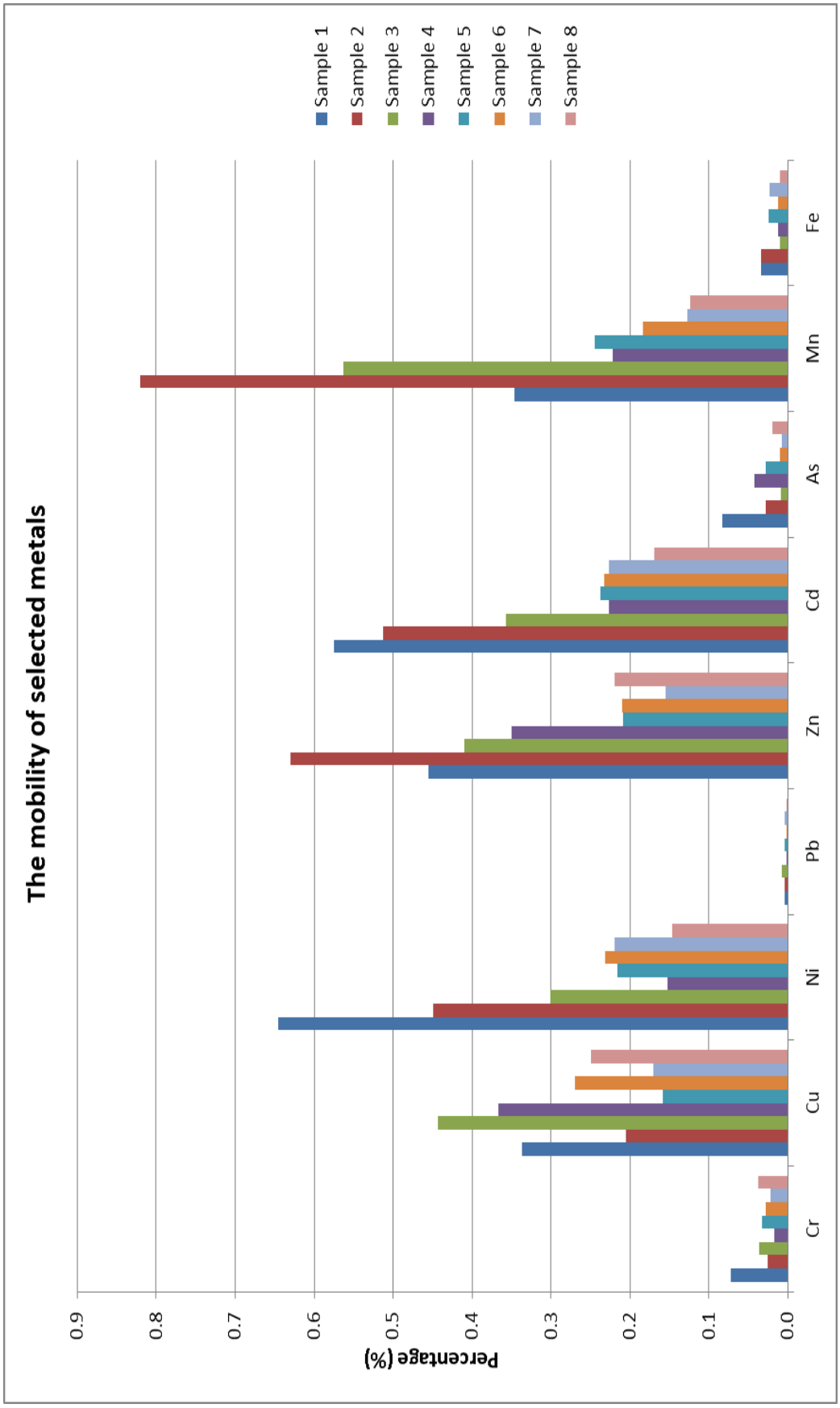

Figure 28: The mobility of selected metals

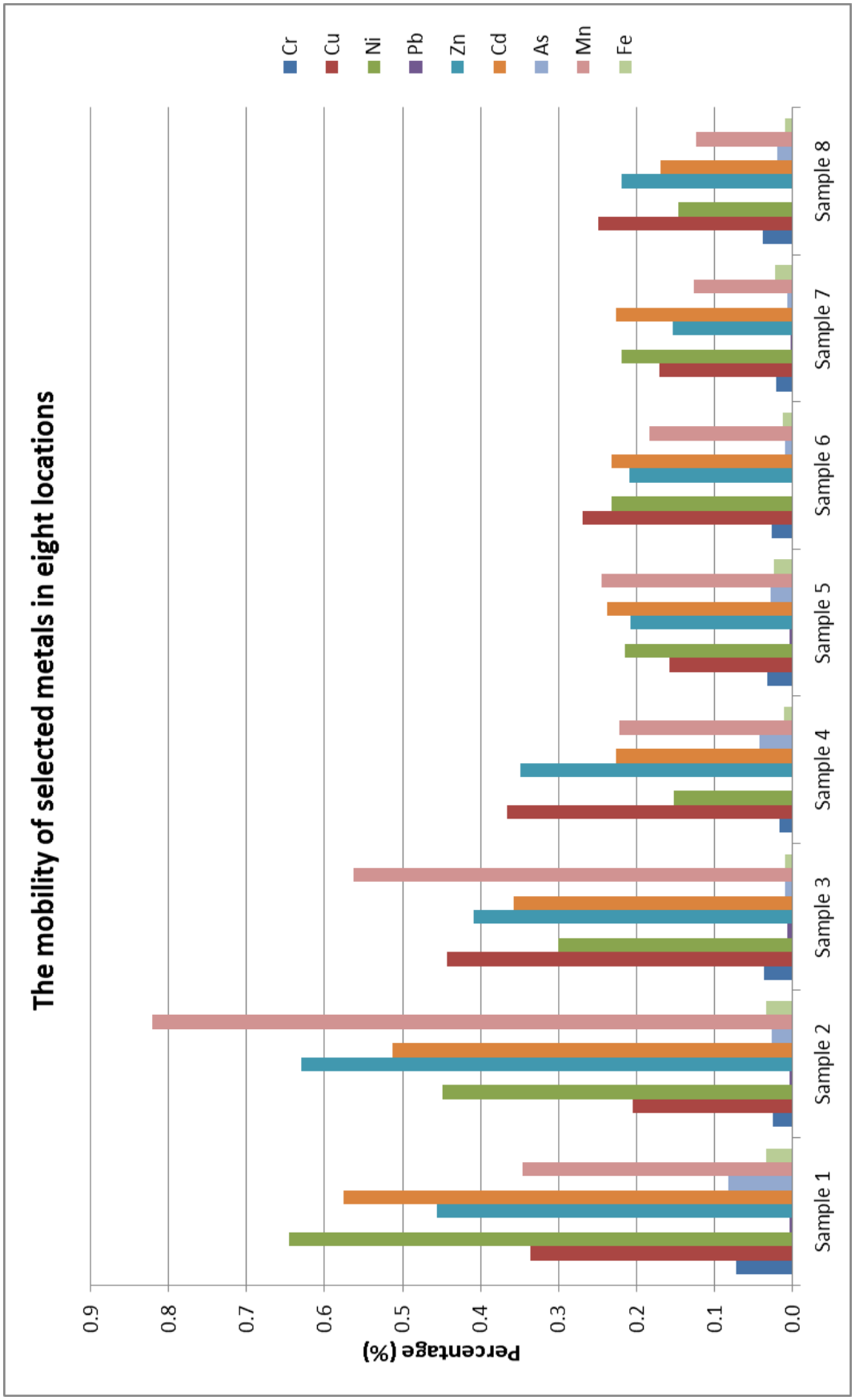

Figure 29: The mobility of selected metals in eight locations

Bioavailability of heavy metals in eight locations

The exchangeable fraction of sediments is very important because of the high mobility of metals from this fraction to the aqueous phase (Uwumarongie-Ilori *et al*., 2011). Metals bound to the Fe-Mn oxides are more thermodynamically unstable and more easily leached than the metals bound to organics and sulfides. The combined conditions of pH and redox potential are required for the release of metals bound to organics and sulfides fractions, which are not easily attainable (Adekola *et al*., 2010).

The exchangeable (step 1) and Fe-Mn oxide (step 2) fractions were grouped as bioavailable, and those bound to organic matter and sulfide (step 3) were grouped as non-bioavailable on the basis of relative mobility and toxicity to the aquatic environment.

The bioavailability of metals for all locations is represented in Table 33. Also, the percentage of bioavailability of each metal for each location was represented in Figures 30 to 37.

The bioavailable fractions represent the fraction for when the pH and redox conditions were favorable. These metals are soluble and could be taken up by aquatic plants or ingested by animals. In addition, the concentration of the bioavailable fraction reached 60%, which is a serious source of environmental concern (Adekola *et al*., 2010). Bioavailability is related to solubility, the metals' bioavailability decreased in the order of exchangeable forms>acid reduction forms>organic forms>residual forms (Naji et al., 2010).

Table 33: The contributions of bioavailability and non-bioavailability of metals for all locations ($mgkg^{-1}$)

Location	Fraction	Cr	Cu	Ni	Pb	Zn	Cd	As	Mn	Fe
1	Bioavailability	0.727	344.3	1.249	10.90	13.55	0.161	68.16	52.08	9927
	Non- bioavailability	1.986	192.2	0.585	1.922	6.448	0.025	4.08	13.70	1109
2	Bioavailability	0.927	494.1	18.758	17.60	409.6	1.241	772.4	1093	15313
	Non- bioavailability	4.212	364.6	5.577	3.425	46.49	0.076	177.0	48.71	2710
3	Bioavailability	2.298	676.3	5.176	10.86	13.14	0.066	1296	249.1	7837
	Non- bioavailability	2.330	198.1	3.225	0.564	6.560	0.021	195	25.66	470.6
4	Bioavailability	1.431	684.0	1.078	10.82	21.83	0.224	2844	44.52	7858
	Non- bioavailability	1.658	125.3	0.917	0.488	6.529	0.029	234.6	15.18	459.7
5	Bioavailability	1.258	472.4	1.760	15.74	9.975	0.079	2877	58.52	8838
	Non- bioavailability	1.946	1142.6	1.918	<LOD	12.06	0.049	186.9	19.81	821.3
6	Bioavailability	1.156	571.8	0.874	14.87	11.81	0.144	3867	46.48	12864
	Non- bioavailability	0.887	217.5	0.556	0.731	9.758	0.031	218.0	32.00	982.0
7	Bioavailability	1.134	459.7	0.800	19.29	8.036	0.086	2540	33.94	13049
	Non- bioavailability	0.898	628.5	0.454	<LOD	11.63	0.038	331.6	49.23	1287
8	Bioavailability	1.066	588.9	1.153	20.34	20.20	0.243	3350	36.31	8045
	Non- bioavailability	0.565	125.9	0.377	0.705	7.190	0.048	158.5	16.73	452.1

Remark: <LOD means that the concentration of Pb is below the limit of detection.

Sampling site 1

Figure 30 shows that the percentages of some metals in the bioavailable fractions were more than 60%. These metals included Cu, Ni, Pb, Zn, Cd, As, Mn and Fe. In particular, Pb, Cd, As and Fe were above 80%. The bioavailability of metals followed the order As> Fe> Cd> Pb> Mn> Ni> Zn> Cu>> Cr.

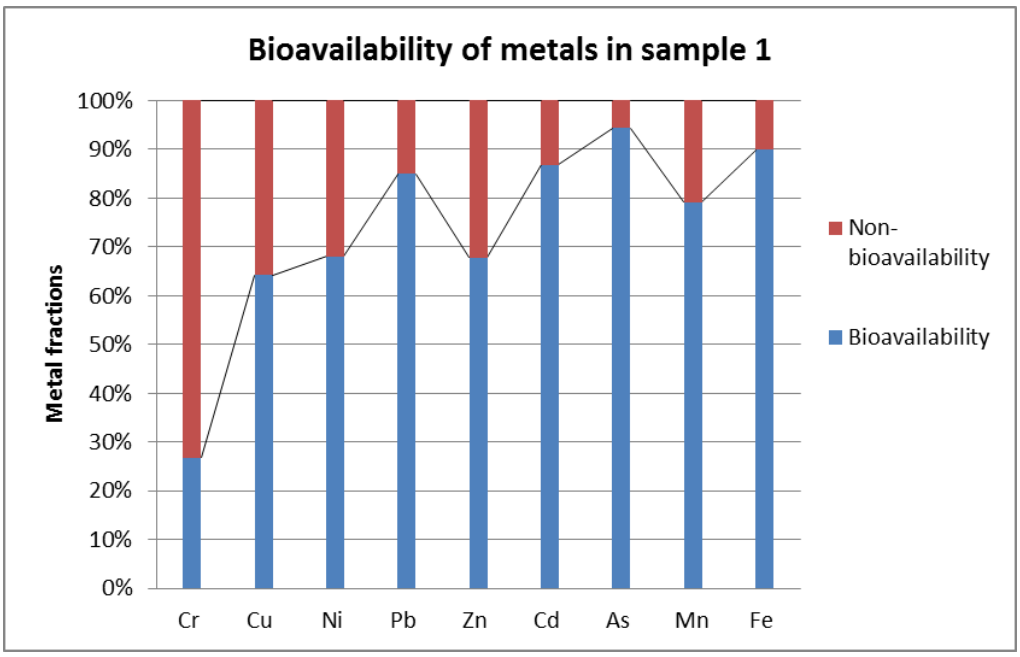

Figure 30: The percentage of bioavailability of metals in sample 1

Sampling site 2

Figure 31 shows that the percentages of some metals in the bioavailable fractions were more than 60%. These metals include Ni, Pb, Zn, Cd, As, Mn and Fe. Most of the metals (e.g. Pb, Zn, Cd, As, Mn and Fe) were higher than 80%. The bioavailability of metals followed the order of Mn> Cd> Zn> Fe> Pb> As> Ni>> Cu>> Cr.

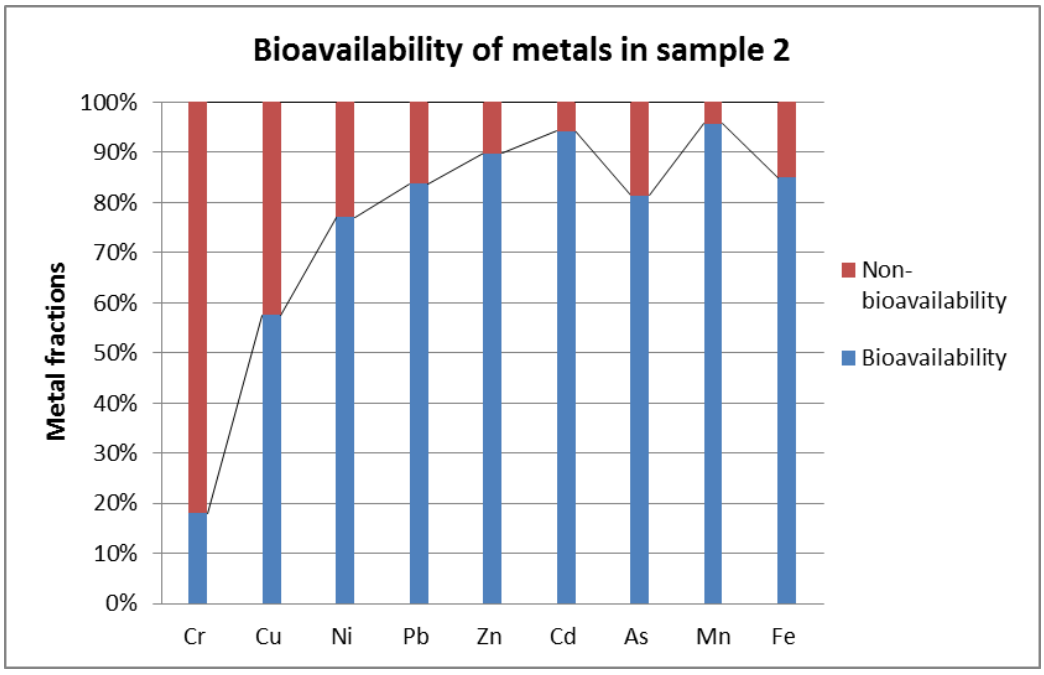

Figure 31: The percentage of bioavailability of metals in sample 2

Sampling site 3

Figure 32 shows that the percentages of all metals in the bioavailable fractions were more than 60% except Cr. Pb, As, Mn and Fe were higher than 80%. The bioavailability of metals followed the order of Pb~ Fe> Mn> As> Cu> Cd> Zn> Ni> Cr.

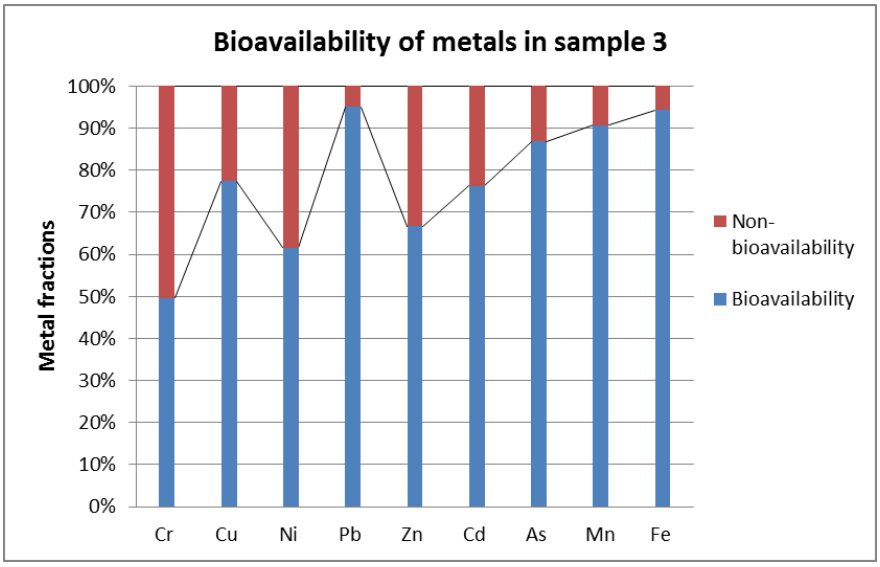

Figure 32: The percentage of bioavailability of metals in sample 3

Sampling site 4

Figure 33 shows that the percentages of some metals in the bioavailable fractions were more than 60%, including Cu, Pb, Zn, Cd, As, Mn and Fe. Some of the metals (e.g. Cu, Pb, Cd, As and Fe) were higher than 80%. The bioavailability of metals followed the order of Pb> Fe> As> Cd> Cu> Zn> Mn> Ni> Cr.

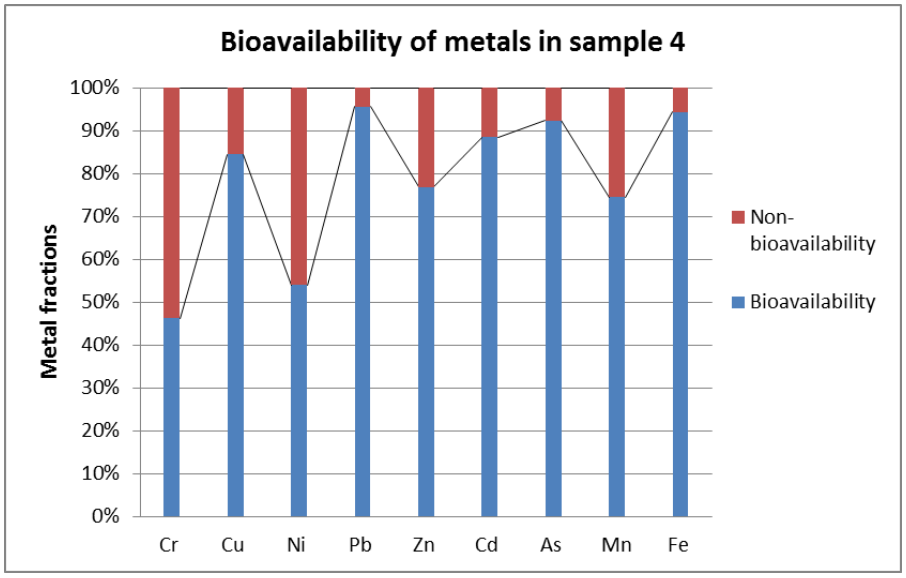

Figure 33: The percentage of bioavailability of metals in sample 4

Sampling site 5

Figure 34 shows that the percentages of half metals in the bioavailable fraction were higher than 60%. These metals include Pb, Cd, As, Mn and Fe. Pb, As and Fe were high than 80%. The bioavailability of metals followed the order of Pb> As> Fe> Mn> Cd> Pb> Zn> Cr> Cu.

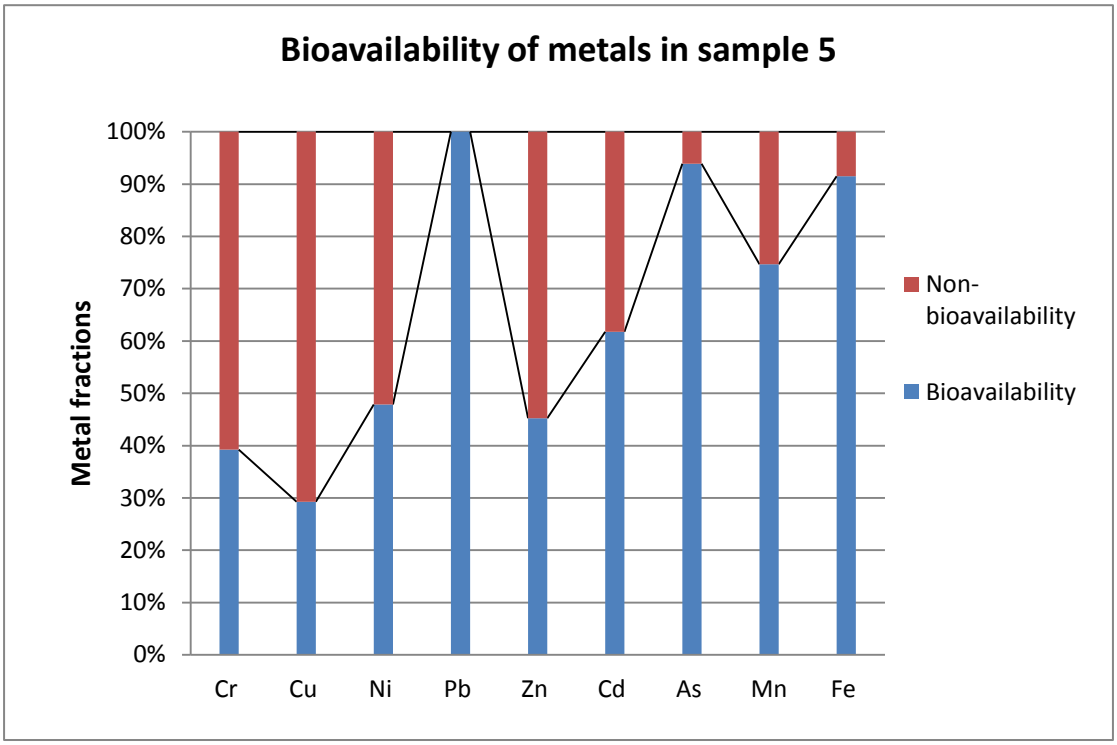

Figure 34: The percentage of bioavailability of metals in sample 5

Sampling site 6

Figure 35 shows that the percentages of some metals in the bioavailable fractions were higher than 60%, including Cu, Ni, Pb, Cd, As and Fe. Some of these metals (e.g. Pb, Cd, As and Fe) were higher than 80%. The bioavailability of metals followed the order of Pb~ As> Fe> Cu> Ni> Mn> Mn> Cr> Zn.

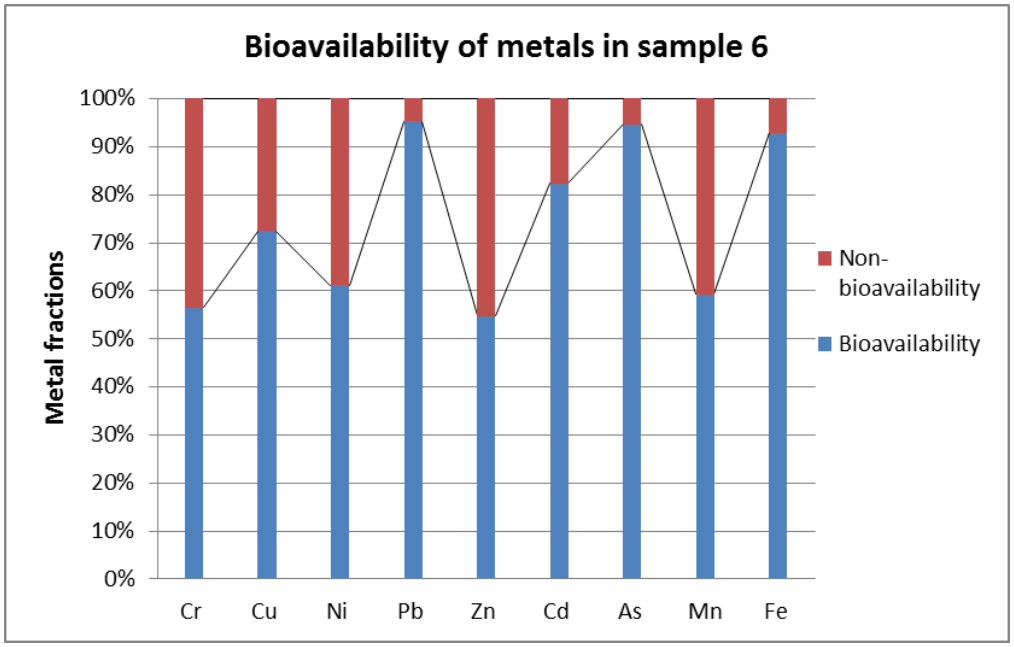

Figure 35: The percentage of bioavailability of metals in sample 6

Sampling site 7

Figure 36 shows that the percentages of half metals in the bioavailable fractions were higher than 60%. These metals includes Ni, Pb, Cd, As and Fe, with Pb, As and Fe higher than 80%. The bioavailability of metals followed the order of Pb> Fe> As> Cd> Ni> Cr> Cu> Zn~ Mn.

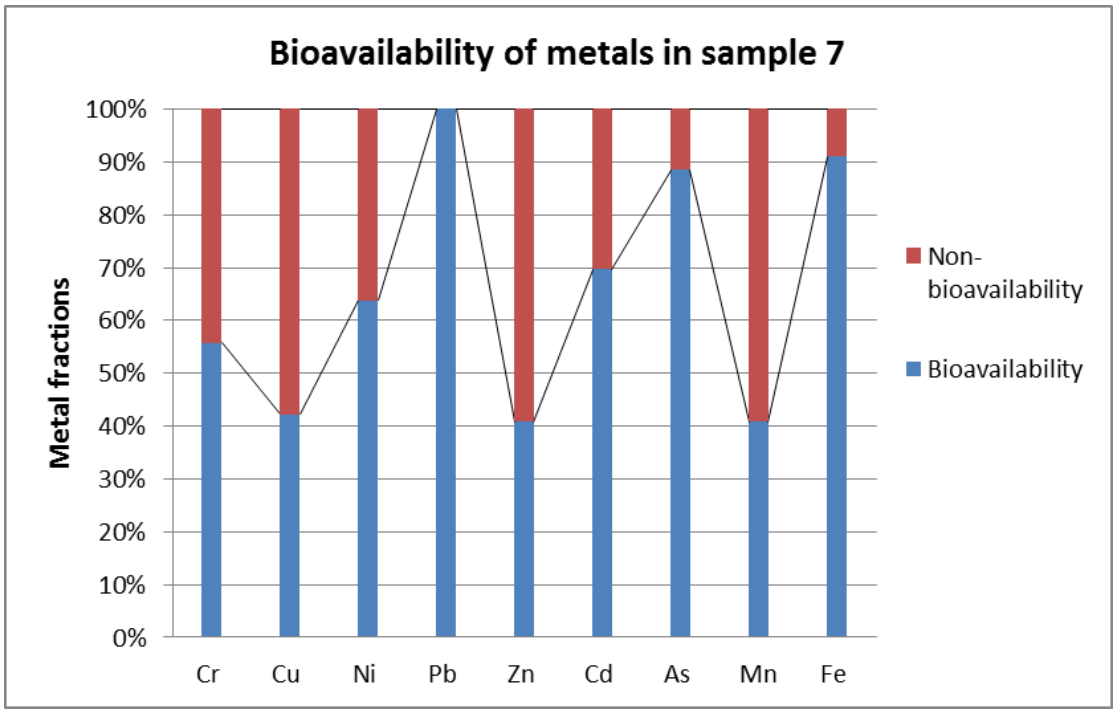

Figure 36: The percentage of bioavailability of metals in sample 7

Sampling site 8

Figure 37 shows that the percentages of all metals in the bioavailable fractions were greater than 60%. A few metals (e.g. Cu, Pb, Cd, As and Fe) were higher than 80%. Generally, the most serious pollution occurred in site 8. The percentage of Pb, As and Fe in the bioavailable fractions were over 90%. The bioavailability of metals followed the order of Pb> As> Fe> Cd> Cu> Ni> Zn> Mn> Cr.

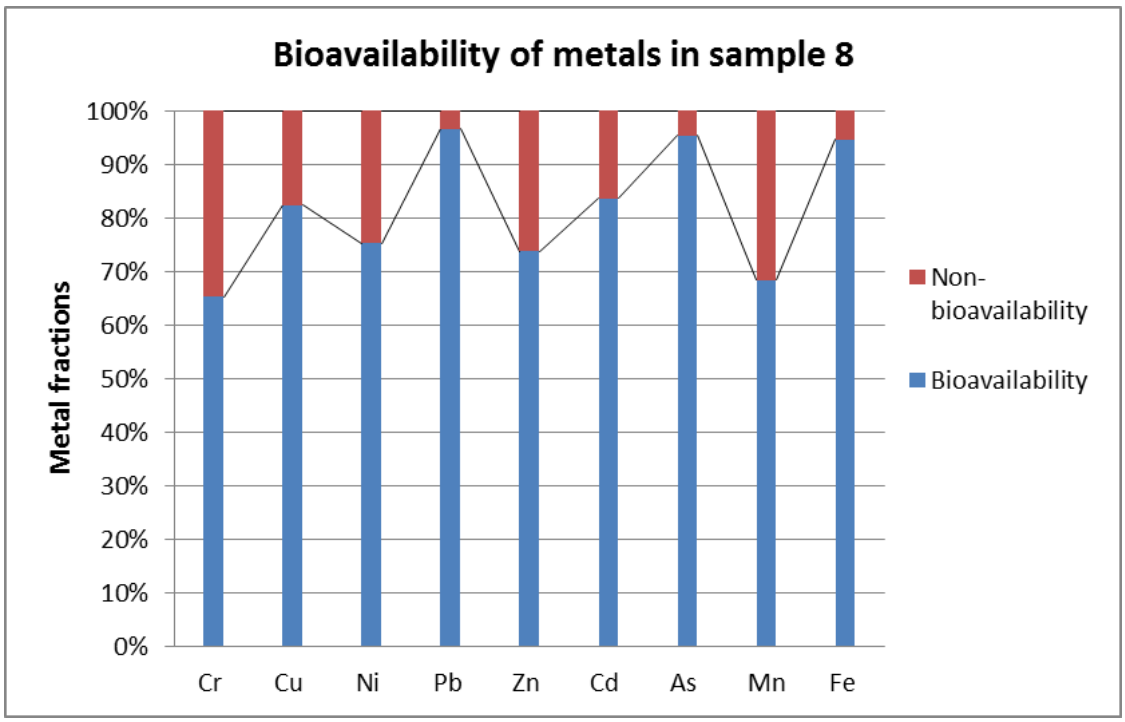

Figure 37: The percentage of bioavailability of metals in sample 8

Figures 30 to 37 show the overall bioavailability of metals in the eight locations. The bioavailability of all the selected metals in all sampling sites decreased in the order of: sampling site 8 > sampling site 3 > sampling site 1 > sampling site 1 > sampling site 6 > sampling site 4 > sampling site 2 > sampling site 5 > sampling site 7. In sample 8, the bioavailability of all metals was over 60%. Pb, As and Fe, in particular, were higher than 90%. The results show that a serious problem exists in site 8. The large amount of metals might be due to the dissolution of Pb, Fe and As minerals (e.g. FeAsS, $FeAsO_4 \cdot 2H_2O$ and PbS). In addition, the Devon Great Consols has produced large amounts of As and Cu in the past. The metals were accumulated in the sediment through the tailing run-off stream.

Figure 38 shows the overall bioavailability of the selected metal concentrations.

Sample 2 has particularly high amounts of Mn and Pb as it was the most contaminated area. The results from sample 2t were not taken into consideration in the order of bioavailability. The bioavailability of metals decreased in the order of: Fe (7837 – 15313 $mgkg^{-1}$) > As (68.1 – 3867 $mgkg^{-1}$) > Cu (344.3 – 684.0 $mgkg^{-1}$) > Mn (33.94 – 249.1 $mgkg^{-1}$) > Pb (10.82 – 20.34 $mgkg^{-1}$) > Zn (8.036 – 21.83 $mgkg^{-1}$) > Cr (0.727 – 2.2985 $mgkg^{-1}$) > Cd (0.066 – 1.241 $mgkg^{-1}$). The results show that the most potential bioavailable metals were found in all the locations, producing high concentrations of bioavailable Fe, As and Cu within the environment. The metals potential was taken up by plants and ingested by organisms in the aquatic system. The anthropogenic inputs (human activities) were different from one location to another, hence the levels of metals were also different (Adekola *et al*., 2010). The high levels of bioavailable metals might present a real threat as these metals are transferred into the food chain from sediment contamination (Yusuf, 2007). Furthermore, these metals might become a cumulative poison in mammals if levels reach above the threshold (Tokaliolu *et al*., 2003). Moreover, there was some variability in the range of the concentrations of each metal in all locations, which could be attributed partly to the weathering and transport properties of minerals and other components of the sediments (Adekola *et al*., 2010). The results match the largest productions of As and Zn in the nineteenth century. Eventually, the bioavailable metals were released into the Tamar River and were hazardous to the nearest city, Gunnislake, a town located downstream on the Tamar River.

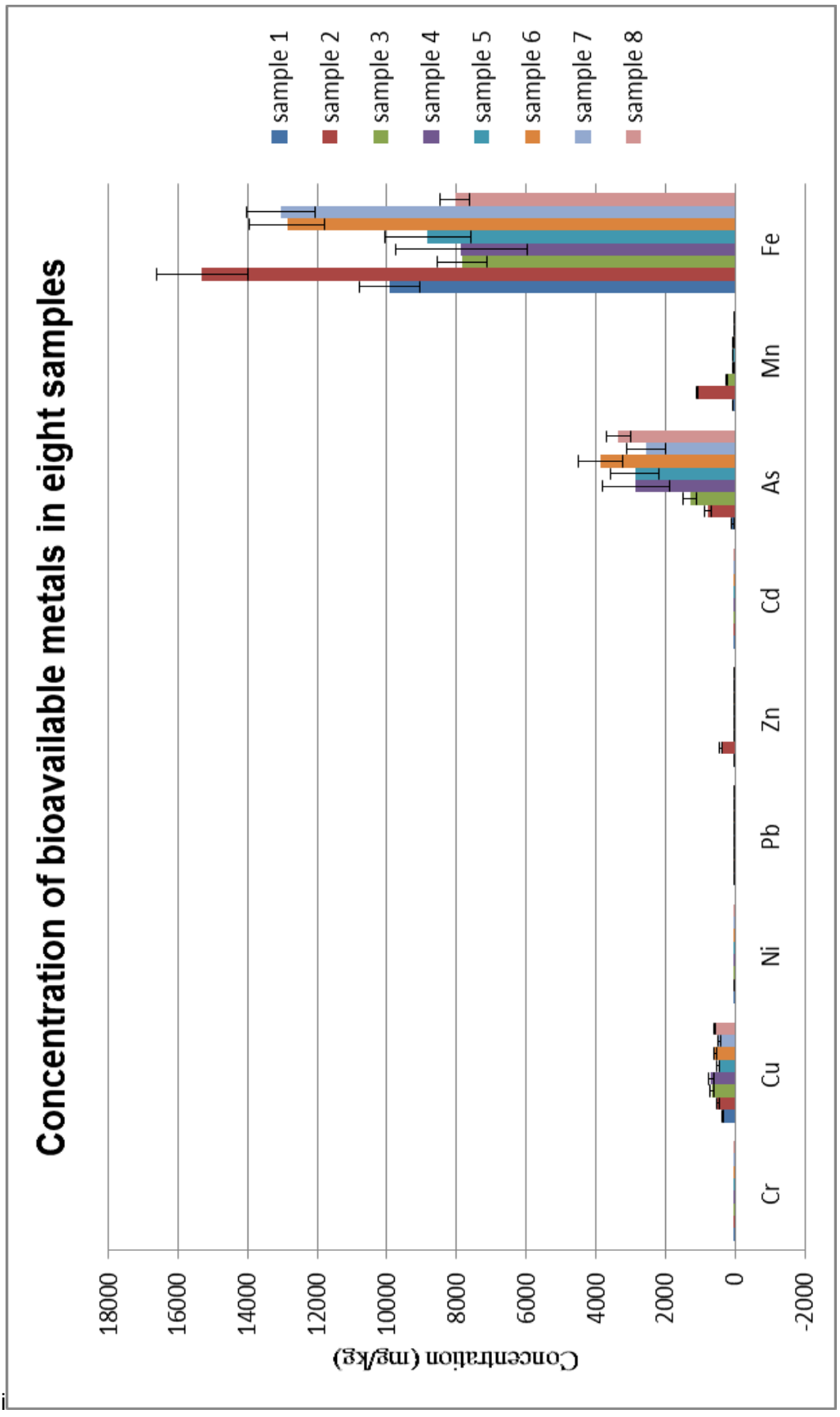

Figure 38: The concentration of bioavailable metals in eight samples (±2SD)

Conclusions and Future Work

To conclude, BCR sequential extraction procedures provide useful information for risk assessments because the amount of metals that can be mobilised under different environmental conditions can be predicted (e.g. weak acidic conditions: Step 1, reducible conditions: Step 2 and oxidisable conditions: Step 3). Decreases in mobility and bioavailability of the metals approximates to the order of the extraction sequence, hence the exchangeable fraction (step 1) could indicate which metals were more mobile and therefore most available for plants to uptake and release into the environment.

The mobility of trace metals, their bioavailability and related eco-toxicity to plants, depends strongly on their specific chemical forms or ways of binding. Consequently, these are the parameters that have to be determined rather than the total element contents in order to assess toxic effects and to study geochemical pathways.

In this investigation, CRM®701 was used to compare different instruments, namely ICP-AES and ICP-MS. The CRM could improve the accuracy and precision of the BCR extraction. In step 1, the overall metal recovery in ICP-AES was close to 100% comparatively and a few metals were over 120%. For a T-Test, more metals were accepted with no difference in significance between the certified values for ICP-AES. It can be seen that ICP-AES was preferable in step 1.

In step 2, the RSD of six metals for ICP-AES were all below 10%, representing a high precision. For recovery, nine out of the 12 metals were higher than 80% across the two instruments. The recovery of ICP-AES was as good as ICP-MS. For the T-Test, most of the metals' results showed that there was difference in the significance between the certified and the experiment values of the two sets of data. On the whole, ICP-AES and ICP-MS were also preferable in step 2.

In step 3, only Cr and Ni had no difference in significance between the two instruments in the F-test. The matrix effects and spectroscopic interference might not be factors that affect the comparison. The RSDs of Cr for the two instruments were both higher than 10% while those of Ni were both lower than 10%. The recovery of Ni for ICP-AES was higher than ICP-MS by 10%. It can be concluded that ICP-AES was more preferable in step 3.

The sediments collected on 1st November 2011 were extracted by the BCR extraction method. A large amount of <250μm sediment was present in samples 2, 4 and 8. Samples 1, 3, 6 and 7 were classified as muddy sandy gravel sediment and the colour was yellowish-brown. All the wet densities of the samples were similar and were higher than 1 gcm^{-3}.The concentrations of the sediments were determined by ICP-AES and ICP-MS. In step 1, Fe (78.66-616.2 $mgkg^{-1}$), Cu (175.9- 387.4 $mgkg^{-1}$) and As (5.976- 128.5 $mgkg^{-1}$) had the highest concentrations. In step 2, Fe (7759- 14697$mgkg^{-1}$), As (62.19- 3827 $mgkg^{-1}$) and Cu (163.9- 387.6 $mgkg^{-1}$) had the highest levels. In step 3, the highest metal content consisted of Fe (452.1- 2710$mgkg^{-1}$), Cu (125.3- 1143 $mgkg^{-1}$), and As (4.084- 331.6 $mgkg^{-1}$) respectively.

In sample 2, especially high levels of Mn (936.5 $mgkg^{-1}$), Zn (287.2 $mgkg^{-1}$) and Fe (616.2 $mgkg^{-1}$) presented in step 1; Zn (122.4 $mgkg^{-1}$) and Mn (156.1 $mgkg^{-1}$) in step 2; and Zn (46.49 $mgkg^{-1}$) and Fe (2710 $mgkg^{-1}$) in step 3. The results demonstrate that site 2 was closest to the contaminated regions, or the historical mine ores, hence some heavy metals (e.g. Mn, Zn, Fe) were discharged into, and accumulated within, the sediment via the tailing run-off streams.

The distribution of the selected metals in the 3 steps may show the differences between the percentages of the eight sample fractions. A high proportion of the step 3 fraction was revealed in Cr (~50% - 72%), while a high proportion of step 2 was shown in Pb (~83% - 100%), As (78% - 93%) and Fe (81% - 93%). A high percentage of Cr in step 3 was due to Cr(III) which has a high tendency to form stable complexes with organic matter. High amounts of Pb, As and Fe in step 2 might be due to Fe precipitation effects in the Fe-Mn oxides and large amounts of Fe-Mn oxides might effectively adsorb more Pb and As.

The distribution of the selected metals in step 1 could reflect the mobility of the metals. A high percentage of metals in the step 1 fraction relates to high mobility and would be released if the conditions became slightly acidic (pH <7). Mn was the most mobile one (0.821% - 0.123%), followed by Ni (0.646% - 0.1475) and Zn (0.630% - 0.154%). These metals might be released in acidic conditions, becoming hazardous to organisms, and accumulated in plants. The overall mobility of all metals decreased in the order of: site 2 > 1 > 3 > 4 > 6 > 5 > 8 > 7.

The bioavailability of metals included the exchangeable and reducible fractions (step 1and 2). The bioavailability of all the selected metals in all sampling sites decreased in the order of: site 8 > 3 > 1 > 6 > 4 > 2 > 5 > 7. In sample 8, the bioavailability of all metals was over 60%. In particular, Pb, As and Fe were higher than 90%. The large amount of metals might be due to the dissolution of Pb, Fe and As minerals (e.g. FeAsS, $FeAsO_4{\cdot}2H_2O$ and PbS). The highest levels of bioavailable metals were of Fe (7837 – 15313 $mgkg^{-1}$), As (68.1 – 3867 $mgkg^{-1}$), and Cu (344.3 – 684.0 $mgkg^{-1}$). The bioavailable metals in location 8 produced high concentrations of bioavailable Fe, As and Cu, which could potentially be up-taken by plants and organisms within the aquatic system. Eventually, the metals would be released into the Tamar River, becoming hazardous to the nearest town, Gunnislake.

For future research, the BCR extraction method could determine the residual fractions (step 4). The residual phase represents metals largely embedded in the crystal lattice of the soil fraction and should not be available for remobilization except under very harsh conditions (Yusuf *et al*., 2007). In addition, total digestion would be required for internal checking, as well as total recovery calculations of all metals collected in the extraction method. The method recovery = (Fraction 1 to 4)/ Total digestion x 100 (Cuong *et al*., 2006). Additionally, the metal content in the water from the Devon Great Consols could be determined through further investigation.

References

Absolute Astronomy, F.D. (2011), *Pourbaix diagram*. Available from: http://www.absoluteastronomy.com/topics/Pourbaix_diagram [Accessed: January 18, 2012].

Adekola, F.A., Abdus-Salam, N., Bale, R.B. & Oladeji, I.O. (2010), "Sequential extraction of trace metals and particle size distribution studies of Kainji Lake sediment, Nigeria", *Chemical Speciation and Bioavailability*, vol. 22, no. 1, pp. 43-49.

Alonso Castillo, M.L., Verdea Alonso, E., Siles Cordero, M.T., Cano Pavon, J.M. & Garcia de Torres, A. (2011), "Fractionation of heavy metals in sediment by using microwave assisted sequential extraction procedure and determination by inductively coupled plasma mass spectrometry", *Microchemical Journal*, vol. 98, pp. 234-239.

Anawar, H.M., Mihaljevic, M., Garcia-SSanchez, A., Akai, J. & Moyano, A. (2010), "Investigation of Sequential Chemical Extraction of Arsenic from Sediments: Variations in Sample Treatment and Extractant", *Soil and Sediment Contamination*, vol. 19, pp. 133-141.

Arain, M.B., Kazi, T.G., Jamali, M.K., Baig, J.A., Afridi, H.I., Jalbani, N. & Sarfraz, R.A. (2009), "Comparison of different extraction approaches for heavy metal partitioning in sediment samples", *Pedosphere*, vol. 19, pp. 476–485.

Asagba, E.U., Okieimen, F.E. and Osokpor, J. (2007), "Screening and speciation of heavy metal contaminated soil from an automobile spare-part market", *Chem. Spec. Bioavail.*, vol. 19, no. 1, pp. 9 – 15.

Ayres, D. C. (1998), *Dictionary of environmentally important chemicals,* Blackie Academic & Professional, London.

Bacon, J.R. & Davidson, C.M. (2008), "Is there a future for sequential chemical extraction?", *Analyst*, vol. 133, pp. 25–46.

Baig, J.A., Kazi, T.G., Arain, M.B., Shah, A.Q., Sarfraz, R.A., Afridi, H.I., Kandhro, G.A., Jamali, M.K. & Khan, S. (2009), "Arsenic fractionation in sediments of different origins using BCR sequential and single extraction methods", *Journal of Hazardous Materials*, vol. 167, pp. 754-751.

Balistrieri, L.S., Muray, J.W. & Paul, B. (1992), "The biogeochemical cycling of trace metals in the water column of Lake Sammamish. Washington; response to seasonally anoxic conditions", *Limnol. Oceanogr*, vol. 37, pp. 529-548.

Baron, J., Legret, M. & Astruc, M. (1990), "Study of interactions between heavy metals and sewage sludge. Determination of stability constants and complexation capacities of complexes formed with Cu and Cd", *Environ. Technol.*, vol. 11, pp. 151-162.

Bertling, S., Wallinder, I.O., Leygraf, Ch. & Kleja, D.B. (2006), "Occurrence and fate of corrosion-induced zinc in runoff water from external structures", *Sci. Total Environ*, vol. 367, pp. 908-923.

Bialkowski, S. (2004), *F – Test*. Available from: Utah State University, Chemistry and Biochemistry Web site: http://ion.chem.usu.edu/~sbialkow/Classes/3600/Overheads/F%20Test/F%20test.html [Accessed: January 22, 2012].

Brown, P.L. & Markich, S.J. (2000), "Evaluation of the free ion activity model of metal-organism interaction: Extension of the conceptual model.", *Aquat. Toxicol.*, vol. 51, pp. 177 – 194.

Campbell, P.G.C. (1995), "Interactions between trace metals and aquatic organisms: A critique of the free-ion activity model.", *Metal Speciation and Bioavailability in Aquatic Systems*, pp. 45 – 102.

Cappuyns, V., Swennen, R. & Niclaes, M. (2007), "Application of the BCR sequential extraction scheme to dredged pond sediments contaminated by Pb–Zn mining: A combined geochemical and mineralogical approach", *Journal of Geochemical Exploration*, vol. 93, pp. 78–90.

Chlopecka, A., Bacon, J.R., Wilson, M.J. & Kay, J. (1996), "Forms of cadmium, lead and zinc in soils from Southwest Poland", *Environ. Qual.*, vol. 25, pp. 69-79.

Choi, S.C., Wai, O.W.H., Choi, T.W.H., Li, X.D. & Yen, Y.F. (2006), "Distribution of cadmium, chromium, copper, lead and zinc in marine sediments in Hong Kong waters", *Environmental Geology*, vol. 51, pp. 455–461.

Christensen, T.H. & Huang, P.M. (1999), "Solid Phase Cadmium and the Reactions of Aqueous Cadmium with Soil Surfaces. In: Cadmium in Soils and Plants", *Kluwer Academic Publisher*, pp. 65-69.

Cuong, D.T. & Obbard.J.P. (2006), "Metal speciation in coastal marine sediments from Singapore using a modified BCR-sequential extraction procedure", *Applied Geochemistry*, vol. 21, pp. 1335-1346.

Devon County Council (2012), *Educational Register of Geological Sites*. Available from:, Devon County Council Web site: http://www.devon.gov.uk/geo-devon-great-consols.pdf [Accessed: March 10, 2012].

Directive 76/464/EEC (2009), *Water pollution by discharges of certain dangerous substances*. Available from: http://ec.europa.eu/environment/water/water-dangersub/76_464.htm [Accessed: January 24, 2012].

Drever, J. I. (1997), *The geochemistry of natural waters: surface and groundwater environments,* Prentice Hall, London.

Fan, W.H., Wang, W.-X., Chen, J.S., Li, X.D. & Yen, Y.F. (2002), "Cu, Ni, and Pb speciation in surface sediments from a contaminated bay of northern China", *Marine Pollution Bulletin*, vol. 44, pp. 820–826.

Fifield, F. W. & Haines, P. J. (2000), *Environmental Analytical Chemistry,* 2nd ed, Blackwell Science.

Gao, X.L., Chen, S.Y. & Long, A.M. (2008), "Chemical speciation of 12 metals in surface sediments from the northern South China Sea under natural grain size", *Marine Pollution Bulletin*, vol. 56, pp. 786–792.

Guo, X., Ma, Y., Wang, X. & Chen, S. (2010), "Re-evaluating the effects of organic ligands on copper toxicity to barley root elongation in culture solution", *Chemical Speciation and Bioavailability*, vol. 22, no. 1, pp. 51-59.

Gleyzes, C., Tellier, S. & Astruc, M. (2002), "Fractionation studies of trace elements in contaminated soils and sediments: a review of sequential extraction procedures", *Trac-Trends in Analytical Chemistry*, vol. 21, pp. 451–467.

Google Map (2012), *Devon Great Consols*. Available from:, Google Web site: http://maps.google.com/maps?hl=zh-TW&tab=Tl [Accessed: January 11, 2012].

Ikem, A., Osibanjo, O., Sridhar, M.K.C. & Sobande, A. (2002), "Evaluation of groundwater quality characteristics near two waste sites in Ibadan and Lagos, Nigeria", *Water Air Soil Pollut.*, vol. 140, pp. 307-333.

Iwegbue, C.M.A., Eghwrudje, M.O., Nwajei, G.E. & Egboh, S.H.O. (2007), "Chemical speciation of heavy metals in the Ase River sediment, Niger Delta, Nigeria", *Chemical Speciation and Bioavailability*, vol. 19, no. 3, pp. 117-127.

Kabata-Pendias, A. & Pendias, H. (2000) *Trace Elements in Soils and Plants,* Washington, CRC Press LLC.

Kartal, S., Aydin, Z. & Tokalioglu, S. (2006), "Fractionation of metals in street sediment samples by using the BCR sequential extraction procedure and multivariate statistical elucidation of the data", *Journal of Hazardous Materials*, vol. 132, pp. 80-89.

Keefer, R.F., Codling, E.E. & Singh, R.N. (1984), "Fractionation of metal-organic components extracted from a sludge-amended soil", *Soil Sci. Soc. Am. J.*, vol. 48, pp. 1054-1059.

Lai, C.-H., Chen, C.-Y., Wei, B.-L. & Yeh, S.-H. (2002) "Cadmium adsorption on goethite-coated sand in the presence of humic acid", Water Res., vol.36, pp. 4943– 4950.

Langmuir, D., Chrostowski, R., Vigneault, B. & Chaney, R. (2004), . Available from: U.S. Environmental Protection Agency, Risk Assessment Forum Web site: http://hk.search.yahoo.com/r/_ylt=Axt7wJPiSm1PuGYAfZ6zygt.;_ylu=X3oDMTE1YWs1cXBpBHNlYwNzcgRwb3MDMgRjb2xvA2hrMgR2dGlkA1ZJUEhLMDNfNDU-/SIG=12mgm3o4m/EXP=1332591458/**http%3a//oaspub.epa.gov/eims/eimscomm.getfile%3fp_download_id=437514 [Accessed: January 13, 2012].

Lambert, M., Pierzynski, G., Erickson, L. & Schnoor, J. (1997), "Remediation of lead, zinc and cadmium contaminated soils", *Contaminated land and its reclamation*, pp. 91 – 102.

Li, X.D., Shen, Z.G., Wai, O.W.H., & Li, Y.S. (2001), "Chemical forms of Pb, Zn and Cu in the sediment profiles of the Pearl River Estuary", *Marine Pollution Bulletin*, vol. 42, pp. 215– 223.

Lopez, D.L., Gierlowski-Kordesch, E. & Hollenkamp, C. (2010), "Geochemical Mobility and Bioavailability of Heavy Metals in a Lake Affected by Acid Mine Drainage: Lake Hope, Vinton County, Ohio", *Water Air Soil Pollut.*, vol. 2010, no. 213, pp. 27-45.

Loring, D.H. & Rantala, R.T.T. (1992), "Manual for the geochemical analyses of marine sediments and suspended particulate matter", *Earth-Science Reviews*, vol. 32, pp. 235-283.

Lu, Y. & Allen, H.E. (2002), "Characterization of copper complexation with natural dissolved organic matter (DOM)—Link to acidic moieties of DOM and competition by Ca and Mg", *Water Res.*, vol. 36, pp. 5083-5101.

Margui, E., Salvado, V., Queralt, I. & Hidalgo, M. (2004), "Comparison of three-stage sequential extraction and toxicity characteristic leaching tests to evaluate metal mobility in mining wastes", *Analytica Chimica Acta*, vol. 524, pp. 151-159.

Marin, B., Valladon, M., Polve, M. & Monaco, A. (1997), "Reproducibility testing of a sequential extraction scheme for the determination of trace metal speciation in a marine reference sediment by inductively coupled plasma-mass spectrometry", *Analytica Chimica Acta*, vol. 342, pp. 91–112.

Mcgrath, S.P. & Smith, S. (1990), "Chromium and nickel", *Heavy metals in soils*, pp. 125 150.

Mclean, J. E. & Bledsoe, B. E. (1992), *Ground water issue: behaviour of metals in soil,* US Env. Prot. Agency EPA, U.S.

Mello, J.W. V., Roy, W. R., Talbot, J. L., and Stucki, J.W. (2006), "Mineralogy and arsenic mobilization in arsenic-rich Brazilian soils and sediments", *J Soils Sediments*, vol. 6, pp. 9–19.

Mok, W.M. & Wai, C.M. (1989), "Distribution and mobilization of arsenic species in the creeks around the Blackbird Mining District, Idaho", *Wat. Res.*, vol. 23, pp. 7–13.

Morel, F. M. & Hering, J. G. (1994), *Principles and applications of aquatic chemistry,* John Wiley Sons, Inc., New York.

Morillo, J., Usero, J., Gracia, I., (2004), "Heavy metal distribution in marine sediments from the southwest coast of Spain", *Chemosphere*, vol. 55, pp. 431–442.

Morrison, H & Vicente-Becketti, V. (2006), *Chemical Sequential Extraction of Estuarine Sediments of Central Queensland*. Available from: Central Queensland University, School of Chemical and Biomedical Sciences Web site: http://hk.search.yahoo.com/r/_ylt=Axt7wJSkQG1PWl4AAWmzygt.;_ylu=X3oDMTE1YzNyNDF1BHNlYwNzcgRwb3MDMQRjb2xvA2hrMgR2dGlkA1ZJUEhLMDNfNDU-/SIG=1474dcguv/EXP=1332588836/**http%3a//association.cqu.edu.au/cqusa_new_site/cqusa%2520site/aaflash/Menu/Site/pso/2002%2520Papers/HelenMorrison.pdf [Accessed: November 18, 2011].

Namiesnik, J. & Rabajczyk, A. (2010), "The speciation and physico-chemical forms of metals in surface waters and sediments", *Chemical Speciation and Bioavailability*, vol. 22, no. 1, pp. 1-24.

Naji, A., Ismail, A. & Ismail, A.R. (2010), "Chemical speciation and contamination assessment of Zn and Cd by sequential extraction in surface sediment of Klang River, Malaysia", *Microchemical Journal*, vol. 95, pp. 285-292.

Nemati, K., Bakar, N.K.A., Sobhanzadeh, E. & Abas, M.R. (2009), "A modification of the BCR sequential extraction procedure to investigate the potential mobility of copper and zinc in shrimp aquaculture sludge", *Microchemical Journal*, vol. 92, pp. 165-169.

Palumbo-Roe, B., Klinck, B. & Cave, M. (2007a), "17 Arsenic speciation and mobility in mine wastes from a copper–arsenic mine in Devon, UK: an SEM, XAS, sequential chemical extraction study", *Trace Metals and other Contaminants in the Environment*, vol. 9, pp. 431-460.

Palumbo-Roe, B. & Klinck, B. (2007b), "Bioaccessibility of arsenic in mine waste-contaminated soils: A case study from an abandoned arsenic mine in SW England (UK)", *Journal of Environmental Science and Health Part A*, vol. 42, no. 9, pp. 1251-1261.

Pickering, J. (1996), "Metal on speciation; soils and sediments (a review)", *Ore Geol. Rev.*, vol. 1, pp. 83 – 146.

Pickering, W.F. (1986), "Metal ion speciation-soils and sediments", *Ore Geol. Rev.*, vol. 1, pp. 83-146.

Popovic, O., Almas, A.R., Manojlovic, M., Muratovic, S. & Singh, B.R. (2011), "Chemical speciation and bioavailability of Cd, Cu, Pb and Zn in Western Balkan soils", *Acta Agriculturae Scandinavica Section B - Soil and Plant Science*, vol. 61, no. 8, pp. 730-738.

Pueyo, M., Rauret, G., Luck, D., Muntau, H., Quevauviller, P.H. & Lopez-Sanchez, J. F. (2001), "Certification of the extractable contents of Cd, Cr, Cu, Ni, Pb and Zn in a freshwater sediment following a collaboratively tested and optimised three-step sequential extraction procedure", *J. Environ. Monit*, vol. 3, pp. 243-250.

Radojevic, M. (2006), *Practical environmental analysis,* 2nd ed, Cambridge, Royal Society.

Ramos, L., Hernandez, L.M. & Gonzalez, M.J. (1994), "Sequential fractionation of copper, lead, cadmium and zinc in soils from or near Donana National Park", *Journal of Environmental Quality*, vol. 23, pp. 50–57.

Rauret, G., Lopez-sanchez, J.F., Sahuquillo, A., Rubio, R., Davidson, C., Ure, A.& Quevauviller, Ph. (1999), "Improvement of the BCR three step sequential extraction procedure prior to the certification of new sediment and soil reference materials", *J. Environ. Monit.*, vol. 1, pp. 57–61.

Ryan, P.C., Wall, A.J., Hillier, S. & Clark, L. (2002), "Insight into sequential chemical extraction procedure from quantitative XRD: a study of trace metal partitioning in sediments related to frog malformities", *Chem. GeoL*, vol. 184, pp. 337- 357.

Rickard, D.T. & Nriagu, J.E. (1978), "Aqueous Environmental Chemistry of Lead", *In The Biogeochemistry of Lead in the Environment. Part A. Ecological Cycles*, pp. 219-284.

Rozan, T.F., Lassman, M. E., Ridge, D.P. & Luther III, G.W. (2000), "Evidence for iron, copper and zinc complexation as multinuclear sulphide clusters in oxic rivers", *Nature*, vol. 406, pp. 879-882.

Simon-Hettich, B., Wibbertmann, A., Wagner, D., Tomaska, L. & Malcolm, H. (2001) *Environmental health criteria 221*, *Zinc*, WHO, Geneva.

Singh, S.P., Tack, F.M. and Verloo, M.G. (1998), "Heavy metal fractionation and extractability in dredged sediment derived surface soils", *Water, Air Soil Pollut.*, vol. 102, pp. 313 –328.

Skoog, D. A, Holler, F. J. & Crouch, S. R. (2007), *Principles of Instrumental Analysis,* 6th ed, David Harris, Canada.

Smedley, P. L., and Kinniburgh, D. G. (2002), "A review of source, behaviour and distribution of arsenic in natural waters", *Appl Geochem*, vol. 17, pp. 517–568.

Spiers, V. (2011), *Country Diary: Great Consols, Tamar Valley*. Available from: Guardian News and Media Limited Web site: http://www.guardian.co.uk/environment/2011/may/18/country-diary-tamar-valley-mining-woodland [Accessed: January 19, 2012].

Sposito, G., Lund, L.J. & Chang, A.C. (1982), "Trace metal chemistry in arid-zone soils amended with sewage sludge 1. Fractionation of Ni, Cu, Zn, Cd and Pb in solid phases Soil Sci.", *Soc. Am. J.*, vol. 46, pp. 260-264.

Taylor, S.R. (2010), "The application of trace element data to problems in petrology", *Physics and chemistry of the earth*, pp. 133-213.

Tessier, A., Campbell, P.G.C & Bisson, M. (1979), "Sequential extraction procedure for the speciation of particulate trace metals", *Analytical Chemistry*, vol. 51, pp. 844–8 51.

The University of Plymouth (2011), *Devon Great Consols Virtual Tour*. Available from: The University of Plymouth, Lab Plus Web site: http://www.ssb.plymouth.ac.uk/labplus/sharples/DGC/DGCOverview.htm [Accessed: October 10, 2011].

Thomas, R.P., Ure, A.M., Davidson, C.M., *et al*. (1994), "Three-stage sequential extraction procedure for the determination of metals in river sediments", *Analytica Chimica Acta*, vol. 286, pp. 423-429.

Tokalioglu, S., Kartal, S. & Birol, G. (2003), "Application of a three-stage sequential extraction procedure for the determination of extractable metal contents in highway soil", *Turk. J. Chem.*, vol. 27, pp. 333 –346.

Turner, A. & Millward, G.E. (2002), "Suspended Particles: Their Role in Estuarine Biogeochemical Cycles", *Estuarine, Coastal and Shelf Science*, vol. 55, pp. 857-883.

Tyler, G. & Olsson, T. (2001a), "Concentrations of 60 elements in the soil solution as related to the soil acidity", *Soil Sci.*, vol. 52, pp. 151-165.

Tyler, G. & Olsson, T. (2001b), "Plant uptake of major and minor mineral elements as influenced by soil acidity and liming", *Plant Soil*, vol. 230, pp. 307-321.

USGS (2012), *U.S. Geological Survey Open-File Report 2006-1187*. Available from:, USGS Web site: http://pubs.usgs.gov/of/2006/1187/htmldocs/folk.htm [Accessed: March 26, 2012].

Uwumarongie-Ilori, E.G., Okieimen, F.E. & Uwumarongie, O.H. (2011), "Speciation of trace metals in chromated-copper-arsenate contaminated sediment of Ogba River", *Chemical Speciation and Bioavailability*, vol. 23, no. 2, pp. 118-124.

Vasile, G.G. & Tanase, I.G. (2008), "COMPARATIVE STUDY OF DIFFERENT EXTRACTION METHODS FOR EVALUATION OF BIOAVAILABILITY OF TERRESTRIAL SEDIMENT – BOUND METALLIC ELEMENTS", *Revue Roumaine de Chimie*, vol. 53, no. 11, pp. 1041-1049.

Vieira, J.S., Botelho, C.M.S. & Boaventura, R.A.R. (2009), "Trace Metal Fractionation by the Sequential Extraction Method in Sediments from the Lis River (Portugal)", *Soil & Sediment Contamination*, vol. 18, pp. 102-119.

Wikipedia (2012), *Particle Size (grain Size)*. Available from:, Wikipedia Web site: http://en.wikipedia.org/wiki/Particle_size_%28grain_size%29 [Accessed: February 5, 2012].

Wilde, F.D. & Radtke, D.B. (2005), General information and guidelines 6.0, *USGS*. Available from: http://water.usgs.gov/owq/FieldManual/Chapter6/Archive/6.0/final508Chapter6.0.pdf [Accessed: January 18, 2012].

Wilson, F.H. & Hawkins, D.B. (1978), "Arsenic in streams, stream sediments, and ground water, Fairbanks Area, Alaska", *Environ. Geol.*, vol. 2, pp. 195–202.

Yi, Y., Wang, Z., Zhang, K., Yu, G. & Duan, X. (2008), "Sediment pollution and its effect on fish through food chain in the Yangtze River", *International Journal of Sediment Research*, vol. 23, pp. 338-347.

Yu, X., Yan, Y. & Wang, W.-X. (2010), "The distribution and speciation of trace metals in surface sediments from the Pearl River Estuary and the Daya Bay, Southern China", *Marine Pollution Bulletin*, vol. 60, pp. 1364-1371.

Yuan, C.-G., Shi, J.-B., He, B., Liu, J.-F., Liang, L.-N. & Jiang, G.-B. (2004), "Speciation of heavy metals in marine sediments from the East China Sea by ICP-MS with sequential extraction", *Environment International*, vol. 30, pp. 769-783.

Yusuf, K.A. (2007), "Sequential Extraction of Lead, Copper, Cadmium and Zinc in Soils near Ojota Waste Site", *Journal of Agronomy*, vol. 6, no. 2, pp. 331-337.